

# **Controlled Ring-Opening Polymerization: Polymers with designed Macromolecular Architecture**

**Kajsa M. Stridsberg**



**Department of Polymer Technology  
Royal Institute of Technology  
Stockholm, Sweden  
2000**

## **Akademisk avhandling**

som med tillstånd av Kungliga Tekniska Högskolan framlägges till offentlig granskning för avläggande av teknisk doktorsexamen fredagen den 3 mars 2000, kl. 10.00 i Kollegiesalen, Administrationsbyggnaden, Valhallavägen 79, KTH, Stockholm. Avhandlingen försvaras på engelska.

ISBN 91-7170-522-8

Printed by Kista Snabbtryck AB, Stockholm, Sweden

# Controlled Ring-Opening Polymerization: Polymers with designed Macromolecular Architecture

Kajsa M. Stridsberg

## ABSTRACT

This thesis summarizes the development of new catalyst systems for ring-opening polymerization and their use in the production of macromolecules with advanced architecture.

The influences of reaction conditions, *i.e.* reaction temperature, solvent and reaction time, on the polymerization kinetics have been evaluated for the ring-opening polymerization (ROP) of 1,5-dioxepan-2-one (DXO) initiated by a cyclic tin-alkoxide. The purpose has been to achieve a controlled ring-opening polymerization of lactones and lactides, resulting in polymers with desirable properties. The mechanism and kinetics of controlled ring-opening polymerization of L-lactide (L-LA) have been investigated, leading to hydroxy telechelic polymers to be used in macromer reactions of various natures.

The ROP mechanism of DXO with stannous octoate as catalyst has been investigated theoretically with hybrid density functional methods. A new mechanism has been proposed which provides an explanation of the experimental observations. The ROP mechanism has been shown to involve the formation of a tin-alkoxide complex, which subsequently coordinates a monomer. It has been demonstrated that the ring-opening of the monomer proceeds via a concerted four-center transition state.

Elastomeric tri-block copolymers have been obtained from L-LA and DXO with a difunctional tin-initiator. A two-step process has been developed to achieve a well-defined tri-block copolymer, poly(L-lactide-*b*-1,5-dioxepan-2-one-*b*-L-lactide) (poly(L-LA-*b*-DXO-*b*-L-LA)), in good yield. Thermal analysis of the poly(L-LA-*b*-DXO-*b*-L-LA) has been used to examine the morphology of the block copolymer. The crystallinity and melting temperature have been shown to increase with increasing amount of L-LA in the copolymer, but the glass transition temperature was only slightly influenced by the polymer composition.

Poly(L-LA-*b*-DXO-*b*-L-LA) has been subjected to hydrolytic degradation in phosphate buffer solution. The influence of molecular weight and chemical composition on the hydrolysability has been investigated. The molecular weight change, weight loss and composition changes have been characterized in order to determine the degradation pathway. The degradation of poly(L-LA-*b*-DXO-*b*-L-LA) was characterized by a significant decrease in molecular weight immediately after immersion in the buffer solution and a progressive increase the amount of L-LA in the remaining copolymer with increasing degradation time. The primary degradation products formed during hydrolysis have been detected as lactic acid and 3-(2-hydroxyethyl)-propanoic acid. Results indicate that the composition had no effect on the rate of degradation. The major factor determining the degradation rate was the original molecular weight.

**Keywords:** controlled ring-opening polymerization, poly(1,5-dioxepan-2-one), poly(L-lactide), kinetics, mechanism, block copolymerization, poly(L-lactide-*b*-1,5-dioxepan-2-one-*b*-L-lactide), characterization, hydrolytic degradation,



## LIST OF ARTICLES

This thesis is a summary of the following papers:

- I. Ring-Opening Polymerization of 1,5-Dioxepan-2-one Initiated by a Cyclic Tin-Alkoxide Initiator in Different Solvents. K. Stridsberg, A.-C. Albertsson, *Journal of Polymer Science: Part A: Polymer Chemistry* **1999**, *37*, 3407
- II. Di-hydroxy Terminated Poly(L-lactide) obtained by Controlled Ring-Opening Polymerization: Investigation of the Polymerization Mechanism, K. Stridsberg, M. Ryner, A.-C. Albertsson, *Macromolecules*, accepted for publication
- III. Controlled Ring-Opening Polymerization of L-lactide and 1,5-dioxepan-2-one forming a Tri-Block Copolymer, K. Stridsberg, A.-C. Albertsson, submitted to *Journal of Polymer Science: Part A: Polymer Chemistry*
- IV. Changes in Chemical and Thermal Properties of the Tri-Block Copolymer Poly(L-lactide-*b*-1,5-dioxepan-2-one-*b*-L-lactide) during Hydrolytic Degradation, K. Stridsberg, A.-C. Albertsson, *Polymer*, accepted for publication

It also contains parts of the following article:

- V. The Mechanism of Ring-Opening Polymerization of Lactones and Lactides with Stannous(II) 2-ethylhexanoate as Catalyst studied with Hybrid Density Functional Methods, K. Stridsberg, M. Ryner, A.-C. Albertsson, H. von Schenck, M. Svensson, submitted to *Macromolecules*



# TABLE OF CONTENTS

1	PURPOSE OF THE STUDY .....	1
2	INTRODUCTION.....	3
2.1	Background.....	3
2.2	Ring-opening polymerization of cyclic esters .....	4
2.2.1	Cationic ring-opening polymerization .....	5
2.2.2	Anionic ring-opening polymerization .....	5
2.2.3	“Coordination-insertion” ring-opening polymerization.....	6
2.3	Organometallic compounds as initiators for the ROP of lactones and lactides.....	7
2.3.1	Stannous(II) 2-ethylhexanoate .....	9
2.3.2	Aluminum tri-isopropoxide .....	10
2.3.3	Tin-alkoxides .....	11
2.3.4	Lanthanide alkoxides.....	12
2.4	Macromolecular architecture .....	12
2.4.1	Homopolymers.....	12
2.4.2	Block copolymers .....	13
2.4.3	Star-shaped (co)polymers.....	14
2.5	Biodegradable polymers.....	15
2.5.1	Polymer degradation .....	15
2.5.2	Polyglycolide and copolymers .....	16
2.5.3	Poly lactide and copolymers.....	16
2.5.4	Poly( $\epsilon$ -caprolactone) and copolymers .....	18
3	SYNTHESIS .....	19
3.1	Materials.....	19
3.2	Initiator.....	19
3.2.1	1,1,6,6-tetra- <i>n</i> -butyl-1,6-distanna-2,5,7,10-tetraoxacyclodecane.....	19
3.3	Monomers .....	20
3.3.1	L-lactide .....	20
3.3.2	1,5-dioxepan-2-one.....	20
3.4	Polymerization.....	21
3.4.1	Homopolymerization of DXO and L-lactide .....	21
3.4.2	Block copolymerization of 1,5-dioxepan-2-one and L-lactide .....	21

4	CHARACTERIZATION .....	23
4.1	Hydrolytic Degradation.....	23
4.1.1	Sample Preparation.....	23
4.1.2	<i>In vitro</i> degradation of the poly(L-lactide- <i>b</i> -1,5-dioxepan-2-one- <i>b</i> -L-lactide) tri-block copolymers. ....	23
4.2	Instrumental Analysis.....	24
4.2.1	Mass Spectroscopy (MS) .....	24
4.2.2	Nuclear Magnetic Resonance Spectroscopy (NMR) .....	24
4.2.3	Size Exclusion Chromatography (SEC) .....	25
4.2.4	Differential Scanning Calorimetry (DSC) .....	25
4.2.5	Solid Phase Extraction (SPE).....	26
4.2.6	Gas Chromatography – Mass Spectroscopy (GC-MS) .....	26
4.2.7	X-ray Diffraction Pattern Analysis .....	26
5	RESULTS AND DISCUSSION .....	27
5.1	Influence of reaction conditions on the homo-polymerization of 1,5-dioxepan-2-one and L-lactide .....	27
5.1.1	Synthesis of 1,1,6,6-tetra- <i>n</i> -butyl-1,6-distanna-2,5,7,10-tetra-oxacyclodecane.....	27
5.1.2	Influence of the reaction temperature on the polyDXO molecular weight and molecular weight distribution .....	29
5.1.3	Dependence of poly(L-lactide) number-average molecular weight and molecular weight distribution on the degree of monomer conversion .....	31
5.1.4	The effect of solvent on the rate of polymerization and the polyDXO molecular weight .....	32
5.1.5	Dependence of poly(L-LA) molecular weight on the monomer-to-initiator ratio .....	34
5.1.6	Influence of hydroxyl-functionality-containing contaminants on the molecular weight and molecular weight distribution .....	35
5.1.7	Catalytic degradation .....	36
5.2	Kinetics of lactide polymerization.....	38
5.2.1	Kinetic models .....	38
5.2.2	Kinetics of lactide polymerization.....	39
5.3	NMR analysis of the propagating species in ROP .....	42
5.3.1	NMR analysis of the reaction mixture.....	42
5.3.2	Initiator efficiency .....	43
5.3.3	Mechanism .....	45
5.4	Study of the ROP mechanism by hybrid density functional methods.....	46
5.4.1	Model system .....	46
5.4.2	Formation of the active species.....	47



5.4.3	Ring-opening of the monomer .....	48
5.4.4	Homo- and copolymerization.....	49
5.5	Block copolymerization of 1,5-dioxepan-2-one and L-lactide forming a tri-block copolymer .....	51
5.5.1	NMR-analysis of the block copolymers.....	53
5.5.2	Influence of the block copolymer composition on the thermal properties .....	55
5.6	Hydrolytic degradation of poly(L-lactide- <i>b</i> -1,5-dioxepan-2-one- <i>b</i> -L-lactide) .....	58
5.6.1	The influence of copolymer composition and original molecular weight on the rate of degradation.....	59
5.6.2	Changes in the copolymer composition during degradation. ....	60
5.6.3	Influence of the decrease in weight-average molecular weight on the weight loss .....	60
5.6.4	Degradation products .....	62
5.6.5	Dependence of the thermal properties on the composition and molecular weight .....	66
6	CONCLUSIONS .....	71
7	ACKNOWLEDGEMENTS .....	73
8	REFERENCES .....	75



# 1 PURPOSE OF THE STUDY

Aliphatic polyesters are an attractive class of polymers, which can be used in biomedical and pharmaceutical applications. One reason for the growing interest in this type of degradable polymers is that their physical and chemical properties can be varied over a wide range by *e.g.* copolymerization. The synthesis of novel polymer structures through ring-opening polymerization has been studied in our group for a number of years.<sup>[1,2,3,4,5]</sup> Degradable materials with new mechanical properties and modified degradation profiles have been produced and characterized. The increasing demands of the larger number of biomedical applications have resulted in an increasing interest in producing macromolecules through controlled polymerization. This thesis is concerned with the synthesis of novel degradable polymers and the ability to tailor the macromolecular structure using new initiator systems.

The aim of the first part of the investigation was to find optimal reaction conditions for the ring-opening polymerization of 1,5-dioxepan-2-one and L-lactide with 1,1,6,6-tetra-*n*-butyl-1,6-distanna-2,5,7,10-tetraoxacyclodecane. The influence of experimental parameters such as monomer-to-initiator ratio and initiator concentration on the chain length, and on the end group composition of the poly(L-LA) macromers has been elucidated.

In order to investigate the reaction mechanism, a thorough study of the kinetics of polymerization has been performed. Polymerization of L-lactide has been carried out in solution with 1,1,6,6-tetra-*n*-butyl-1,6-distanna-2,5,7,10-tetraoxacyclodecane as initiator. The results of the kinetic experiments have been utilized to understand the action of the initiator in more detail.

The reaction mechanism of one of the most utilized and effective catalysts for ring-opening polymerization, stannous octoate, has been under debate for the last decade. Despite the long use of this catalyst in both industrial use and polymer research, several questions about the structure of the reactive species and ring-opening of the monomer still remain. In this

thesis, a theoretical approach has been used to achieve information about the mechanisms of both initiation and propagation. For the calculations regarding the reaction mechanism, hybrid density functional methods have been used.

The newly developed tin-alkoxide initiator system has been used to synthesize well-defined block copolymers. Special attention has been paid to tri-block copolymers consisting of a soft inner poly(1,5-dioxepan-2-one) block associated with semi-crystalline poly(L-lactide) outer blocks. The effect of copolymer composition on the thermal properties has been determined.

The hydrolytic degradation of the elastomeric tri-block copolymer poly(L-lactide-*b*-1,5-dioxepan-2-one-*b*-L-lactide) has been investigated. The effects of composition changes and molecular weight variations on the degradability, degradation rate and physical properties during hydrolysis have been determined. The results have been analyzed in relation to the hydrolytic degradation of the respective homopolymers and random copolymers.

## 2 INTRODUCTION

The ability to control precisely the synthesis of advanced macromolecular structures has been an important objective in polymer research during the last decades. The development of macromolecules with strictly defined structures and properties, aimed at biomedical applications, leads to complex and advanced architecture and diversification of the hydrolyzable polymers.

### 2.1 Background

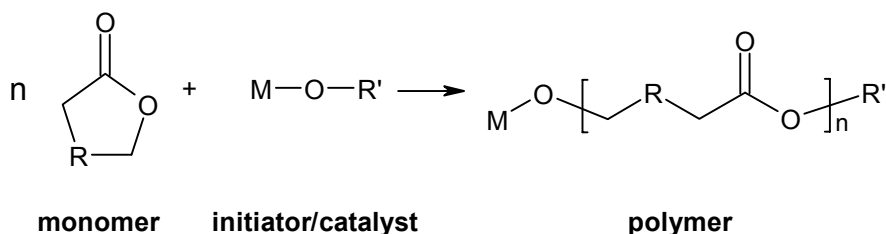
Polylactones and polylactides can be prepared by two different approaches, by polycondensation of hydroxy-carboxylic acids or by ring-opening polymerization (ROP) of cyclic esters. The polycondensation technique is less expensive than ROP, but it is difficult to obtain high molecular weight polymers, to achieve specific endgroups, and to prepare well-defined copolyesters. The ROP of lactones and lactides has been thoroughly investigated during the last 40 years, due to its versatility to produce a variety of biomedical polymers in a controlled manner. Carothers and co-workers first extensively explored the ROP technique for lactones, anhydrides, and carbonates.<sup>[6,7,8,9]</sup> Since then the method has been applied to a diversity of monomers to produce all types of polymers, and a number of initiator and catalyst systems have been developed. In many cases, the resulting polymers exhibit useful properties as engineering products.

There are several reasons for studying the polymerization of cyclic esters. First, to exploit the potential of synthetic polymer chemistry to prepare a variety of polymers with control of the major variables affecting polymer properties. Experimental conditions have to be optimized in order to find the best polymerization system for technological and industrial processes. Factors such as economy, toxicology and technical apparatus development are important. A second reason for studying ROP is to enable various advanced macromolecules, including homopolymers with well-defined structures or end-groups, to be prepared, as well as copolymers with different architectures, *e.g.* block, graft or star copolymers. The physical, mechanical,

and degradation properties of these various macromolecules are studied to determine the structure-to-property relationship. The third reason for studying these kinds of systems is that they are valuable models for the examination of the kinetics<sup>[10]</sup> and mechanisms<sup>[11]</sup> of elementary reactions in polymerization.

## 2.2 Ring-opening polymerization of cyclic esters

Poly lactones and poly lactides of high molecular weight are exclusively produced by the ring-opening polymerization of the corresponding cyclic monomers. A polyester is formed when cyclic esters are reacted with a catalyst or initiator. Scheme 2.2.1 presents the reaction pathway for the ring-opening polymerization of cyclic esters.



**Scheme 2.2.1** Schematic representation of the ring-opening polymerization of a cyclic ester. R = (CH<sub>2</sub>)<sub>0-3</sub> and/or (CHR’)

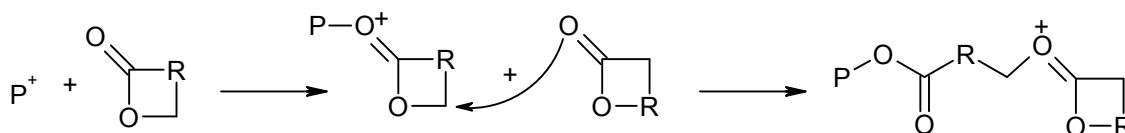
Each macromolecule formed will generally contain one chain end terminated with a functional group originating from the termination reaction and one terminus end-capped with a functional group originating from the initiator. By altering the catalyst or initiator and the termination reaction, the nature of the functional groups can be varied to fit the application of the polymer. The types of initiator and end-group play an important role in both the thermal stability and hydrolytic stability of the resulting polyester.<sup>[12,13,14]</sup> Functional groups accessible to post polymerization reactions can also be introduced into the polymer structure this way.

The ring-opening reaction can be performed either as a bulk polymerization, or in solution, emulsion or dispersion.<sup>[15,16]</sup> A catalyst or initiator is necessary to start the polymerization. Under rather mild conditions, high-molecular weight aliphatic polyesters of low polydispersity can be prepared in short periods of time. Problems associated with condensation polymerization, such as the need for exact stoichiometry, high reaction temperatures and the removal of low molecular weight by-products (*e.g.* water) are excluded in ROP.<sup>[17]</sup>

Depending on the initiator, the polymerization proceeds according to three different major reaction mechanisms,<sup>[18]</sup> *i.e.* cationic, anionic, or “coordination-insertion” mechanism.<sup>[19,20,21]</sup> In addition, radical, zwitterionic<sup>[22]</sup> or active hydrogen<sup>[18]</sup> initiation is possible although such techniques are not used to any great extent.

### 2.2.1 Cationic ring-opening polymerization

Among the cyclic esters, 4-, 6- and 7-membered rings form polyesters when reacted with cationic catalysts.<sup>[18,23,24,25]</sup> The cationic ring-opening polymerization involves the formation of a positively charged species which is subsequently attacked by a monomer (Scheme 2.2.2). The attack results in a ring-opening of the positively charged species through an S<sub>N</sub>2-type process.

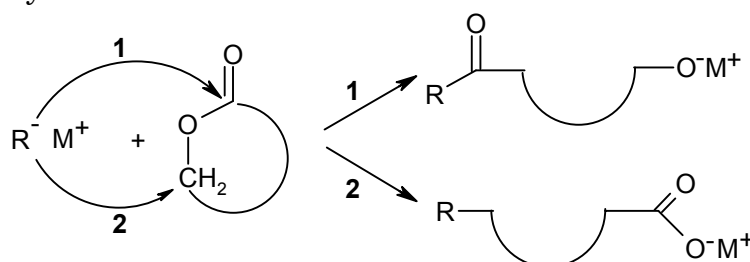


**Scheme 2.2.2** The reaction pathway for the ring-opening polymerization of a cyclic ester by cationic initiation.

The cationic polymerization is difficult to control and often only low-molecular weight polymers are formed. When the bulk and solution polymerization of 1,5-dioxepan-2-one (DXO) with cationic initiators was studied the highest molecular weight achieved was about 10 000.<sup>[23]</sup>

### 2.2.2 Anionic ring-opening polymerization

Anionic ring-opening polymerization of cyclic ester monomers takes place by the nucleophilic attack of a negatively charged initiator on the carbonyl carbon or on the carbon atom adjacent to the acyl-oxygen, resulting in a linear polyester (Scheme 2.2.3).<sup>[26,27]</sup> The propagating species is negatively charged and counter-balanced with a positive ion. Depending on the nature of the ionic propagating chain end and the solvent, the reacting complex varies from completely ionic to almost covalent.

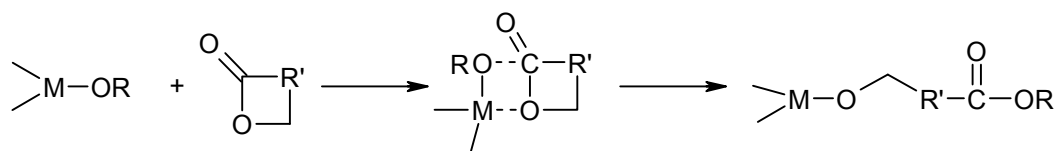


**Scheme 2.2.3** The reaction pathway for the ring-opening polymerization of a cyclic ester by anionic initiation. Ring-opening of monomer by 1) acyl-oxygen bond cleavage and 2) alkyl-oxygen bond cleavage.

One of the best controlled methods leading to high molecular weight polymers is anionic polymerization carried out in a polar solvent. The Jedlinski group developed living anionic ROP methods of 4- and 5-membered ring lactones and has reported well-defined polymers and copolymers of high molecular weight.<sup>[28]</sup> The anionic ring-opening of four membered rings ( $\beta$ -lactones) occurs through alkyl-oxygen or acyl-oxygen cleavage giving a carboxylate or alkoxide.<sup>[29]</sup> Larger lactones, such as  $\epsilon$ -caprolactone or lactide, react only by an attack of the anion on the carbonyl carbon atom with acyl-oxygen scission and the formation of an alkoxide as the growing species.<sup>[30,31]</sup> A problem associated with the anionic ROP is the extensive back-biting, and in some cases only polyesters of low molecular weight are achieved.<sup>[32]</sup>

### 2.2.3 “Coordination-insertion” ring-opening polymerization

The pseudo-anionic ring-opening polymerization is often referred to as “coordination-insertion” ROP, since the propagation is thought to proceed by coordination of the monomer to the active species and then insertion of the monomer into the metal-oxygen bond by rearrangement of the electrons.<sup>[19,20]</sup> Scheme 2.2.4 shows a schematic presentation of the coordination-insertion mechanism. The growing chain remains attached to the metal through an alkoxide bond during the propagation. The reaction is terminated by hydrolysis forming a hydroxyl end-group. With functional alkoxy-substituted initiators, macromers with end-groups active in post polymerization reactions are produced.



**Scheme 2.2.4** The proposed reaction pathway for the ring-opening polymerization of a cyclic ester by the coordination-insertion mechanism.

The coordination-insertion type of polymerization has been thoroughly investigated since it may yield well-defined polyesters through living polymerization.<sup>[20]</sup> When two monomers of similar reactivity are used, block copolymers can be formed by sequential addition to the “living” system.<sup>[58]</sup>



## 2.3 Organometallic compounds as initiators for the ROP of lactones and lactides

The synthesis of novel initiators and the ROP of existing or new monomers and macromers substituted with functional groups provide a very interesting and promising strategy to produce structurally advanced macromolecules.

A large variety of organometallic compounds, *i.e.* metal alkoxides and metal carboxylates, have been studied in order to achieve effective polymer synthesis.<sup>[33]</sup> Many reactions catalyzed by metal complexes are highly specific, and, by careful selection of metal and ligands, reactions can be generated to form a desired polymer structure.<sup>[34,35]</sup> The covalent metal alkoxides with free p or d orbitals react as coordination initiators and not as anionic or cationic initiators.<sup>[36]</sup> Figure 2.3.1 summarizes some of the most frequently used initiators and catalysts.

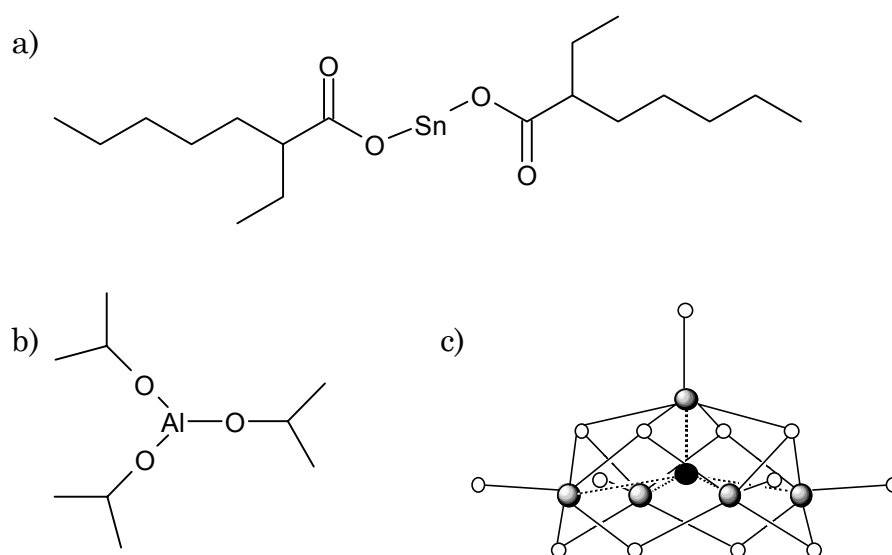
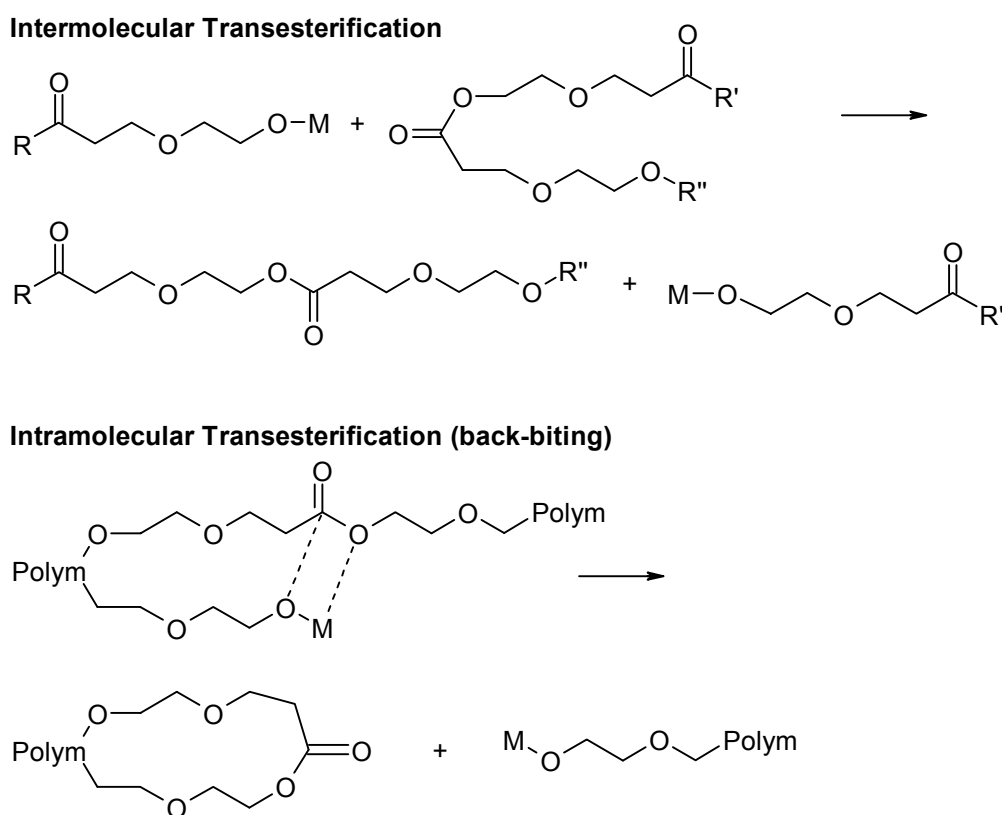


**Figure 2.3.1** Chemical structure of initiators used in ROP of lactones and lactides. a) stannous octoate b) aluminum isopropoxide c) lanthanide isopropoxide. Lanthanum atoms are represented by gray circles, and oxygen atoms by white circles. The black circle represents the bridging oxygen atom connecting all lanthanum atoms. Alkyl groups are left out for clarity

### *Transesterification reactions*

It is well known from the ring-opening polymerization of lactones and lactides that the catalyst or initiator causes transesterification reactions at elevated temperatures,<sup>[37]</sup> or at long reaction times (Scheme 2.3.2).<sup>[38]</sup> Intermolecular transesterification reactions modify the sequences of copolyesters and prevent the formation of block copolymers. Intramolecular transesterification reactions, *i.e.* back-biting, cause degradation of the polymer chain and the

formation of cyclic oligomers.<sup>[39]</sup> Both types of transesterification reactions broaden the molecular weight distribution.



**Scheme 2.3.2** Reaction scheme for intermolecular and intramolecular transesterification reactions

As displayed in the proposed scheme, each intramolecular transesterification randomly breaks the polymer chain. In this way, an attack on the polymer chain leads to a free residual polymer and a new randomized, modified polymer. According to this, an original copolymer with a blocky structure would be converted to a randomized copolymer after undergoing  $n$  transesterifications.<sup>[40,41]</sup>

Parameters that will influence the number of transesterifications are temperature, reaction time, and type of and concentration of catalyst or initiator.<sup>[42]</sup> Depending on the metal used, the initiator is more or less active towards side-reactions such as transesterification reactions.<sup>[43,44]</sup> The relative reactivity of different metal alkoxide initiators towards chains already formed has been reported to be:  $\text{Bu}_2\text{Sn}(\text{OR})_2 > \text{Bu}_3\text{SnOR} > \text{Ti}(\text{OR})_4 > \text{Zn}(\text{OR})_2 > \text{Al}(\text{OR})_3$ .<sup>[43]</sup>

The lactide configuration influences the degree of transesterification reactions taking place during polymerization.<sup>[45]</sup> The contribution of

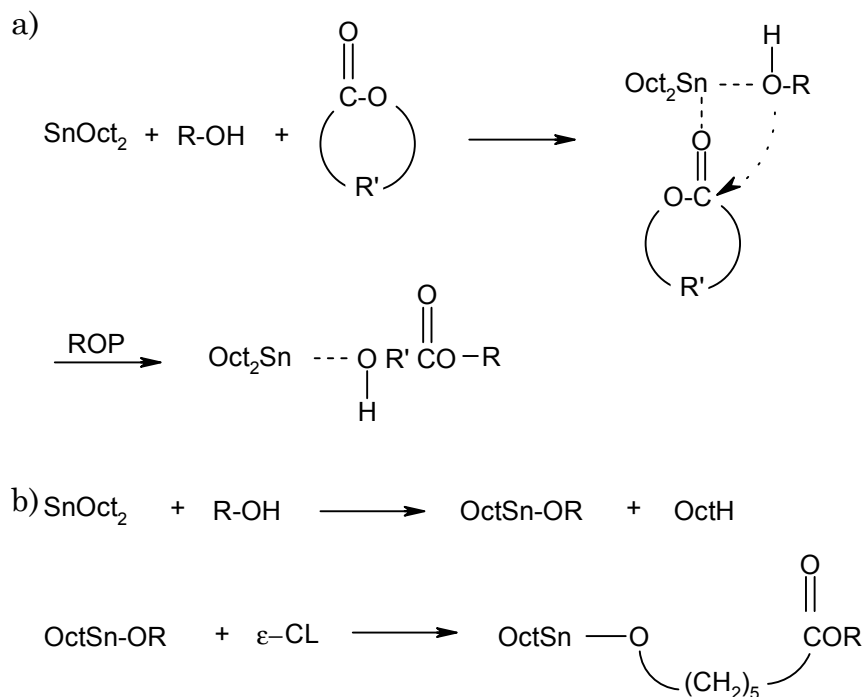
transesterification processes in the case of D,L-lactide was found to be considerably higher than that observed when L,L-lactide was polymerized. The difference in number of side-reactions was attributed partly to the polymer chain stiffness. The poly(D,L-lactide) is more flexible than the poly(L,L-lactide) due to the atactic lactide blocks.

When  $\epsilon$ -caprolactone and L-lactide are block copolymerized, the monomer addition sequence is very important. AB block copolymers can be prepared by ROP with SnOct<sub>2</sub> as catalyst and ethanol as initiator provided that  $\epsilon$ -CL is polymerized first.<sup>[46]</sup> If the L-LA block is synthesized first and the hydroxyl terminated macromer formed is used to initiate polymerization of  $\epsilon$ -CL, the polymer formed is totally randomized.

### 2.3.1 Stannous(II) 2-ethylhexanoate

Stannous(II) 2-ethylhexanoate, commonly referred to as stannous octoate [Sn(Oct)<sub>2</sub>], is a frequently used catalyst in the ROP of lactones and lactides.<sup>[40,47,48,49,50,51]</sup> Stannous octoate has been approved as a food additive by the Food and Drug Administration (FDA). The mechanism of polymerization has been widely discussed, and despite several proposals<sup>[11,46,52,53]</sup> the ROP mechanism remains unclear. The SnOct<sub>2</sub> is not thought to be the actual initiator since the molecular weight does not depend on the monomer-to-SnOct<sub>2</sub> molar ratio. The most promising mechanism is a coordination insertion mechanism where a hydroxyl functional group is thought to coordinate to SnOct<sub>2</sub>, forming the initiating tin-complex. The SnOct<sub>2</sub> catalyst is a strong transesterification agent, and resulting copolymers normally have a randomized microstructure.<sup>[38]</sup> An increase in reaction temperature or reaction time increases the amount of transesterification reactions.

Investigations of the coordination-insertion mechanism have resulted in two slightly different reaction pathways. Kricheldorf and coworkers have proposed a mechanism<sup>[11]</sup> where the coinitiating alcohol functionality and the monomer are both coordinated to the SnOct<sub>2</sub>-complex during propagation. Penczek and coworkers have presented a mechanism<sup>[52]</sup> where the SnOct<sub>2</sub>-complex is converted into a tin-alkoxide before complexing and ring-opening of the monomer. Scheme 2.3.3 shows the two different proposals.



**Scheme 2.3.3** The main ring-opening polymerization mechanism proposals with stannous(II) 2-ethylhexanoate as catalyst, a) complexation of a monomer and alcohol prior to ROP b) formation of a tin-alkoxide before ROP of  $\epsilon$ -caprolactone.

The ROP of lactide with  $\text{SnOct}_2$  is fairly slow and it is desirable for economic and commercial reasons to increase the rate of polymerization. The addition of an equimolar amount of triphenyl phosphine improves the rate and as an additional advantage this compound delays the occurrence of the undesirable back-biting reactions.<sup>[54]</sup>

### 2.3.2 Aluminum tri-isopropoxide

ROP initiated with aluminum tri-isopropoxide has been investigated extensively by several research groups,<sup>[39,42,55,56,57,58,59]</sup> since it yields well-defined polymers through living polymerization.<sup>[60,61]</sup> A living polymerization is a chain polymerization which proceeds in the absence of the kinetic steps of termination or chain transfer.<sup>[60]</sup>

Polymerization with aluminum tri-isopropoxide is assumed to proceed through a coordination-insertion mechanism, which consists of monomer complexation to the active species, and then insertion by rearrangement of the covalent bonds. The mechanism leads to cleavage of the acyl-oxygen bond of the monomer and the metal-oxygen bond of the propagating species. The propagation is characterized by the almost total absence of side-reactions such as transesterification reactions, at least until complete monomer

conversion has occurred.<sup>[62,63,64]</sup> Some results indicate that transesterification reactions may take place during the polymerization of L-LA.<sup>[64]</sup> However, the main rearrangement of the polymer occurs when the monomers are completely consumed. The initiator is active at low temperatures (reaction temperatures of 0-25°C are often reported) and the initiator is preferentially used in solution polymerization.

Most metal alkoxides are aggregated in solution and, as a result, an induction period during which the initiator is rearranged to form the active species often characterizes the polymerization. Only a few of the M-OR bonds are not involved in coordination to the metal atom and can consequently behave as initiation centers. The type and size of the aggregates depend on the solvent polarity, the nature of the substituents, and the presence of coordinative ligands such as amines<sup>[65]</sup> and alcohols.<sup>[66,67]</sup> The groups involved in coordinative aggregation are not active in propagation. Significant advances in the understanding of the “coordination-insertion” ROP mechanism have been made through the kinetic studies by Duda and Penczek.<sup>[10,39,65,66]</sup>

Recently, systems have been developed where the aluminum alkoxide is covalently bonded to solid porous silica.<sup>[68]</sup> This system takes advantage of the exchange reaction between the alkoxide and the hydroxyl-terminated free molecules to produce a catalytic process, *i.e.* to produce a larger number of polymer chains than aluminum complexes present. The initiator/catalyst used can easily be recovered by filtration and recycled. In addition, the polymers obtained are free from metal residues.

### 2.3.3 Tin-alkoxides

Mono-tin-alkoxides, tin-dialkoxides and cyclic tin-alkoxides have been utilized as initiators in the ring-opening polymerization of cyclic esters. The tin-alkoxides are known to form cyclics during synthesis and the dibutyl tin-alkoxides are known to exist as monomers and dimers.<sup>[69]</sup> The cyclic tin-alkoxides were originally studied because of their resistance towards hydrolysis.<sup>[70]</sup>

The tributyl derivatives have been thoroughly studied since they are easily synthesized by nucleophilic substitution of commercial tributyl tin chloride, and they are easy to handle due to their moisture resistance and they are relatively soluble in lactones.<sup>[71]</sup> The tin-alkoxides have been reported to be an effective transesterification catalyst initiating polymerization at moderate temperatures.<sup>[72]</sup>

The polymerization of lactones with tin-alkoxides is thought to follow the coordination-insertion mechanism. The ring-opening of the monomer

proceeds through acyl-oxygen cleavage with retention of the configuration. Tin(IV) complexes have been used to produce predominantly syndiotactic poly( $\beta$ -hydroxybutyrate),<sup>[73,74]</sup> macrocyclic poly( $\beta$ -hydroxybutyrate),<sup>[75]</sup> poly( $\epsilon$ -caprolactone) and polylactide.<sup>[71,72]</sup>

### 2.3.4 Lanthanide alkoxides

Ring-opening polymerization of lactones and lactides using lanthanide alkoxide based initiators is a relatively recent discovery. The first example of lactone polymerization by lanthanide alkoxide complexes was reported in a DuPont patent written by McLain and Drysdale in 1991.<sup>[76]</sup> In general, the activity of these catalysts is much higher than that determined for aluminum alkoxides, especially in lactide polymerization.<sup>[77,78,79]</sup> Polymers of relatively high molecular weight and narrow MWD are formed. The negative side reactions such as macrocycle formation, transesterification and racemization are absent.

Yttrium isopropoxide and yttrium 3-oxapentoxide initiators were the first lanthanide alkoxides described in the literature for the ROP of  $\epsilon$ -CL.<sup>[80]</sup> The discovery of lanthanide-based initiator systems allowed the block copolymerization of  $\epsilon$ -caprolactone with compounds such as ethylene,<sup>[81]</sup> tetrahydrofuran,<sup>[82]</sup> L-lactide,<sup>[83]</sup> trimethylene carbonate<sup>[84]</sup> and methyl methacrylate.<sup>[85]</sup> This type of initiator has also been used to prepare poly( $\beta$ -butyrolactone)s.<sup>[86,87]</sup>

## 2.4 Macromolecular architecture

Many recent advances in polymer synthesis have involved the development of new controlled polymerization systems proceeding via a variety of mechanistic types. A number of architectures may be produced as a result of the great versatility of the ROP of cyclic esters. Different strategies have been applied for the design of new polymeric materials.

### 2.4.1 Homopolymers

Several factors are known to affect the ring-opening polymerization of cyclic esters. The main factors are the reaction conditions, *i.e.* the nature of the initiator, type of solvent, reaction temperature, and also the ring size of the monomer used, and the substituents on the monomer ring.<sup>[88,89,90]</sup> Cyclic esters of four, seven and eight membered rings polymerize, whereas the five-membered ester does not. In the case of six-membered rings, the polymerizability depends on the substituents.<sup>[88]</sup>

## 2.4.2 Block copolymers

Block copolymerization is one method of mixing chemically different polymers. The block copolymers have received much attention, since the different homopolymer properties are maintained in the block copolymer, and this allows easy modification of the polymer characteristics.

Block copolymers are most readily prepared by the sequential addition of monomers to systems polymerizing under living conditions. However, this approach is of limited importance since the monomers involved must all be capable of polymerizing by the selected propagating mechanism. The order of monomer addition must be such that the macroinitiator generated by the preceding monomer must be capable of rapidly initiating the polymerization of the succeeding monomer. The last condition limits the combination of monomers which can be used in block copolymerization. Figure 2.4.1 shows a schematic presentation of a tri-block copolymer.

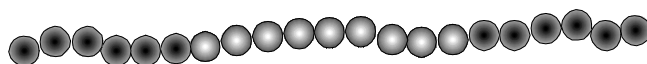


**Figure 2.4.1** A schematic presentation of an ABA tri-block copolymer with two A-blocks (●) and one B-block (○).

The preparation of prepolymers<sup>[91]</sup> or macromers with functional end-groups, so called telechelic polymers, is another approach to structurally unconventional architecture. The functional end-groups are introduced either by functional initiation or end-capping of living polymers, or by a combination of the two. In this way, monomers which not able to copolymerize can be incorporated in a copolymer. Telechelic prepolymers can be linked together using chain extenders such as diisocyanates.<sup>[92]</sup> In this process, it is essential that the structure and end groups of the prepolymers can be quantitatively and qualitatively controlled.<sup>[93]</sup>

One simple way of producing segmented (blocky) copolymers is reactive extrusion.<sup>[94]</sup> If two homopolymers are mixed and the mixture is subjected to high temperature, intermolecular transesterification reactions produce a block structure. If only a limited amount of transesterification reactions are allowed to take place, a block-type copolymer will form.

Thermoplastic tri-block copolymers are interesting since they possess novel properties different from those of the homo- or copolymers. The thermoplastic elastomers have many of the physical properties of rubbers, *i.e.* softness, resilience and flexibility. The unique properties of this kind of copolymer are due to the microphase separation of the hard crystalline domains dispersed in a continuous amorphous matrix (Figure 2.4.2). Such

phase morphology provides a physical network of flexible chains cross-linked by crystalline microdomains. The advantage over natural vulcanized rubbers are that thermoplastic elastomers are readily soluble in an appropriate solvent and processed as thermoplastics.<sup>[95]</sup>

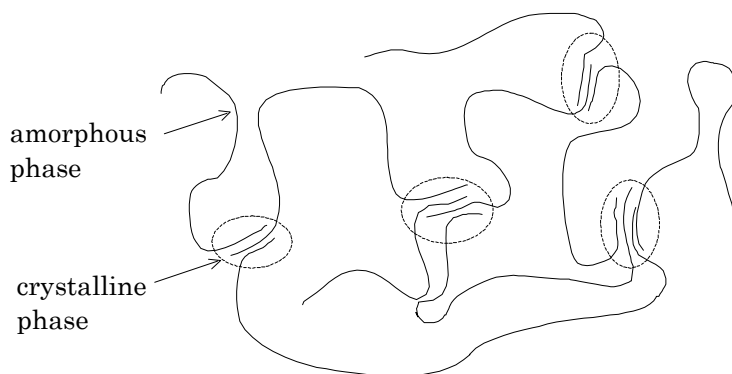


**Figure 2.4.2** Schematized picture of a block copolymer with one hard-phase-forming block and one soft-phase-forming block, giving rise to phase separation.

### 2.4.3 Star-shaped (co)polymers

Macromolecular structures such as star copolymers have been synthesized in the search for polymers with new mechanical and thermal properties and a varied degradation profile. Figure 2.4.3 shows a schematic representation of four-armed homo- and block copolymers.

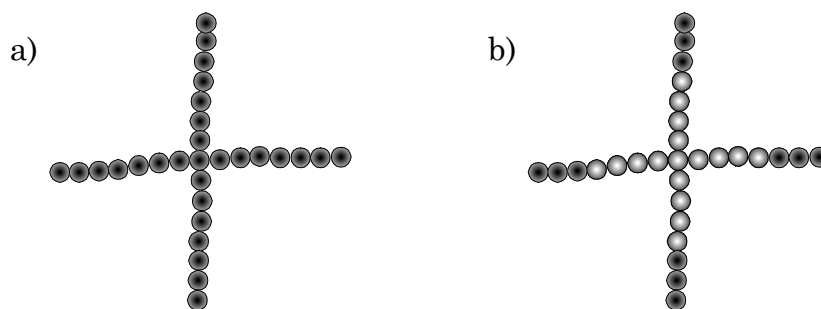


**Figure 2.4.3** Schematic representation of a four-armed star-shaped homopolymer b) star-shaped block copolymer.

Star-shaped polymers can be prepared by using a multifunctional initiator *e.g.* pentaerytritol and a catalyst which initiates ROP of the selected monomer. A second approach is to use telechelic prepolymers that are linked together after polymerization.

Aliphatic star-shaped polyesters of L-lactide have been synthesized<sup>[96,97]</sup> with multifunctional hydroxyl compounds as initiators. The crystallinity of



the star-shaped poly(L-lactide) was found to be higher than that of the corresponding linear counterpart. The degradation rate at the later stages of degradation was also faster, which was explained by the higher concentration of chain ends facilitating auto-catalysis. Star-shaped poly(L-LA) has also been block copolymerized with trimethylene carbonate /  $\epsilon$ -caprolactone.<sup>[98]</sup> This resulted in a less brittle and considerably toughened material.

The unique thermal and solution properties of star-shaped block copolymers of poly(ethylene oxide)-poly( $\epsilon$ -caprolactone) and poly(ethylene oxide)-poly(L-LA) have been studied.<sup>[99]</sup> The results, *e.g.* lower crystallinity and lower swelling with increasing degree of branching, may be used to influence the formulation, drug loading and *in vivo* fate of drug and polymers in drug delivery applications.

## 2.5 Biodegradable polymers

Biodegradable polymers are receiving increasing attention for their use in a wide variety of surgical and pharmaceutical applications<sup>[100]</sup> as well as in disposable packages.<sup>[101]</sup> Novel synthetic polymer materials may provide considerable improvement in medical applications due to their tailored thermal and mechanical properties and their decomposition to non-toxic products. Among various families of biodegradable polymers, aliphatic polyesters have a leading position since hydrolytic and/or enzymatic chain cleavage yields hydroxy carboxylic acids, which in most cases are ultimately metabolized.<sup>[100,102,103]</sup> Typical examples of synthetic, biodegradable polymers used in medical applications are polylactide,<sup>[102]</sup> polyglycolide,<sup>[104]</sup> and poly( $\epsilon$ -caprolactone).<sup>[105]</sup> The key properties, *e.g.* the rate of degradation, tensile properties and surface chemical composition, can be optimized by copolymerization<sup>[106]</sup> or blending of homo- and/or copolymers.

### 2.5.1 Polymer degradation

There are two principal ways by which polymer chains can be hydrolyzed, passively by chemical hydrolysis or actively by enzymatic reaction. The latter is most important for naturally occurring polymers such as polysaccharides and poly(hydroxy alkanoate)s *e.g.* polyhydroxybutyrate and polyhydroxyvalerate.<sup>[103,107]</sup> Many synthetic aliphatic polyesters utilized in medical applications degrade mainly by pure hydrolysis.<sup>[103]</sup>

There are several factors that influence the rate of degradation including the type of chemical bond in the polymer back-bone, hydrophilicity, molecular weight, crystallinity, copolymer composition, and the presence of low molecular weight compounds.<sup>[108,109]</sup> Other concerns are related to the loss of mechanical stability of polymers during degradation, which can be

undesirable when it is too fast, or to the toxicity of high concentrations of degradation products. Many biodegradable polymers contain some kind of hydrolyzable bonds. Polymers containing anhydride<sup>[110]</sup> or ortho-ester<sup>[111]</sup> bonds are the most reactive ones with a fast rate of degradation, ester bonds degrade somewhat more slowly, and carbonates<sup>[112]</sup> are almost totally resistant to hydrolysis.

### 2.5.2 Polyglycolide and copolymers

Polyglycolide was one of the first synthetic polymers used as a degradable surgical suture.<sup>[104]</sup> Figure 2.5.1 shows the glycolide monomer and polymer structure. This aliphatic polyester is biodegradable and exhibits negligible toxicity when implanted in tissue. It is also possible to fabricate a strong fiber of this polyester with satisfactory mechanical properties.

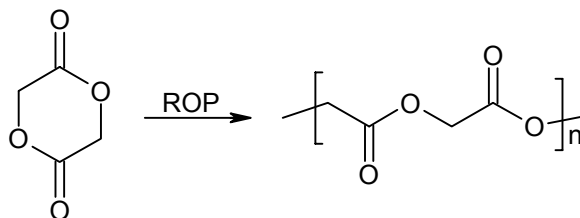


**Figure 2.5.1** The chemical structure of glycolide and the resulting repeating unit.

The polyester of glycolide has a melting point around 219°C and is difficult to dissolve in most organic solvents. In order to produce materials suitable for specific medical applications, glycolide has been copolymerized with a number of monomers.<sup>[113]</sup>

### 2.5.3 Polylactide and copolymers

Due to the presence of two chiral centers, there are three forms of the lactide monomer (Figure 2.5.2). Repeating units with different configurations have been used to produce stereocopolymers where the physical and mechanical properties and the rate of degradation are easily adjusted.

The most efficient way of preparing polylactides is the ring-opening polymerization by coordination initiators.<sup>[114]</sup> This method usually allows a controlled synthesis leading to quite a narrow molecular weight distribution. Polymerization of the different stereofoms results in materials with different properties. The polymers derived from the pure L,L-lactide or D,D-lactide monomers are semi-crystalline, relatively hard materials with melting temperatures around 184°C<sup>[115]</sup> and glass transition temperatures of about 55°C.<sup>[116]</sup> The L,L-lactide and D,D-lactide are normally termed L-lactide and D-

lactide, respectively. Polymerization of the *rac*-(D,L)-lactide and meso-lactide results in an amorphous material with a glass transition similar to that of the semi-crystalline counterparts.<sup>[115]</sup> Polylactides are highly sensitive to heat, especially at temperatures higher than 190°C. Heating these materials above this temperature results in a noticeable decrease in weight-average molecular weight.<sup>[115]</sup>

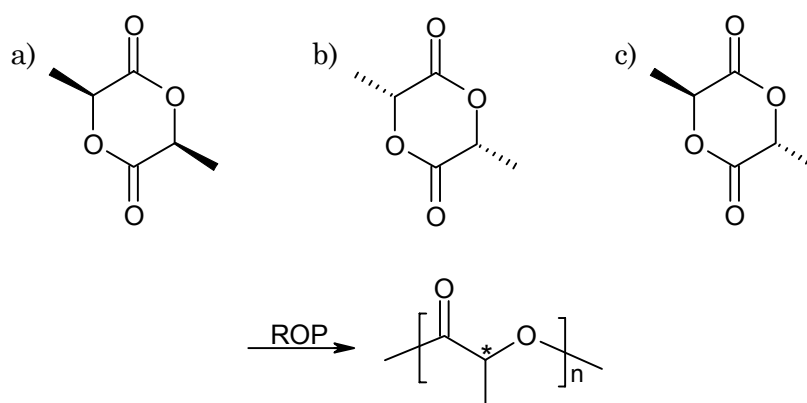


**Figure 2.5.2** Structure of the different stereofoms of the lactide monomer and the resulting repeating unit, the chiral center marked with \*. a) L,L-lactide, b) D,D-lactide, and c) meso-lactide

Poly(L-lactide) is biocompatible and when it is implanted in the body, it will in the course of time undergo hydrolytic scission to lactic acid, which is a natural intermediate in carbohydrate metabolism.<sup>[102]</sup> The *in vitro* degradation of poly(L-LA) is generally rather slow compared to the degradation of poly(D,L-LA). The higher degradability is probably due to the greater water absorption in the amorphous domains. Copolymers of L-lactide with several types of monomers *e.g.* glycolide, or  $\epsilon$ -CL have been investigated.<sup>[113]</sup> Copolymerization is an important tool to modify the properties of the resulting copolymers and adjust them to the needs of a given application.

The crystallinity, brittleness and melting point of poly(L-LA) can be decreased by incorporation of comonomer units such as 1,5-dioxepan-2-one (DXO). The large difference in reactivity ratio between the DXO and the lactides leads to a microstructure with a more blocky nature than is expected from a random copolymerization.<sup>[50]</sup> The copolymers have properties very different from those of the homopolymers. They show a low stiffness and high elasticity compared to poly(L-LA). The DXO/LA copolymers are interesting materials with possible applications in *e.g.* the biomedical field.<sup>[117]</sup> The *in vitro* / *in vivo* degradation has been studied and it was found that the copolymer hydrolyzed mainly by ester bond cleavage.<sup>[118,119]</sup>

## 2.5.4 Poly( $\epsilon$ -caprolactone) and copolymers

Poly( $\epsilon$ -caprolactone) has been investigated thoroughly because of the possibility of blending this aliphatic polyester with a number of commercial polymers such as PVC and bisphenol A polycarbonate.<sup>[17]</sup> It is interesting as a packaging material and in biomedical applications due to its degradability to non-toxic degradation products. Figure 2.5.3 shows the monomer structure and the resulting repeating unit.

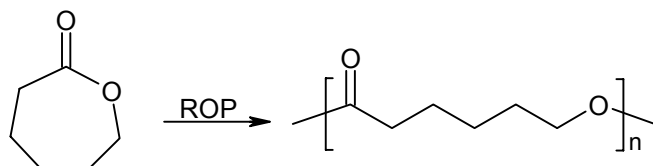


**Figure 2.5.3** The chemical structure of  $\epsilon$ -caprolactone and the resulting repeating unit.

The poly( $\epsilon$ -caprolactone) material has a long degradation time, which is usually a disadvantage in medical applications. The *in vivo* degradation of poly(D,L-lactide) was 2.8 times faster than the poly( $\epsilon$ -caprolactone) chain cleavage under the same conditions.<sup>[106]</sup> Different approaches have been used to copolymerize  $\epsilon$ -caprolactone to increase the degradation rate. Copolymers of  $\epsilon$ -caprolactone and D,L-lactide of all compositions degraded much more rapidly than their component homopolymers.<sup>[106]</sup> This observation has been attributed to morphological differences, specifically a reduction in crystallinity and a lowering of the glass transition temperature.

Random copolymers of  $\epsilon$ -caprolactone with 1,5-dioxepan-2-one (DXO) have been investigated.<sup>[51,120,121]</sup> The copolymers were crystalline up to a DXO content of 40%, and it was concluded that the DXO units were incorporated into the poly( $\epsilon$ -caprolactone) crystals. The block copolymerization has also been investigated and the resulting material was shown to exhibit thermoplastic elastomeric properties.<sup>[58]</sup>

## 3 SYNTHESIS

### 3.1 Materials

Dibutyltin oxide (Aldrich Chemie, Germany) and ethylene glycol (Merck, Germany) were obtained commercially and were used as received. Toluene (Merck, Germany) was dried over Na-wire before use. Dichloromethane (KEBO Lab, Sweden) and chloroform, HPLC-grade (Merck, Germany) were dried by stirring over CaH<sub>2</sub> for 24 h prior to distillation under an inert atmosphere. Anhydrous chloroform (Aldrich, Germany) and anhydrous 1,2-dichloroethane (Aldrich, Germany) were used without further purification. Ethylene glycol (Aldrich, Germany) and *m*-chloroperoxybenzoic acid (ACROS, Belgium) were used as received. 4H-tetrahydropyran-4-one (Maybridge Chemical Co. Ltd., UK) was used as received.

### 3.2 Initiator

#### 3.2.1 1,1,6,6-tetra-*n*-butyl-1,6-distanna-2,5,7,10-tetraoxacyclodecane

The 1,1,6,6-tetra-*n*-butyl-1,6-distanna-2,5,7,10-tetraoxacyclodecane was synthesized as follows. Dibutyltin oxide and ethylene glycol were weighed into a round-bottomed flask containing dry toluene. The reaction vessel was heated to 135°C and the slurry was refluxed for 22 h. After the complete reaction, the theoretical amount of water had been collected in a Dean & Stark trap. The slurry was then cooled in a refrigerator, the product was precipitated as white crystals and the solvent was poured off. The precipitate was first purified by recrystallisation twice from dry toluene, and then by filtration from a hot slurry. The tin-alkoxide was dried at 130°C under vacuum for 14 h. The melting point of the final product was 222-226°C (litt. 223-226°C).<sup>[122]</sup> The initiator was characterized by mass spectroscopy and <sup>1</sup>H-NMR. The <sup>1</sup>H-NMR-spectrum of the initiator in CDCl<sub>3</sub> showed two triplets at 3.65 and 1.9 ppm and two multiplets at 1.35 and 1.4 ppm, in agreement with the expected structure. The mass spectrum of the tin-alkoxide shows a peak

at  $m/z = 293$  corresponding to the cyclic five membered ring but also at higher values due to fragmentation of the dimer.

### 3.3 Monomers

#### 3.3.1 L-lactide

L-lactide (L-LA) was purchased from Serva Feinbiochemica, Germany, and purified through recrystallization in toluene and dried under reduced pressure ( $10^{-2}$  mbar) overnight. Figure 3.3.1 shows the chemical structure of the L-LA monomer.

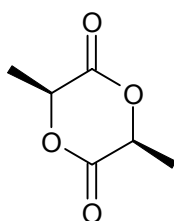


Figure 3.3.1 Chemical structure of L-lactide (L-LA)

#### 3.3.2 1,5-dioxepan-2-one

1,5-dioxepan-2-one<sup>[123]</sup> (DXO) was synthesized from 4H-tetrahydropyran-4-one according to the literature.<sup>[50]</sup> Before polymerization, DXO was purified by distillation twice and then dried over  $\text{CaH}_2$  in an inert atmosphere and distilled under reduced pressure. 120 g *m*-chloroperoxybenzoic acid was dissolved in dichloromethane, the aqueous phase was poured off and the organic solution was dried over magnesium sulfate. 36.6 g tetrahydro-4H-pyran-4-one was added dropwise to the filtered solution. After 16 h, the reaction mixture was added to a slurry containing 50 g sodium bisulfite and 400 mL dichloromethane. Sodium bicarbonate was added until no further gas evolution was detected. The organic phase was separated and the solvent was evaporated. Yield DXO: 38 g. Figure 3.3.2 shows the chemical structure of the DXO monomer.

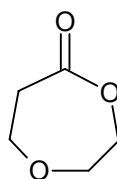


Figure 3.3.2 Chemical structure of 1,5-dioxepan-2-one (DXO)

## 3.4 Polymerization

### 3.4.1 Homopolymerization of DXO and L-lactide

Monomer and initiator were weighed into a previously silanized round-bottomed flask equipped with a magnetic stirring bar inside a dry box (MBraun MB 150B-G-I, Germany). The flask was closed with a three-way valve. The desired amount of solvent was transferred to the flask using a syringe. The reaction vessel was then immersed in the thermostated oil bath for the desired time. The temperature was held constant ( $\pm 1^\circ\text{C}$  of preset value) using an Ikatron ETS D3 temperature-regulator (IKA Labortechnik, Germany).  $^1\text{H-NMR}$  and SEC samples, for the kinetic investigation, were withdrawn from the reaction mixture at various times with a flamed syringe under flushing with an inert gas (Ar). After removing the solvent, the monomer conversion was determined by  $^1\text{H-NMR}$  from monomer and polymer signals. The polymer formed was precipitated into cold hexane. All glassware were silanized, using  $\text{Me}_2\text{Cl}_2\text{Si}$ , and flame-dried in an inert atmosphere before use.

### 3.4.2 Block copolymerization of 1,5-dioxepan-2-one and L-lactide

The desired amounts of DXO and initiator were weighed into a silanized round-bottomed flask under a nitrogen atmosphere inside a dry box. The flask was fitted with a magnetic stirring bar and sealed with a three-way valve. Solvent was transferred to the flask using a syringe. Polymerization was started by immersing the flask in a thermostated oil bath. The second monomer, L-lactide, was charged into a round-bottomed flask, as described above. The monomer was dissolved in chloroform and transferred with a syringe to the reaction vessel containing the initiator-polymer complex after almost complete conversion of DXO. All glassware was flame-dried prior to use. The polymer formed was precipitated three times in a mixture consisting of hexane and methanol (95/5).





## 4 CHARACTERIZATION

### 4.1 Hydrolytic Degradation

#### 4.1.1 Sample Preparation

For degradation studies, films were prepared as follows: Dichloromethane solutions of different tri-block poly(L-lactide-*b*-1,5-dioxepan-2-one-*b*-L-lactide)s were prepared to have a total polymer concentration of 0.16 g/ml and cast onto flat glass plates followed by solvent evaporation at room temperature. The resulting films were dried *in vacuo* for 2 weeks. Circular plates 12 mm in diameter and weighing approximately 0.02 g were obtained from the solution-cast films.

#### 4.1.2 *In vitro* degradation of the poly(L-lactide-*b*-1,5-dioxepan-2-one-*b*-L-lactide) tri-block copolymers.

Samples were subjected to hydrolytic degradation in a saline buffer of pH 7.4 at 37°C. The saline buffer contained per liter of water the following: 9 g NaCl, 10.73 g Na<sub>2</sub>HPO<sub>4</sub>×7H<sub>2</sub>O, 2.12 g NaH<sub>2</sub>PO<sub>4</sub>. The pH of the buffer solution was adjusted to pH 7.4 by the addition of NaOH. The degradation experiments were performed in 10 ml of the saline solution. In order to prevent microbial growth, 100 µl 0.04 weight % NaN<sub>3</sub> was added to the solution. The samples were subjected to a gentle shaking motion during hydrolysis to achieve a homogeneous solution. Samples were drawn from the test environment after 1, 2, 5, 10, 15 and 23 weeks of degradation. A 2 ml aliquot of the aqueous solution was withdrawn for analysis of the degradation products. The remaining polymer films were washed with deionized water before drying under vacuum for two weeks prior to analysis.

## 4.2 Instrumental Analysis

### 4.2.1 Mass Spectroscopy (MS)

The purity and structure of the initiator 1,1,6,6-tetra-*n*-butyl-1,6-distanna-2,5,7,10-tetraoxacyclodecane were determined with a Finnigan SSQ 7000 mass-spectrometer using a direct inlet probe. The spectrometer temperature was held at 50°C for 0.5 minutes and was then raised to 300°C at a rate of 100°C/min. The mass spectrum of 1,1,6,6-tetra-*n*-butyl-1,6-distanna-2,5,7,10-tetraoxacyclodecane shows a peak at  $m/z = 293$  corresponding to the cyclic five-membered ring and also peaks at higher values matching the fragmentation of the dimer.

### 4.2.2 Nuclear Magnetic Resonance Spectroscopy (NMR)

Nuclear magnetic resonance spectroscopy (NMR) was used to analyze the reaction progress, the chemical composition of the polymers formed, the polymerization mechanism and the number-average molecular weight. The monomer conversion was determined by <sup>1</sup>H-NMR spectroscopy from the relative intensities of the resonance peaks for the monomer and the polymer protons. The chemical structure and the monomer sequence of the block copolymers were determined by <sup>13</sup>C-NMR spectroscopy. <sup>1</sup>H-NMR spectra were obtained using a Bruker AC-400 Fourier-Transform Nuclear Magnetic Resonance spectrometer (FT-NMR) operating at 400 MHz. A 25 mg sample was dissolved in 0.5 ml chloroform-*d*<sub>1</sub> (CDCl<sub>3</sub>) in a 5 mm diameter sample tube. Non-deuterated chloroform was used as an internal standard ( $\delta = 7.26$  ppm). The 100.61 MHz <sup>13</sup>C-NMR spectra were obtained with a 100 mg sample dissolved in 0.5 ml CDCl<sub>3</sub> using a Bruker AC-400 FT-NMR spectrometer. The number-average molecular weight was calculated from the <sup>1</sup>H-NMR spectra of the polymers. The peaks originating from the ethylene glycol bridge and the -CH- group in the poly(L-lactide) and -CH<sub>2</sub>- group next to the carbonyl carbon in the polyDXO unit respectively were used to calculate the molecular weight.

DEPT (Distortionless Enhancement by Polarization Transfer) and heteronuclear multiple quantum coherence – gradient selected (hmqc-gs) spectra were obtained by a Bruker DMX-500 Fourier-Transform Nuclear Magnetic Resonance spectrometer operating at 500.13 MHz and 125.77 MHz respectively. DEPT (135°) spectra were obtained using a standard Bruker microprogram utilizing 1.3 seconds acquisition time, and 2 seconds delay. <sup>1</sup>J(C,H) was set to 130 Hz. 2D <sup>1</sup>H-<sup>13</sup>C hmqc-gs spectra were acquired and processed with a standard Bruker microprogram. A total of 20 scans were accumulated with a relaxation delay of 2 s. The spectrum was obtained with

3255.2 Hz spectral width over the  $F_1$  (proton) axis and 24509.8 Hz along the  $F_2$  (carbon) axis.

The reaction progress was followed *in situ* by  $^1\text{H-NMR}$  utilizing the Bruker AC-400. The monomer and initiator were charged into a silanized round bottomed flask and closed by a rubber septum inside a dry-box. Deuterated solvent,  $\text{CDCl}_3$ ; was transferred through the septum with a syringe. The mixture was then transferred to a 5 mm NMR-tube equipped with a rubber septum, and subsequently frozen in liquid nitrogen to prevent any reaction from occurring before insertion into the NMR magnet. The tube was inserted into the heated probe and a  $^1\text{H-NMR}$  spectrum was recorded every 20 minute in order to follow the disappearance of peaks originating from monomer and occurrence of peaks from the polymer. A reaction temperature of  $50^\circ\text{C}$  in the NMR probe was used.

### 4.2.3 Size Exclusion Chromatography (SEC)

Size exclusion chromatography (SEC) was used to monitor the molecular weight change during polymerization and degradation. Spectra of homopolymers from 1,5-dioxepan-2-one were recorded with a Waters model 510 apparatus with a Waters 410 differential refractometer equipped with three PLgel  $10\mu\text{m}$  mixed-B columns,  $300\times 7.5$  mm (Polymer Labs.). An IBM-compatible PC was used to record and process the data. THF was used as eluent, at a flow rate of 1.0 ml/min. Narrow MWD polystyrene standards were used for calibration, range 1700 - 706 000 g/mol.

Tri-block copolymers from L-lactide and 1,5-dioxepan-2-one, and homopolymers of L-lactide were analyzed using a Waters 717plus autosampler and a Waters model 510 apparatus equipped with two PLgel  $10\mu\text{m}$  mixed-B columns,  $300\times 7.5$  mm (Polymer Labs., UK). Spectra were recorded with an PL-ELS 1000 evaporative light scattering detector (Polymer Labs., UK) connected to an IBM-compatible PC. Millennium<sup>32</sup> version 3.05.01 software was used to process the data. Chloroform was used as eluent, at a flow rate of 1.0 ml/min. Narrow MWD polystyrene standards were used for calibration, range 1700 – 706 000 g/mol. SEC measurements were performed on both cyclic and deactivated chains (*i.e.*, into hexane/methanol precipitated chains).

### 4.2.4 Differential Scanning Calorimetry (DSC)

The thermal properties of the synthesized tri-block copolymers were investigated by differential scanning calorimetry (DSC), using a Mettler-Toledo DSC instrument with a DSC 820 module. A scanning rate of  $10^\circ\text{C}/\text{min}$  was used and the samples were heated in a nitrogen atmosphere. Calibration

was performed with Zn and In. The second scan was used to record the heat of fusion and the glass transition temperature. In evaluating the crystallinity of the tri-block copolymer, it was assumed that the only contribution to the heat of fusion was from the poly(L-lactide) segments. According to earlier results obtained by DSC, poly(DXO) is totally amorphous having a  $T_g$  between  $-35$  and  $-40^\circ\text{C}$ .

#### 4.2.5 Solid Phase Extraction (SPE)

The following procedure was used for sample preparation and isolation of degradation products from the aqueous solutions: 2 ml of buffer solution containing degradation products was acidified to a pH of 1-2 with HCl, and 2 mg of the internal standard, 2-hydroxyvaleric acid sodium salt (Sigma, Germany) was added. A SPE ENV+ column (100 mg, Sorbent AB) was pre-washed with one equivalent of methanol (HPLC-grade, Kebo Lab AB), and then equilibrated with one equivalent of acidified buffer solution. The acidified sample solution was applied immediately after pre-washing and the column was then allowed to dry before elution with an organic solvent, acetonitrile (HPLC-grade, Kebo Lab, Sweden).

#### 4.2.6 Gas Chromatography – Mass Spectroscopy (GC-MS)

GC-MS was used in the identification and quantification of degradation products formed in the saline buffer solutions. The samples were analyzed utilizing a Finnigan GCQ gas chromatograph - mass spectrometer. The GC was equipped with a DB-5MS capillary column from J&W (30 m  $\times$  0.25 mm i.d.) Helium was used as carrier gas. The samples was analyzed utilizing the following temperature program of the column: the temperature was held at  $40^\circ\text{C}$  for 10 minutes and then allowed to rise from 40 to  $250^\circ\text{C}$  at a heating rate of  $10^\circ\text{C}/\text{min}$ . The injector maintained a temperature of  $200^\circ\text{C}$ .

#### 4.2.7 X-ray Diffraction Pattern Analysis

X-ray diffraction was used to investigate the influence of the chemical structure of the tri-block copolymers on the crystalline phase formed. Wide angle X-ray diffraction analysis was performed on a Philips generator PW 1830, nickel-filtered  $\text{CuK}\alpha$ -radiation ( $\lambda=1.542 \text{ \AA}$ ), with a Warhus camera. No change in the X-ray pattern of the polymers with different compositions was observed.

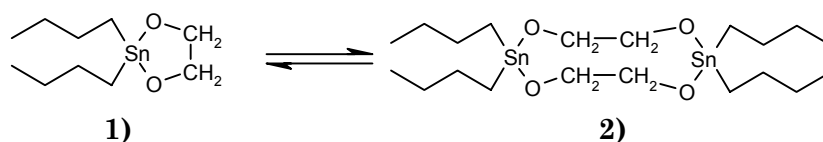
## 5 RESULTS AND DISCUSSION

### 5.1 Influence of reaction conditions on the homopolymerization of 1,5-dioxepan-2-one and L-lactide

The importance of the reaction conditions was examined for the homopolymerization of 1,5-dioxepan-2-one (DXO) and L-lactide (L-LA) initiated with 1,1,6,6-tetra-*n*-butyl-1,6-distanna-2,5,7,10-tetraoxacyclodecane. The influence of monomer conversion, temperature, solvent and initiator concentration on the molecular weight, molecular weight distribution and rate of polymerization was investigated.

#### 5.1.1 Synthesis of 1,1,6,6-tetra-*n*-butyl-1,6-distanna-2,5,7,10-tetraoxacyclodecane

The initiator 1,1,6,6-tetra-*n*-butyl-1,6-distanna-2,5,7,10-tetra-oxacyclodecane was synthesized from dibutyltin oxide and ethylene glycol. After purification, the initiator formed was characterized by mass spectroscopy and <sup>1</sup>H-NMR. The structure of the tin-alkoxide has previously been thoroughly investigated by several research groups.<sup>[124,125,126]</sup> The analysis performed in this study revealed the existence of two tin-alkoxide compounds, a monomer and a dimer. Scheme 5.1.1 shows the equilibrium between the five-membered monomer and the 10-membered dimer of the tin-alkoxide.



**Scheme 5.1.1** Equilibrium between 1) the monomer and 2) the dimer of 1,1,6,6-tetra-*n*-butyl-1,6-distanna-2,5,7,10-tetraoxacyclodecane.

The direct inlet spectrum of the synthesized initiator is shown in figure 5.1.2, together with the mass spectra of the two compounds.

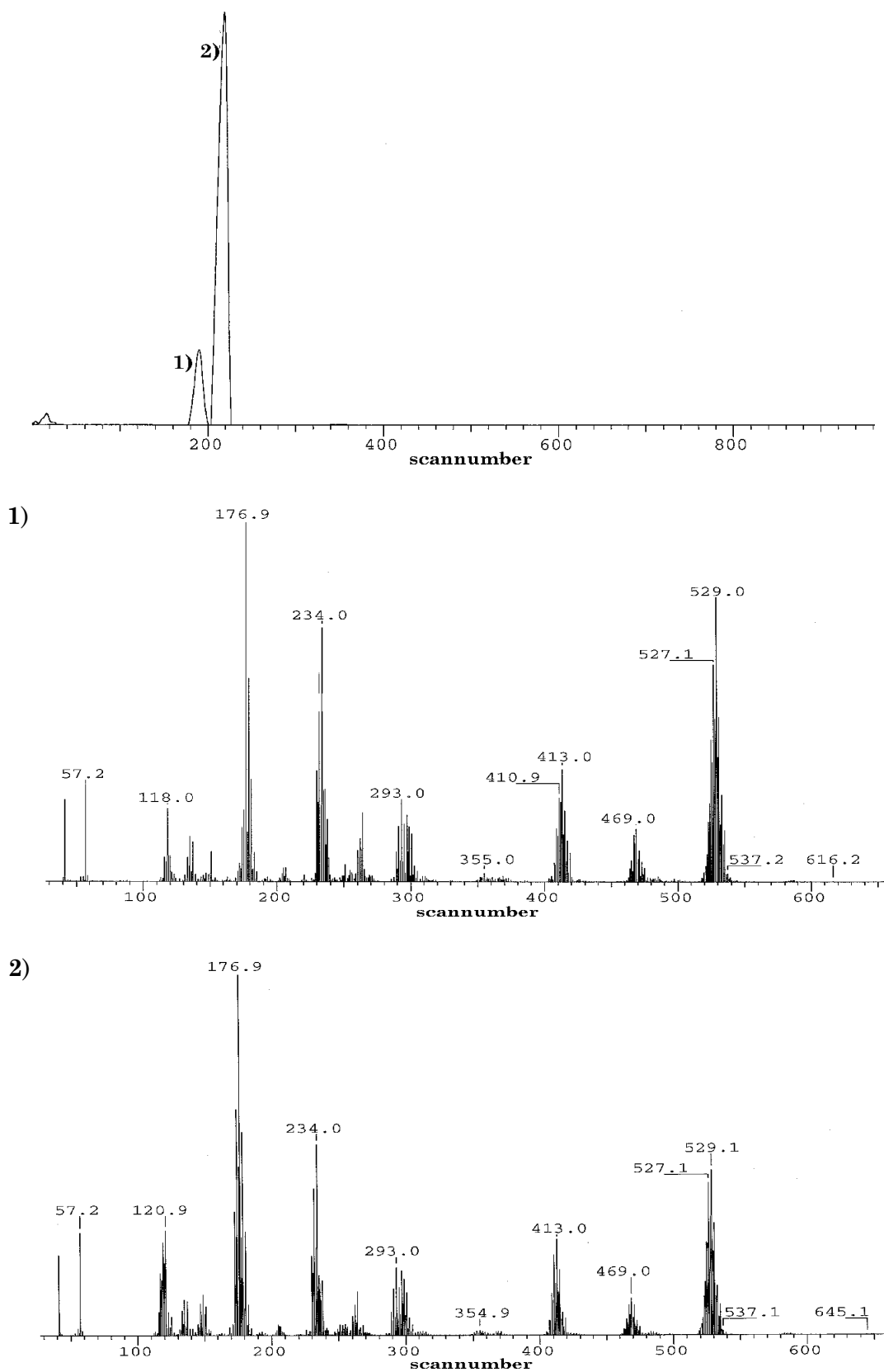


**Figure 5.1.1** The direct inlet spectrum of the monomer and dimer of the 1,1,6,6-tetra-*n*-butyl-1,6-distanna-2,5,7,10-tetraoxacyclodecane initiator. 1) mass spectrum of peak no. 1, and 2) mass spectrum of peak no. 2

The direct inlet spectrum of the initiator clearly shows the existence of two compounds with similar fragmentation patterns. The compounds have been identified as the monomer and dimeric form of the tin-alkoxide.

It has been suggested that the polymerization of lactones and lactides with the cyclic tin-alkoxide proceeds by insertion at the tin-oxygen bond. However, it has not been clarified whether one or both tin-oxygen bonds are active in polymerization. The polymerization of cyclic esters with the tin-alkoxide results in di-hydroxy terminated polymers, suitable for post-polymerization reactions.

### 5.1.2 Influence of the reaction temperature on the polyDXO molecular weight and molecular weight distribution

The influence of reaction temperature,  $T_p$ , on the number-average molecular weight ( $\bar{M}_n$ ) of the polymer formed was examined with SEC and  $^1\text{H-NMR}$ . Polymerizations were carried out at 30, 40, 50, and 60°C to a high monomer conversion. Propagation was terminated by quenching the reaction mixture and the solvent was subsequently evaporated. Polymerization was performed with a monomer-to-initiator ratio of 100. Figure 5.1.2 shows the number-average molecular weight as a function of the DXO monomer conversion.

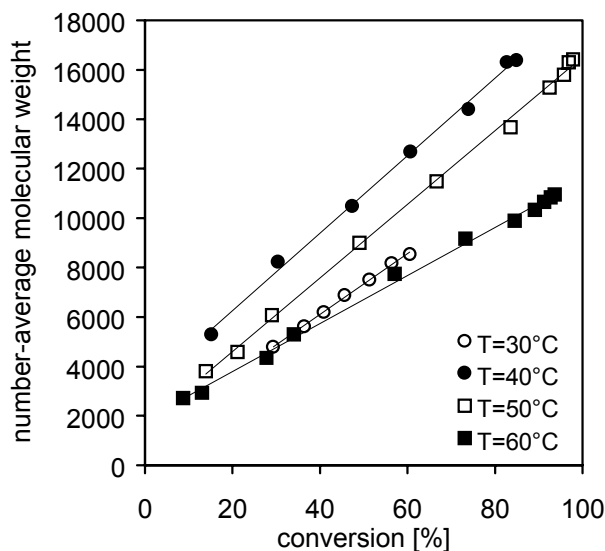


**Figure 5.1.2** The number-average molecular weight as a function of monomer conversion at different polymerization temperatures. Polymerization of DXO in chloroform with an initial monomer concentration of 1 mol/l.

As expected, the rate of polymerization was observed to increase with increasing polymerization temperature ( $T_p$ ). However, the figure shows that the  $\bar{M}_n$  of the polymer formed reached a maximum at a  $T_p$  of 40°C, and that

a further increase in  $T_p$  resulted in a decrease in molecular weight. A decrease in  $T_p$  to 30°C also yielded a polymer with a lower molecular weight. The lower  $\bar{M}_n$  at 30°C was a result of the long reaction times required at this temperature which induced transesterification reactions. At 50 and 60°C the polymerization was quantitative after a much shorter period of time, but the molecular weight obtained was lower. The decrease in  $\bar{M}_n$  at 50 and 60°C was also due to an increase in the amount of transesterification reactions, as an effect of the higher temperature.

The molecular weight distribution (MWD) was also monitored as a function of DXO monomer conversion at the different reaction temperatures. Figure 5.1.3 shows the MWD for the polymerizations performed. The increase in the amount of transesterification reactions at higher temperature was also indicated by the MWD. An increase in polymerization temperature resulted in a broader MWD at higher monomer conversion. The increase in MWD can be explained by the presence of intermolecular transesterification reactions. The decrease in  $\bar{M}_n$  indicates that an intramolecular process also occurs, leading to lower molecular weight cyclic compounds. This has previously been shown to occur for the polymerization of lactide with aluminum isopropoxide.<sup>[62]</sup>

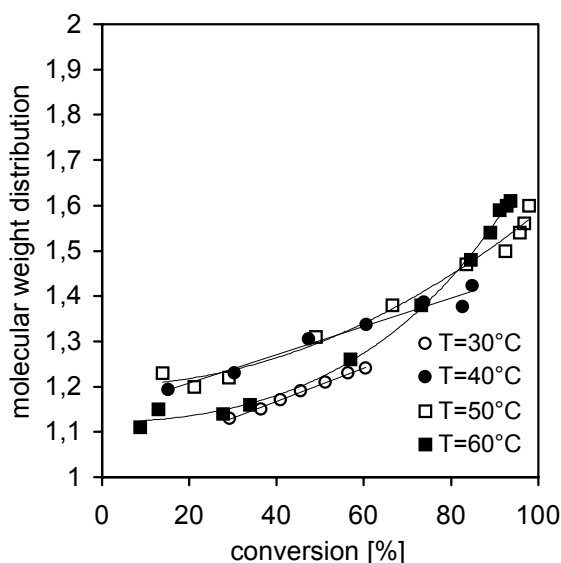


**Figure 5.1.3** The effect of temperature on the molecular weight distribution as a function of monomer conversion. Polymerization of DXO was conducted with an initial monomer concentration of 1 mol/l.

The limiting factor determining the lowest possible polymerization temperature was the rate of polymerization. At high temperatures, the limiting factor was the occurrence of transesterification reactions. An optimized reaction temperature was found at 40°C for the polymerization of



the DXO, where the reaction rate was sufficient and the amount of side reactions was kept at a minimum.

The polymerization of DXO was characterized by an induction period, with the polymerization starting after approximately 70 minutes reaction. This behavior was proposed to be due to a rearrangement of the initiator, to form the actual initiating species. The induction period was influenced by the reaction temperature, a higher  $T_p$  resulted in a shorter induction period.

The rate of homopolymerization of L-LA was lower than the corresponding rate of homopolymerization of DXO. Therefore, the subsequent polymerization of L-LA was performed only at the highest reaction temperature of 60°C.

### 5.1.3 Dependence of poly(L-lactide) number-average molecular weight and molecular weight distribution on the degree of monomer conversion

The progress of the reaction was monitored by  $^1\text{H-NMR}$  and SEC. The analyses were performed on the crude reaction mixture to avoid artifacts during *e.g.* fractionation of the samples during precipitation. Figure 5.1.4 shows the number-average molecular weight and molecular weight distribution of the poly(L-LA) as a function of the monomer conversion. The figure shows that the  $\bar{M}_n$  increased linearly with increasing conversion and that the MWD remained narrow throughout the polymerization reaction.

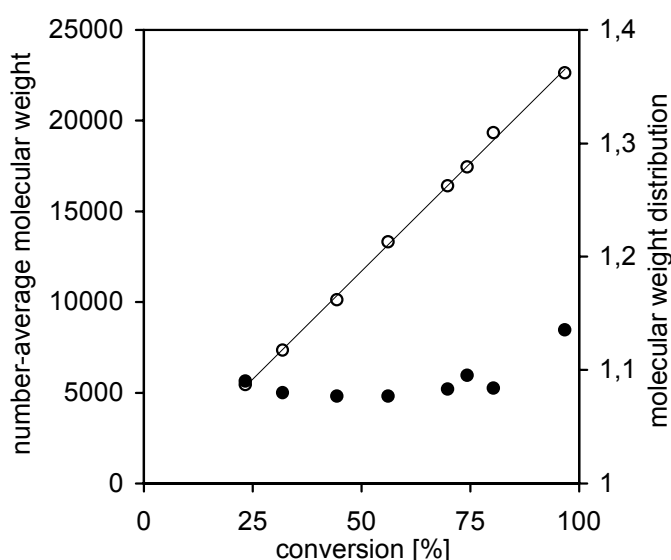


**Figure 5.1.4** The influence of L-LA monomer conversion on the number-average molecular weight (○) and the molecular weight distribution (●). Polymerization conducted at 60°C with an initial monomer-to-initiator ratio = 100

The linearity of the plot of number-average molecular weight versus conversion indicates that the amount transfer reactions was low throughout the reaction. The increase in molecular weight was proportional to the degree of monomer conversion. Under these specific conditions and by withdrawing the product as soon as the polymerization came to completion, a well-defined polymer with a narrow molecular weight distribution was obtained.

No induction period was observed during polymerization of L-lactide, contrary to what has been reported for many other metal alkoxide initiator systems.<sup>[55]</sup>

#### 5.1.4 The effect of solvent on the rate of polymerization and the polyDXO molecular weight

The effect of the reaction medium on the polymerization was evaluated using dichloromethane, chloroform and 1,2-dichloroethane as solvents. These solvents have the dielectric constants,  $\epsilon = 10.4$ , 9, and 4.8 D respectively. Chlorinated solvents were used exclusively to minimize the difference in the ability of the solvent to coordinate to the active species. Figure 5.1.5 shows the semi-logarithmic plot of  $-\ln([M]/[M]_0)$  as a function of the reaction time.

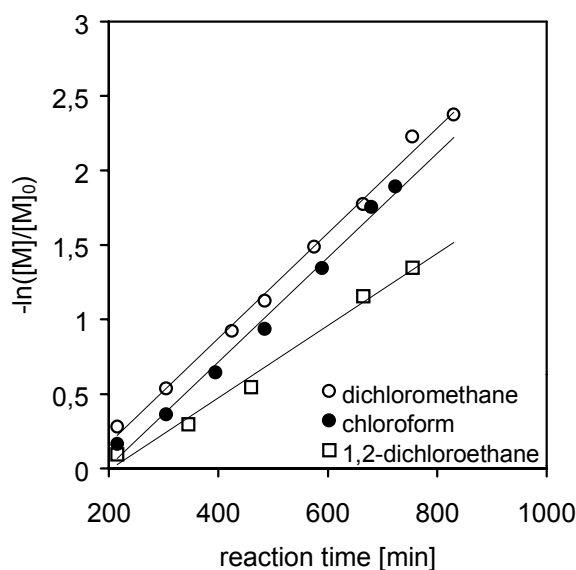


**Figure 5.1.5** The influence of solvent on  $-\ln([M]/[M]_0)$  as a function of reaction time. Polymerization conducted with an initial monomer concentration of 1 mol/l at a reaction temperature of 40°C.

The figure shows that the apparent rate of polymerization was similar in the different chlorinated solvents. A slightly lower rate of polymerization was found in 1,2-dichloroethane probably due to lower miscibility of the initiator in this solvent. The low solubility of the initiator resulted at first in a non-

transparent reaction medium, which became clear after a few minutes of polymerization. The data summarized in Table 5.1.1 indicate that the propagation of cyclic esters probably proceeds with a coordinative character.

**Table 5.1.1** Influence of solvent on the rate of 1,5-dioxepan-2-one polymerization initiated with 1,1,6,6-tetra-*n*-butyl-1,6-distanna-2,5,7,10-tetraoxacyclododecane at 40°C.

solvent	$k_{app} \times 10^3$ [min <sup>-1</sup> ]	dielectric constant [D]
dichloromethane	3,5	10,4
chloroform	3,5	9
1,2-dichloroethane	2,5	4,8

The effect of the reaction medium on the number-average molecular weight of the polymer formed was evaluated. Figure 5.1.6 shows the number-average molecular weight as a function of the degree of monomer conversion.

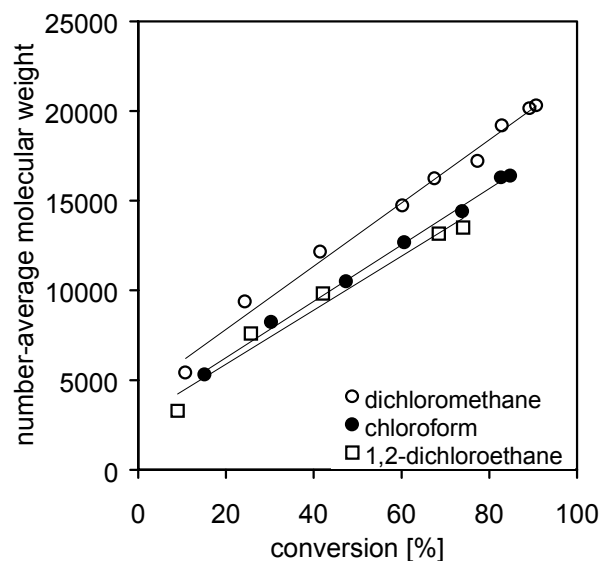


**Figure 5.1.6** The effect of the reaction medium on the number-average molecular weight of the polymer formed. Polymerization of DXO at 40°C with an initial monomer-to-initiator ratio = 100.

The polymers formed exhibited almost the same number-average molecular weight at the same monomer conversion. Results show that the change of solvent did not influence the number of chains produced by the initiator. The  $M_n$  was linearly dependent on the monomer conversion in all solvents.

### 5.1.5 Dependence of poly(L-LA) molecular weight on the monomer-to-initiator ratio

The number-average molecular weight of the polymers obtained was determined by  $^1\text{H-NMR}$ . The peaks originating from the ethylene glycol bridge ( $\delta = 4.35$  ppm) and the  $-\text{CH}-$  group in the polymer back-bone ( $\delta = 5.18$  ppm) was used to calculate the molecular weight. Molecular weights were also determined by SEC. The molecular weights calculated from  $^1\text{H-NMR}$  were systematically lower than those determined by SEC, but the order was the same. The SEC was calibrated with polystyrene standards, and the SEC results were therefore used as a quantitative tool to check the peak shape and molecular weight distribution. It has been reported that molecular weights determined by NMR analysis of the polylactides were lower than those determined by SEC.<sup>[93]</sup> The higher the molecular weight the larger was the difference between the results of these analyses. Figure 5.1.7 shows the linear relationship between the number-average molecular weight and the monomer-to-initiator.

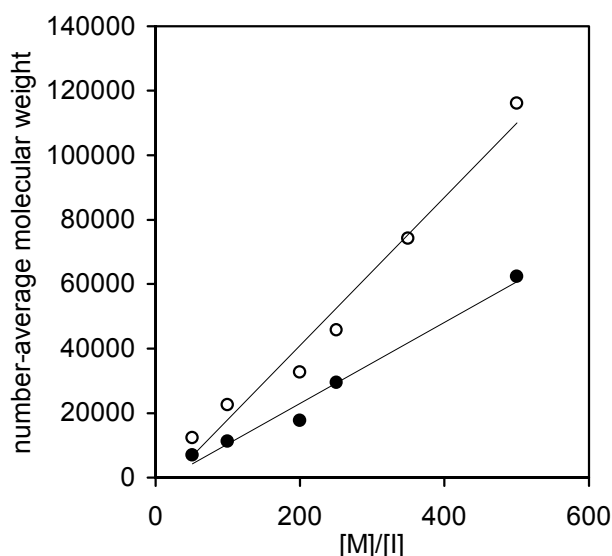


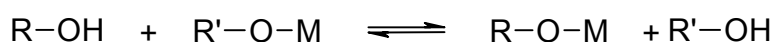
**Figure 5.1.7** The influence of monomer-to-initiator ratio on the number-average molecular weight: Molecular weight determined by  $^1\text{H-NMR}$  (●) and SEC (○). Polymerization of L-lactide in chloroform at  $60^\circ\text{C}$ .

A good correlation was observed between the molecular weight values theoretically expected from the monomer-to-initiator ratio and the values obtained experimentally. The linear relationship held even for both low and high molecular weight poly(L-lactide)s, contrary to what has been reported for the bulk polymerization.<sup>[126]</sup>

The linear relationship indicated that the total number of polymer chains was a function of the initiator concentration. It was also observed that the increase in molecular weight was proportional to the increase in monomer-to-initiator ratio. It can be deduced from the slope of the straight-line relationship between  $\overline{M}_n$  and the monomer-to-initiator ratio that one initiator moiety initiates only one polyester chain.

### 5.1.6 Influence of hydroxyl-functionality-containing contaminants on the molecular weight and molecular weight distribution

It is important to investigate the effect of hydroxyl-containing species due to the large influence which traces of such compounds normally have on the ring-opening polymerization with metal alkoxide initiators. It has been reported that free hydroxyl compounds interchange with alkoxide groups covalently bonded to the metal alkoxide initiators (Scheme 5.1.2).<sup>[66,127]</sup> The free hydroxyl-terminated species are exchanged giving an increase in the total number of polymer chains formed.



**Scheme 5.1.2** Exchange of alkoxide ligands covalently attached to the metal atom in the initiator.

Table 5.1.2 shows the results of the homopolymerization of L-LA and DXO with and without the addition of water.

**Table 5.1.2.** The influence of water on the outcome of polymerization.

Monomer	Amount H <sub>2</sub> O <sup>a)</sup>	reaction time [min]	conversion <sup>b)</sup> [%]	yield [%]	M <sub>n</sub> <sup>c)</sup>	MWD <sup>c)</sup>
L-LA	-	1440	93,3	82,1	29400	1,12
L-LA	1 equiv.	1440	73,5	66,9	9700	1,15
DXO	-	360	90,3	79,1	29400	1,46
DXO	1 equiv.	360	91,7	49,4	10000	1,65

Polymerizations conducted in chloroform at 60°C, initial monomer concentration = 0.5M

<sup>a)</sup> compared to amount of Sn

<sup>b)</sup> determined by <sup>1</sup>H-NMR from crude reaction mixture

<sup>c)</sup> number-average molecular weight determined by SEC; CHCl<sub>3</sub> was used as eluent, flowrate 1.0ml/min

The deliberate contamination with water caused the molecular weight of the resulting polymer to decrease. The decrease in molecular weight was a

consequence of an increase in the total number of polymer chains formed when water was added, but the decrease was also partly due to a decrease in L-LA monomer conversion and to an increase in transesterification reactions for the DXO polymerization. These results show that avoiding contact with even traces of water is essential for the reproducibility of the polymerization.

### 5.1.7 Catalytic degradation

The literature reports the effective ring-closing depolymerization of  $\epsilon$ -caprolactone utilizing  $\text{Bu}_2\text{Sn}(\text{OMe})_2$  resulting in a mixture of cyclic oligomers.<sup>[128]</sup> In most cases, the depolymerization is undesirable but the concept has been investigated as a tool for recycling suitable polymers.<sup>[129]</sup> Parameters that influence the amount of transesterification are temperature, reaction time, and type of and concentration of catalyst or initiator.

In the case of 1,5-dioxepan-2-one, transesterification reactions occur if the polymer chains are left in contact with the active centers after polymerization. Any active center can give rise either to an insertion step or to a transfer reaction. Figure 5.1.8 shows the SEC chromatograms of the depolymerization reaction.

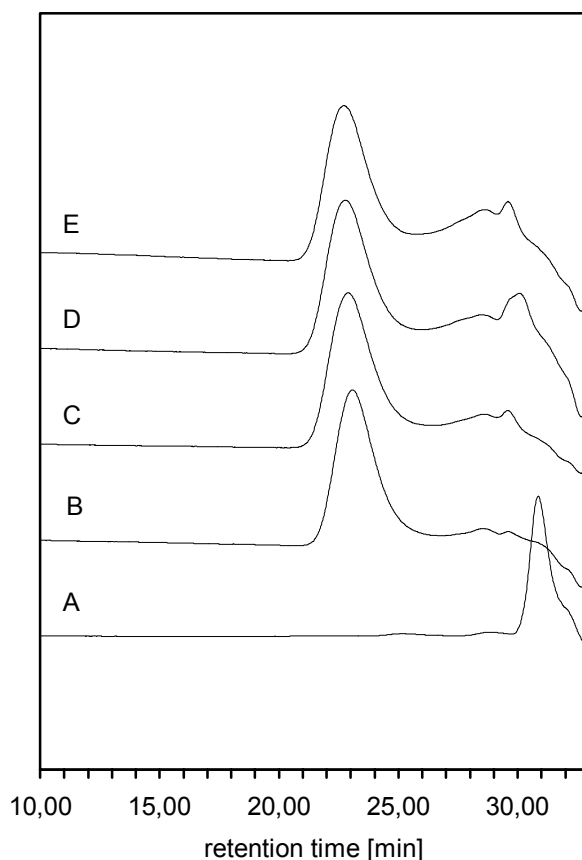


**Figure 5.1.8** SEC chromatograms of the polymerization mixture at various times after full monomer conversion. A) pure DXO monomer, B) 18 h, C) 40 h, D) 67 h, E) 82 h.

The distribution broadened and was modified in different ways when the polymer was left for a longer period of time in the reaction medium. The curve became bimodal after 18 h reaction time, with an increase in the amount of low molecular weight products at longer times. This is probably due to inter- and intra-molecular transesterifications catalyzed by the tin-alkoxide. It was found that the degradation reaction became significant when the polymerization came near to completion. Oligomers were produced by degradation of the initially formed linear polymers.

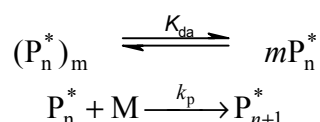
The numerical values show that longer degradation times broadened the MWD and also led to an increase in weight-average molecular weight. The increase in molecular weight was probably due to intermolecular transesterifications, not changing the  $\bar{M}_n$  markedly but increasing the  $\bar{M}_w$ .

## 5.2 Kinetics of lactide polymerization

The kinetics of polymerization were investigated in order to study the mechanism of controlled ring-opening polymerization of L-lactide. The results of the kinetic experiments were utilized to understand the action of the initiator in more detail. Polymerizations of L-lactide were conducted with various monomer-to-initiator ratios.

### 5.2.1 Kinetic models

Ring-opening polymerization reactions initiated with a metal alkoxide initiator are generally characterized by an equilibrium between the free and the aggregated metal alkoxide:<sup>[10,130,131]</sup>



where  $P_n^*$ ,  $(P_n^*)_m$  and  $M$  denote respectively non-aggregated active centers, aggregated active centers and monomer.  $K_{da}$  is the aggregation equilibrium constant,  $k_p$  the propagation rate constant and  $m$  the degree of aggregation. The aggregation causes a temporarily termination of the growing species, since the chains are propagating only if they are non-aggregated. Due to the difference in reactivities between the aggregated compounds, the kinetics of polymerization are influenced.

In order to solve the kinetic equations corresponding to this system, Penczek and co-workers have recently proposed a method to determine the degree of aggregation from the curved plots of  $\ln(k_{app})$  versus  $\ln[I]_0$ .<sup>[132]</sup> The solution for the general case of the  $m$ -aggregate formation is:

$$(k_{app})^{1-m} = -m / K_{da} (k_p)^{m-1} + k_p [I]_0 (k_{app})^{-m} \quad (1)$$

and in the logarithmic form:

$$\ln(k_{app}) = 1/m \ln[I]_0 + C \quad (2)$$

This equation allows a straight linear interpretation of the experimental data. When the logarithm of the apparent rate constant is plotted versus the logarithm of the initial initiator concentration, the slope of the line gives the



external order in the initiator. The equation is valid for polymerization in which a fast reversible aggregation of the active centers takes place.

### 5.2.2 Kinetics of lactide polymerization

The polymerization of L-lactide was monitored in time by manual sampling followed by  $^1\text{H-NMR}$  analysis to determine the degree of monomer conversion. The kinetics of the L-lactide polymerization were investigated in chloroform at  $60^\circ\text{C}$ . Figure 5.2.1 shows the semi-logarithmic plot of  $-\ln([M]/[M]_0)$  versus reaction time,  $t$ .  $[M]_0$  is the initial lactide monomer concentration and  $[M]$  the lactide concentration at a given reaction time  $t$ .

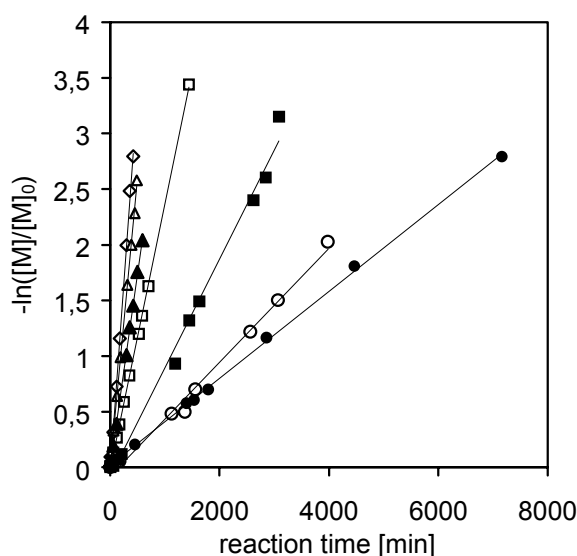


**Figure 5.2.1** The semi-logarithmic plot of  $-\ln([M]/[M]_0)$  versus the reaction time for different monomer-to-initiator ratios.  $M/I = \diamond 25, \triangle 35, \blacktriangle 50, \square 100, \blacksquare 250, \circ 360, \bullet 400$

The linearity of the plot shows that the propagation was first order with respect to lactide monomer when polymerized at  $60^\circ\text{C}$  in chloroform, and no induction period was observed. The absence of induction period indicates that the initiator was reactive from the beginning, no rearrangement of initiator aggregates was necessary to form the active species. The nature of the metal, alkoxide groups, solvent and temperature does not generally influence the first order in monomer.<sup>[66,133]</sup> The linearity of the plot of  $-\ln([M]/[M]_0)$  versus the reaction time also illustrates that no termination reactions occurred during polymerization, *i.e.* the number of propagating chains remained the same throughout the reaction. The kinetic equation describing this system is:

$$-d[M]/dt = k_{app}[M]$$

In order to determine the order in initiator for the polymerization of L-LA, the apparent rate constant was calculated from Figure 5.2.1. Figure 5.2.2 shows the apparent rate constant ( $k_{app} = -\ln([M]/[M]_0)/t$ ) as a function of the initial initiator concentration.

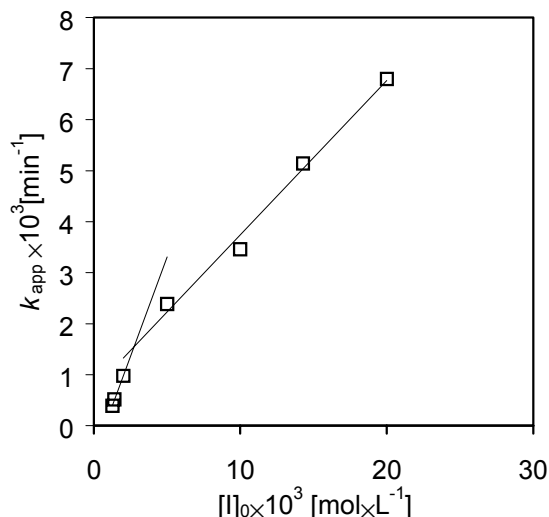


**Figure 5.2.2** Dependence of the apparent rate constant ( $k_{app}$ ) on the initial initiator concentration  $[I]_0$ . Polymerization of lactide was conducted in chloroform at 60°C.

If the polymerization is concluded to be first order in initiator, the  $k_{app}/[I]$  ratio must be constant as long as the number of active sites is independent of the initiator concentration. When the polymerization proceeds with reversible aggregation, the plot is generally curved. Figure 5.2.2 shows two distinct steps with different slopes, which reveals a change in the external order with respect to the initiator.

The external order in initiator was determined by plotting the logarithmic values of  $k_{app}$  versus the logarithm of  $[I]_0$ . Figure 5.2.3 shows the dependence of  $\ln(k_{app})$  on the initial initiator concentration. The external order in initiator increases from a value of approximately 3/4 at  $[I]_0 \approx 5$  mmol/l and higher to a value of 2 at  $[I]_0 \approx 2$  mmol/l and lower. It is thus clear that the tin-alkoxide growing centers do associate in chloroform. The change in the kinetic order in initiator was attributed to the change in proportions of aggregated and non-aggregated species.

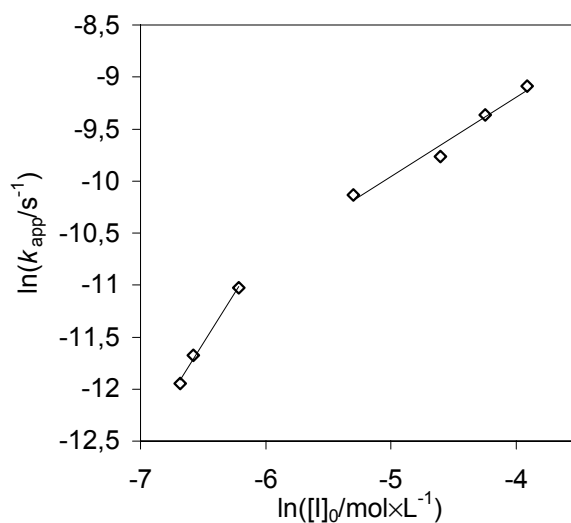


**Figure 5.2.3** Dependence of the logarithm of the apparent rate constant,  $\ln(k_{\text{app}})$ , on the logarithm of the initiator concentration,  $\ln([I]_0)$ . Polymerization of L-lactide in chloroform at 60°C; initial monomer concentration 0.5 mol/l.

This kind of change in external order in initiator has previously been reported for the polymerization of  $\epsilon$ -caprolactone initiated with aluminum isopropoxide.<sup>[130]</sup> It was reported that plots of  $\ln(k_{\text{app}})$  versus  $\ln[I]_0$  should always be curved. However, many publications do not report this behavior due to the limited range of  $[I]_0$  applied.<sup>[10]</sup>

### 5.3 NMR analysis of the propagating species in ROP

NMR spectroscopy can be used to determine three important parameters of the microstructure of polymers, specifically the composition of copolymers, the monomer sequence and in many cases the end groups.<sup>[134,135,136,137]</sup>

#### 5.3.1 NMR analysis of the reaction mixture

To identify the species involved in solution polymerization, and to obtain NMR assignments, <sup>1</sup>H-NMR spectra of the reaction mixture were recorded. A monomer-to-initiator ratio of 8 was used to make it possible to detect peaks originating from the initiator which were incorporated in the polymer chain and/or participated in the reaction. Figure 5.3.1 shows the <sup>1</sup>H-NMR spectrum of the reaction mixture after approximately 55% of the initiator was activated and the peak assignments.

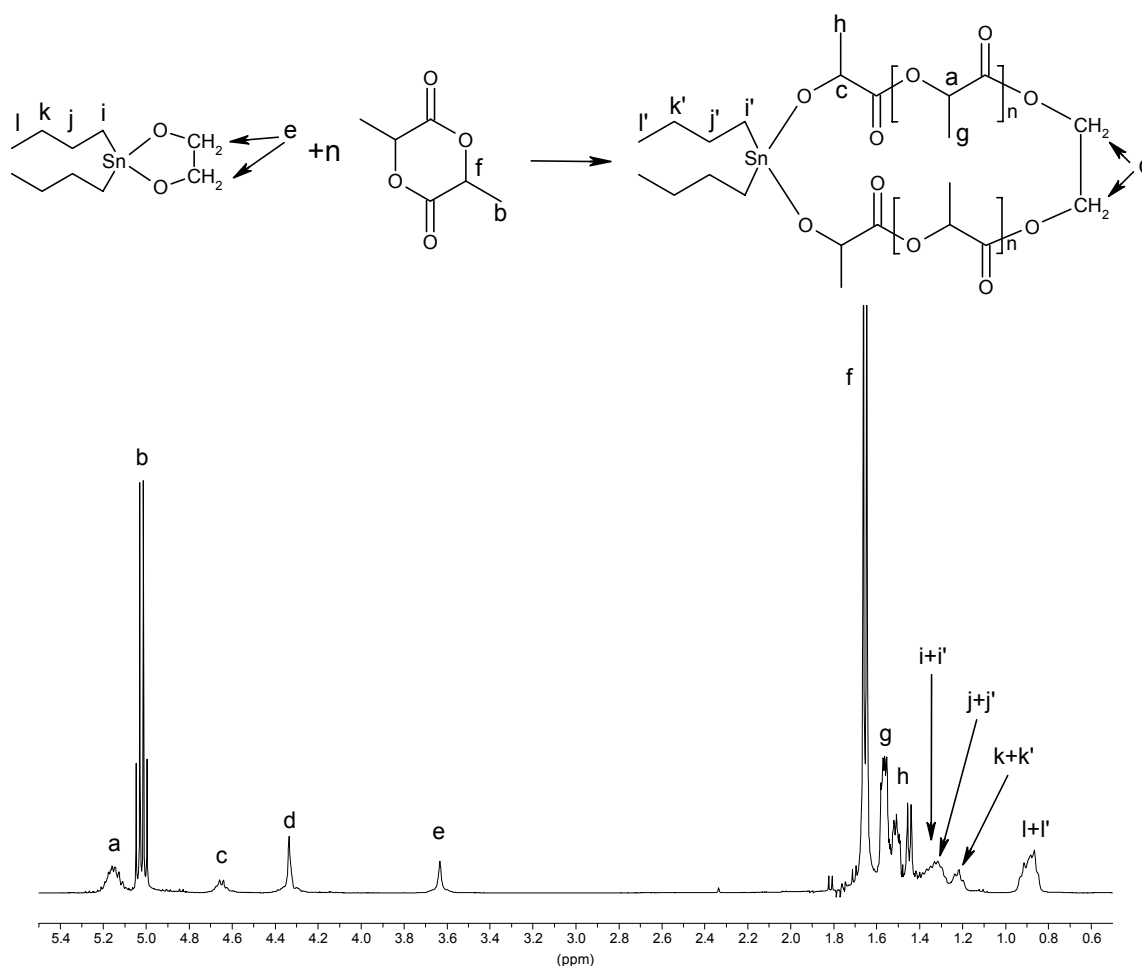


**Figure 5.3.1** <sup>1</sup>H-NMR of the active reaction mixture and the peak assignment. Polymerization conducted in chloroform at 50°C with an initial monomer-to-initiator ratio = 8.

The polymer peaks were assigned partly according to the literature.<sup>[91]</sup> The peaks originating from the metal alkoxide and peaks emerging during polymerization were analyzed, in addition to conventional  $^1\text{H}$ - and  $^{13}\text{C}$ -NMR, with DEPT and 2D  $^1\text{H}$   $^{13}\text{C}$  hmqc-gs. In DEPT ( $135^\circ$ ), the carbons attached to an odd number of hydrogens (methine ( $-\text{CH}-$ ) and methyl carbons ( $-\text{CH}_3-$ )) produce signals with positive amplitudes while carbons coupled to an even number ( $-\text{CH}_2-$ ) give signals with negative amplitudes. The 2D  $^1\text{H}$   $^{13}\text{C}$  hmqc-gs technique reveals the direct coupling between the  $^{13}\text{C}$  and  $^1\text{H}$  nucleus.

The peak at 4.35 ppm was determined using the above described NMR techniques to originate from the  $-\text{CH}_2-$  group in the ethylene glycol bridge incorporated in the growing polymer chain. Figure 5.3.2 shows the DEPT  $135^\circ$  spectrum of the reaction mixture. The peak at 63.1 ppm was determined to be a  $-\text{CH}_2-$  group due to the negative amplitude of this peak. From the 2D spectrum (not shown) this was correlated to the peak at 4.35 ppm, which hence was assigned to the ethylene glycol bridge.

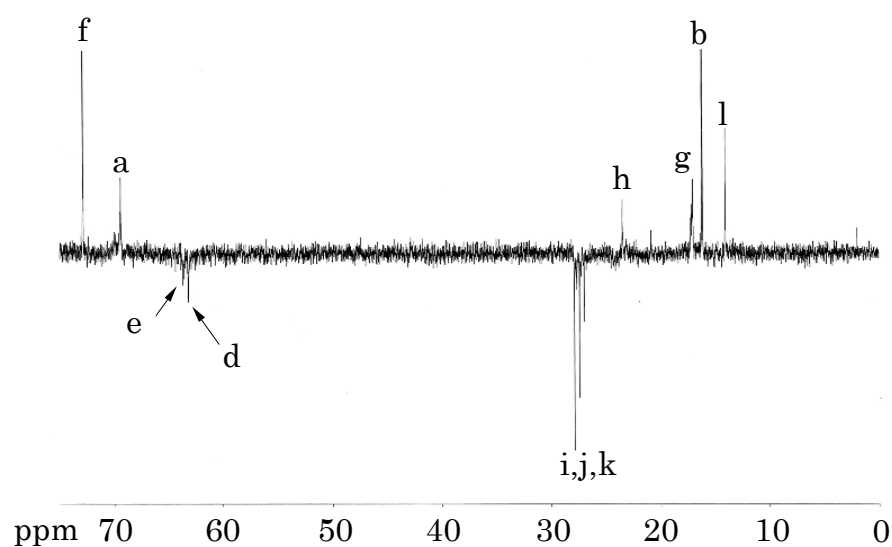


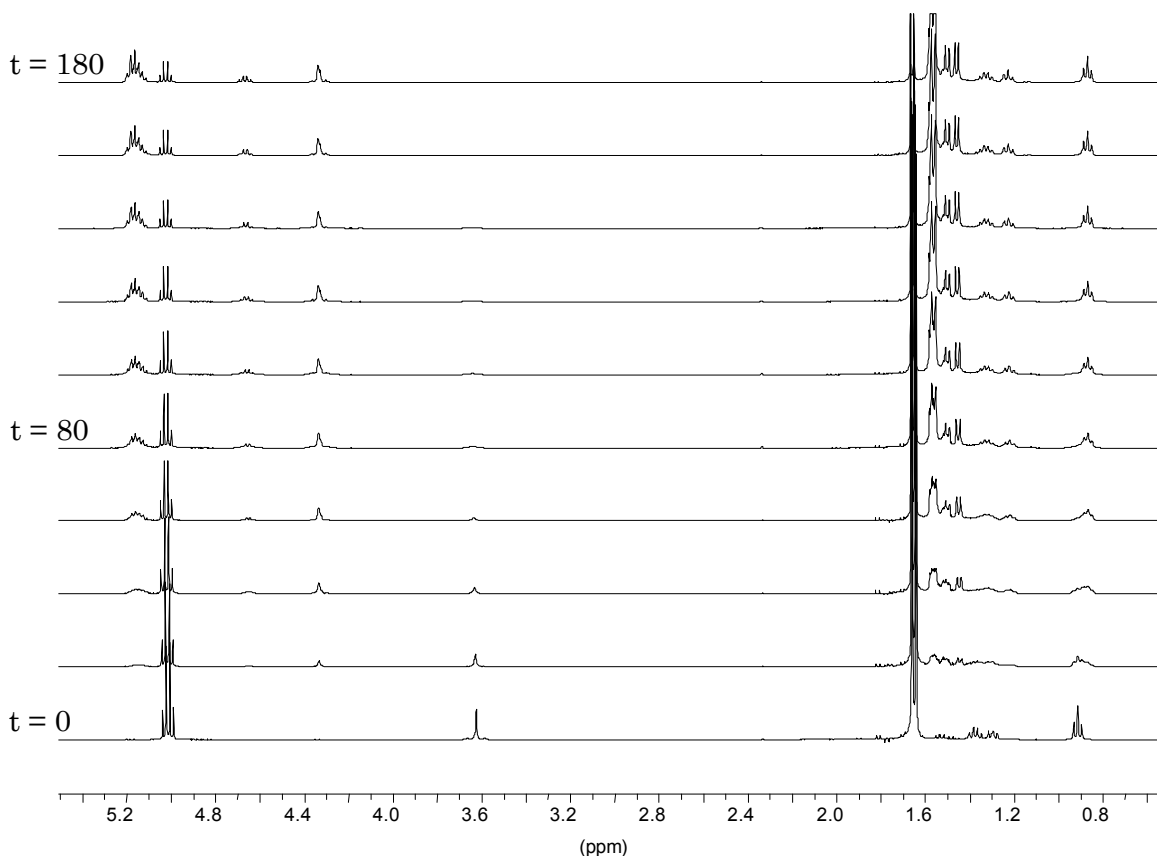
**Figure 5.3.2** DEPT  $135^\circ$  spectrum of the reaction mixture, polymerization of lactide conducted in chloroform- $d_1$  at  $50^\circ\text{C}$ . Peak notation according to the previous figure.

### 5.3.2 Initiator efficiency

The choice of a homogeneous solution as reactive medium and of moderate reaction temperatures was aimed at avoiding all the problems related to the phase separation of the reagents and to limit the number of transesterification reactions. The purpose was also to obtain a complete

reaction of the initiator, since the initiator efficiency has been shown to be limited in bulk polymerization of lactones and lactides.<sup>[126]</sup>

The reaction progress and the initiator efficiency were examined by running the polymerization of L-LA in chloroform- $d_1$  in a silanized NMR-tube. Figure 5.3.3 shows the sequence of  $^1\text{H}$ -NMR spectra of the reaction mixture, a spectrum being recorded every 20 minutes.



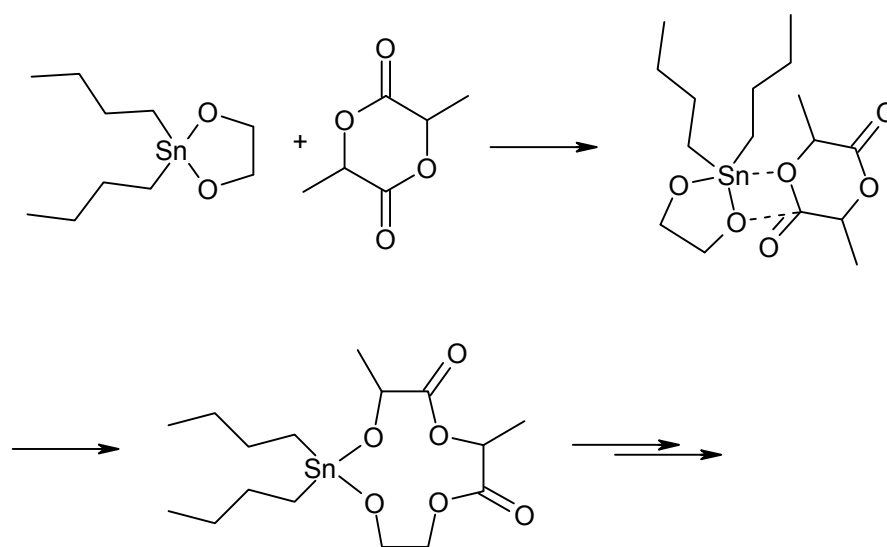
**Figure 5.3.3**  $^1\text{H}$ -NMR spectra showing the reaction progress, from bottom to top, of the polymerization of L-LA in deuteriochloroform, monomer-to-initiator ratio = 8, initial monomer concentration = 0.5 mol/l.

Figure 5.3.3 clearly shows that all the initiator was consumed and reactive in the propagation under these reaction conditions. The peak originating from the ethylene glycol bridge in the original initiator ( $\delta = 3.63$  ppm) disappeared and a peak from the ethylene glycol bridge incorporated in the polymer chain ( $\delta = 4.34$  ppm) emerged as the tin-alkoxide was consumed. Propagation continued after all the initiator had reacted, and almost complete monomer consumption was achieved. These results indicate that both tin-oxygen bonds were active and participated in the propagation.

Proton signals originating from -CH- groups next to free hydroxyl groups are normally found at 4.35 ppm.<sup>[138]</sup> According to the DEPT spectrum, the peaks at this shift originated from -CH<sub>2</sub>- groups. This experiment shows that the propagation proceeds by an insertion mechanism.

### 5.3.3 Mechanism

The NMR results indicate that hydroxy telechelic poly(L-LA)s were readily obtained and that the molecular weights of those polymers can be controlled by the amount of initiator added. From the nature of the end groups it must be concluded that the DXO or L-lactide was inserted into the Sn-O bond of the initiator through the selective cleavage of the acyl-oxygen bond of the monomer. The polymer chains remain attached to the initiator through an alkoxide link throughout the reaction. Scheme 5.3.1 shows a schematic presentation of the mechanism of propagation of lactide polymerization. A similar mechanism has earlier been proposed in the case of L-LA polymerization in bulk with the same initiator.<sup>[126]</sup>



**Scheme 5.3.1** The reaction mechanism of L-LA polymerization with the 1,1,6,6-tetra-*n*-butyl-1,6-distanna-2,5,7,10-tetraoxacyclo-decane initiator.

This type of insertion mechanism has also been proposed for lactone polymerization with aluminum alkoxide catalysts.<sup>[133]</sup>

## 5.4 Study of the ROP mechanism by hybrid density functional methods

Stannous octoate is suitable for the ROP of lactones and lactides because of its solubility and ease of handling. Moreover, the catalyst has been approved by the Food and Drug Administration (USA) as a food additive.

The starting point for this investigation was the mechanism proposals contributed by Penczek and coworkers<sup>[52]</sup> and Kricheldorf and coworkers.<sup>[11]</sup> Their suggested reaction schemes are given in Figure 2.3.3, Section 2.3.1. This polymerization system is relatively complex but, due to the extensive use of this catalyst, there are a large amount of experimental data for a number of homopolymerizations and copolymerizations. Hybrid density functional (HDF) methods have been used as a theoretical instrument to investigate the ROP mechanism of lactones and lactides. HDF provides valuable theoretical information about chemical reactions and experimental results, which can be utilized to gain insight into the reaction mechanism.

### 5.4.1 Model system

The model system used in this study was the ROP of DXO with stannous octoate as catalyst and methanol as initiator. Figure 5.4.1 shows the chemical structures of the components involved in the reaction.

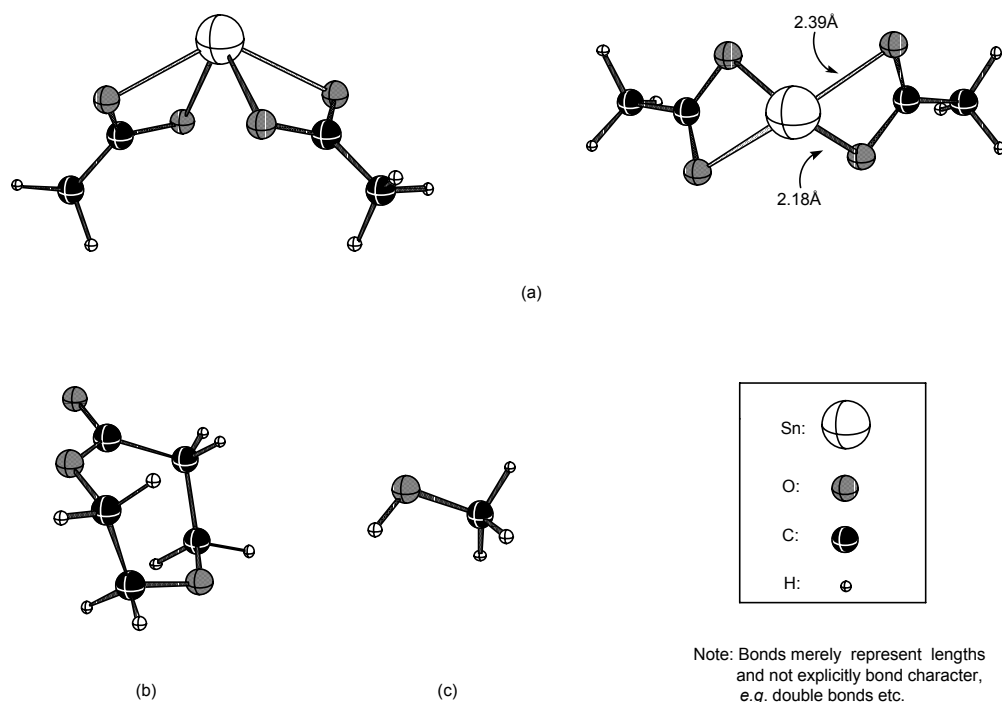


**Figure 5.4.1** The optimized structures of the components in the polymerization system a) stannous oct' b) 1,5-dioxepan-2-one c) methanol.



Functional groups which are not essential for the understanding of the ROP mechanism have been removed to reduce computational costs. The 2-ethylhexanoate ligands of the catalyst have been replaced with acetoxy groups ( $\text{SnOct}'_2$ ).

#### 5.4.2 Formation of the active species

Previous investigations have shown that hydroxyl-containing species in the reaction mixture coordinate strongly to the tin complex.<sup>[11]</sup> The complexation has been investigated by  $^{119}\text{Sn}$ -NMR, where the spectra of mixtures of stannous octoate with hydroxyl functional compounds such as benzyl alcohol, water or ethyl acetate reveals a large shift in the tin peak compared to that of pure stannous octoate.<sup>[11]</sup>

In order to determine the structure of the reactive species in ROP, the relative energies of different complexes have been determined. The calculations show that the addition of hydroxyl-containing groups to the tin complex is highly favored over monomer coordination. In the model system, methanol had a calculated enthalpy of coordination of 15.2 kcal/mol. In contrast to this strong coordination of alcohols, the coordination of the DXO monomer to the plain stannous oct' structure was markedly weaker and had an enthalpy of only 6.2 kcal/mol. Figure 5.4.2 shows the structure of the complex consisting of methanol and stannous oct'.

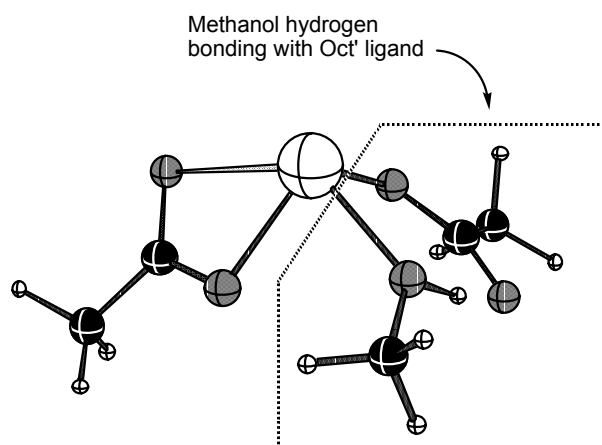


**Figure 5.4.2** One methanol coordinated to  $\text{SnOct}'$  stabilized by hydrogen bonding to the acetoxy ligand.

The strongly favored coordination of the alcohol over the monomer was due to hydrogen bonding between the hydroxyl group and the Oct' ligand. After the first alcohol moiety was complexed to the stannous Oct' a second alcohol was coordinated in the same manner.

The formation of the active species takes place by hydrogen transfer from one hydroxyl group to the Oct' ligand forming an alkoxide group. This hydrogen migration is highly endothermic with a barrier of 12.0 kcal/mol. Proton transfer can be facilitated by the presence of surrounding hydroxyl functionalities acting as transfer bridges. It has been suggested that the octoate ligand dissociates from the complex when the alcohol is converted to the alkoxide.<sup>[52]</sup> However, the calculations imply that both Oct' ligands remain attached to the tin atom during the propagation, the dissociation of a ligand being thermodynamically unfavorable.

In the next step, the second alcohol is substituted by a monomer forming the actual ROP species. Our calculations indicate that the addition of a monomer to the tin-alcohol complex (structure 4, Figure 5.4.4) is slightly endothermic (1.0 kcal/mol).

### 5.4.3 Ring-opening of the monomer

The ring-opening of the monomer proceeds by a nucleophilic attack by the tin-coordinated alkoxide on the carbonyl carbon of the DXO. The reaction passes through a four-centered transition state (Figure 5.4.3), with a high activation barrier of 26.4 kcal/mol for the ring-opening.

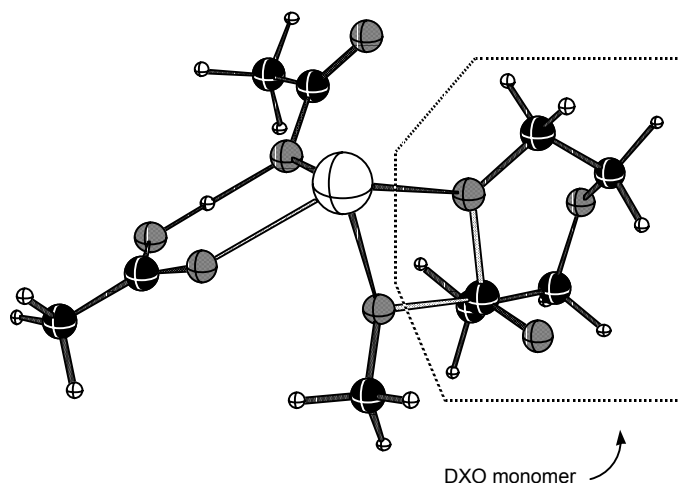


**Figure 5.4.3** The transition state structure (structure 6, Figure 5.4.4).

After ring-opening of the monomer, the polymer formed remained attached to the tin-complex. The structure was stabilized by the transfer of the hydrogen back to the alkoxide and by the addition of a second alcohol-terminated species (complex 9, Figure 5.4.4).

The complete reaction profile for the ROP of DXO with SnOct' as catalyst and methanol as initiator is shown in Figure 5.4.4. The figure

summarizes the formation of the active species, the subsequent ring-opening of the monomer and formation of the energetically most favorable complex **9**.

(1-2):	-15.2	kcal/mol	Coordination of 1st MeOH
(2-3):	-14.1	kcal/mol	Coordination of 2nd MeOH
(3-4):	+12.0	kcal/mol	Hydrogen transfer to ligand
(4-5):	+1.0	kcal/mol	MeOH substituted by DXO
(5-6):	+17.4	kcal/mol	Progression to ring-opening transition state
(6-7):	-24.5	kcal/mol	Ring opening of DXO
(7-8):	-3.2	kcal/mol	Proton transfer to polymer chain end
(8-9):	-12.5	kcal/mol	Coordination of MeOH
(9-10):	+26.4	kcal/mol	Progression to ROP transition state

(1):	SnOct <sub>2</sub>
(2):	MeOHSnOct <sub>2</sub>
(3):	(MeOH) <sub>2</sub> SnOct <sub>2</sub>
(4):	MeOH(MeO)Sn(Oct'H)Oct'
(5):	DXO(MeO)Sn(Oct'H)Oct'
(6):	Transition state for ring-opening
(7):	Pol-OSn(Oct'H)Oct'
(8):	Pol-OHSnOct <sub>2</sub>
(9):	MeOH(Pol-OH)SnOct <sub>2</sub>
(10):	Transition state for ROP

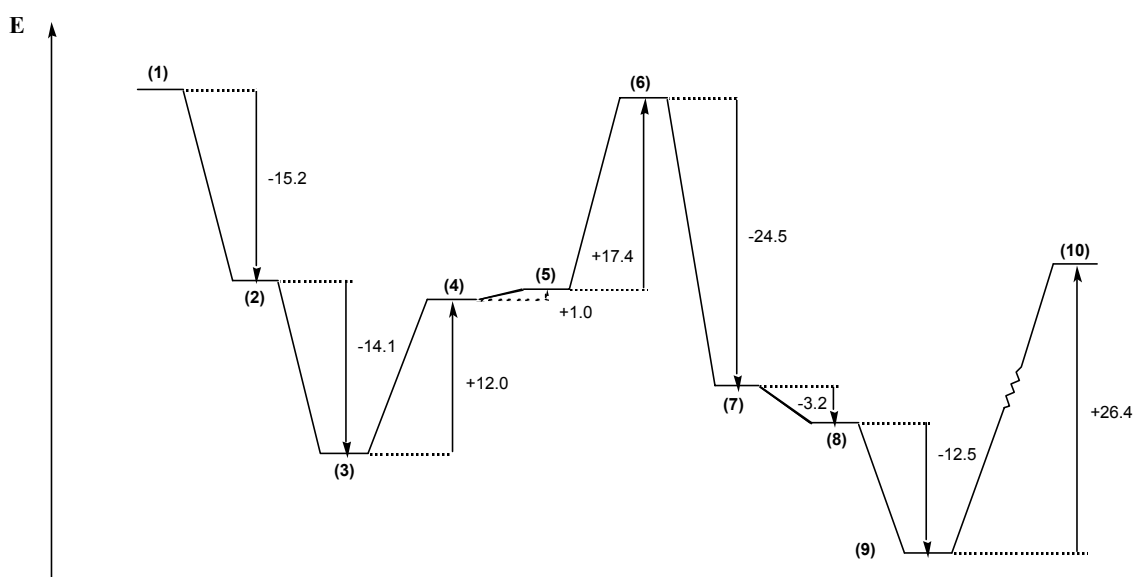


**Figure 5.4.4** Schematic presentation of the calculated reaction profile for the ROP of 1,5-dioxepan-2-one with stannous octoate as catalyst and methanol as initiator.

#### 5.4.4 Homo- and copolymerization

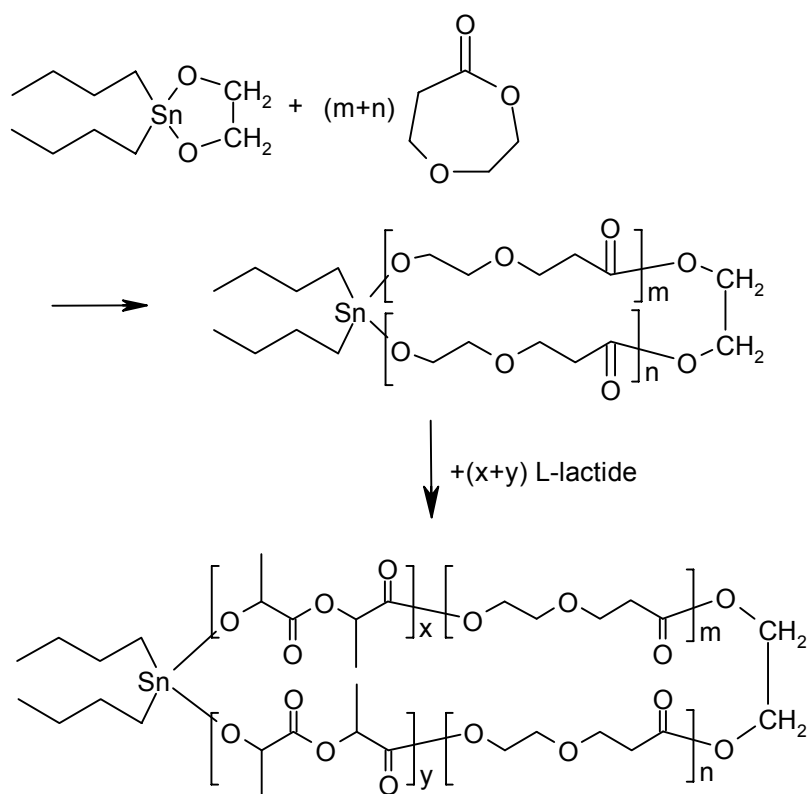
The L-LA monomer is known to homopolymerize slightly more slowly than DXO with SnOct<sub>2</sub> as catalyst under the same reaction conditions.<sup>[114,139]</sup> The activation energy (step **9** – **10**) was determined to be 29.2 kcal/mol, which is 2.8 kcal/mol higher than that for DXO. These values from the calculations agree with the experimentally found results; the L-LA will polymerize more slowly due to the higher activation barrier.

It has been reported that the copolymerization of DXO and L-LA with SnOct<sub>2</sub> as catalyst results in a polymer with a more blocky structure than is expected from a random copolymerization.<sup>[50]</sup> The calculations show that the transition state for the L-LA monomer ring-opening is 2.7 kcal/mol lower than the transition state for the DXO ring-opening. This means a 97% selective

consumption of the L-LA monomer. This is confirmed experimentally, but the resulting polymer is randomized by transesterification reactions.<sup>[50]</sup>

## 5.5 Block copolymerization of 1,5-dioxepan-2-one and L-lactide forming a tri-block copolymer

To understand the relationship between the polymer properties and the microstructure, it is important to study how to control the macromolecular structure, molecular weight and distribution of hard and soft segments. The block copolymers were synthesized from L-lactide and 1,5-dioxepan-2-one to achieve a material with mechanical properties different from those of the corresponding homopolymers, and to improve material factors such as elasticity, toughness, and elongation at break, as well as to modify the degradation profile. The initial requirement in the selection or design of a novel material is that it should be non-toxic, both initially and during degradation, and have the correct balance of mechanical properties.<sup>[140]</sup> Scheme 5.5.1 shows the reaction pathway for the synthesis of tri-block copolymers from L-LA and DXO.



**Scheme 5.5.1** The polymerization sequence for the synthesis of tri-block poly(L-lactide-*b*-1,5-dioxepan-2-one-*b*-L-lactide).

From the very start of our work with hydrolyzable polymers, it was realized that block copolymers could be of interest since they have the capability of combining properties of two different homopolymers into one

unique structure.<sup>[141]</sup> One of the proposed block copolymerization methods was based on the sequential addition of monomers to a living polymerization system initiated with aluminum isopropoxide.<sup>[58]</sup> However, the addition of DXO to a system of living poly(L-LA) macromers was not suitable for block copolymerization of L-LA and DXO. The difference in reactivity ratio was too large,<sup>[50]</sup> the macromer formed when polymerizing L-LA did not initiate polymerization of DXO.

Tri-block copolymers of L-LA and DXO were synthesized in a new two-step process as described in scheme 5.5.1. Table 5.5.1 summarizes the initial amounts of monomer and initiator and the reaction conditions used.

**Table 5.5.1.** Polymerization conditions for the block copolymerization between L-lactide and 1,5-dioxepan-2-one. All polymerizations were conducted in chloroform at 60°C

Polym. No.	$\overline{DP}_0$ in monomer feed <sup>a</sup> L-LA/DXO/L-LA	n (DXO) <sub>0</sub> <sup>b</sup> mmol	n (L-LA) <sub>0</sub> <sup>b</sup> mmol	reaction time DXO [hours]	reaction time L-LA [hours]	[DXO] <sub>0</sub> <sup>c</sup> [mol/l]	[L-LA] <sub>0</sub> <sup>c</sup> [mol/l]
1	50/200/50	27,2	13,5	8	28	1	0,36
2	25/300/25	24,6	4,1	12	14	1	0,14
3	50/300/50	28,2	10,0	12	28	1	0,30
4	75/300/75	19,4	10,0	12	42	1	0,30
5	50/400/50	32,8	10,0	16	28	1	0,20

All polymerizations were conducted with tin-alkoxide 1 as initiator (Scheme II)

<sup>a)</sup>  $DP_0(DXO) = [DXO]_0/[I]_0$ ;  $DP_0(L-LA) = [L-LA]_0/[I]_0$

<sup>b)</sup> total amount of monomer

<sup>c)</sup> monomer concentration in the reaction mixture

Because of the controlled character of the propagation reaction and the low MWD of the products obtained, it was possible to perform a block copolymerization giving well-defined tri-block copolymers. The middle block consisting of DXO was first polymerized through ROP to high conversion before addition of L-LA. In the second step, the L-LA was added and subsequently polymerized giving a tri-block copolymer. The use of the cyclic difunctional tin-alkoxide gave a tri-block copolymer with hydroxyl functionalities at both chain ends. Table 5.5.2 shows the result of the sequential addition block copolymerization.

It follows from the SEC analysis that the addition of L-LA monomer gave an increase in molecular weight without the formation of any homopolymer. The poly(DXO) macro-initiator formed during the first step, easily initiated the polymerization of L-LA. A narrow molecular weight distribution was obtained. The NMR analysis of the polymer formed gave much lower molecular weight values than the SEC analysis, as previously experienced when analyzing the homopolymers of poly(L-LA) (see Section

5.1.5 for further details). The SEC results were therefore mainly used as a tool to check the peak shape and MWD.

**Table 5.5.2.** Molecular weight determination of the of the tri-block copolymer poly(L-lactide-*b*-1,5-dioxepan-2-one-*b*-L-lactide) by  $^1\text{H-NMR}$  and SEC analysis

Polym. No.	$\bar{M}_n$ (DXO-block) <sup>a</sup> [g/mol]	$\bar{M}_n$ (L-LA-block) <sup>a</sup> [g/mol]	$\bar{M}_n$ (DXO-block) <sup>b</sup>	MWD <sup>c</sup>	$\bar{M}_n$ (DXO + L-LA) <sup>b</sup>	MWD <sup>c</sup>
1	23500	10000	43000	1.30	54700	1.27
2	33400	2700	58500	1.35	63100	1.29
3	33500	10000	59500	1.36	69100	1.30
4	36500	15700	61700	1.33	78600	1.26
5	42800	6100	75800	1.26	76400	1.25

Molecular weight measurements were performed on precipitated samples.

<sup>a</sup>) number-average molecular weight determined by  $^1\text{H-NMR}$

<sup>b</sup>) number-average molecular weight determined by SEC, polystyrene used as standard

<sup>c</sup>) molecular weight distribution, determined by SEC, chloroform used as eluent

### 5.5.1 NMR-analysis of the block copolymers

The microstructure of the tri-block copolymers prepared was quantitatively and qualitatively studied with  $^1\text{H-}$  and  $^{13}\text{C-NMR}$ . Table 5.5.3 summarizes the results from the  $^1\text{H-NMR}$  analysis of the block copolymerization of L-LA and DXO.

**Table 5.5.3.** Results from the  $^1\text{H-NMR}$  analysis of the block copolymerization of 1,5-dioxepan-2-one and L-lactide initiated by tin alkoxide, in chloroform at 60°C

Polym. No.	'conversion <sup>a</sup> DXO [%]	conversion <sup>a</sup> L-LA [%]	yield <sup>b</sup> [%]	DXO/L-La <sup>c</sup> [mol-%]
1	99,7	98,2	73,1	73/27
2	99,6	91,4	69,0	93/7
3	99,7	97,6	78,3	80/20
4	99,7	99,5	76,1	75/25
5	99,8	71,6	82,1	89/11

<sup>a</sup>) monomer conversion determined by  $^1\text{H-NMR}$

<sup>b</sup>) amount of polymer formed after precipitation in hexane/methanol

<sup>c</sup>) molar composition of the precipitated copolymer as determined by  $^1\text{H-NMR}$

The polymerization was shown to proceed to a high level of monomer conversion in all the experiments conducted. The polymers formed were obtained in good yield, although, some material was lost during the rigorous purification procedure. The isolated copolymers contained in general slightly

lower amounts of L-LA than expected, taking into account the conversion of the respective monomers.

The microstructure of the block copolymers was examined with  $^{13}\text{C}$ -NMR. The main NMR spectrum shows only the peaks originating from the main chain carbons in the L-LA and DXO repeating units. No additional peaks from initiator residues were detectable, apart from the ethylene glycol bridge which was incorporated in the polymer main chain. The expansion spectra of the carbonyl region of the prepared tri-block copolymer poly(L-LA-*b*-DXO-*b*-L-LA) are shown in Figure 5.5.1.

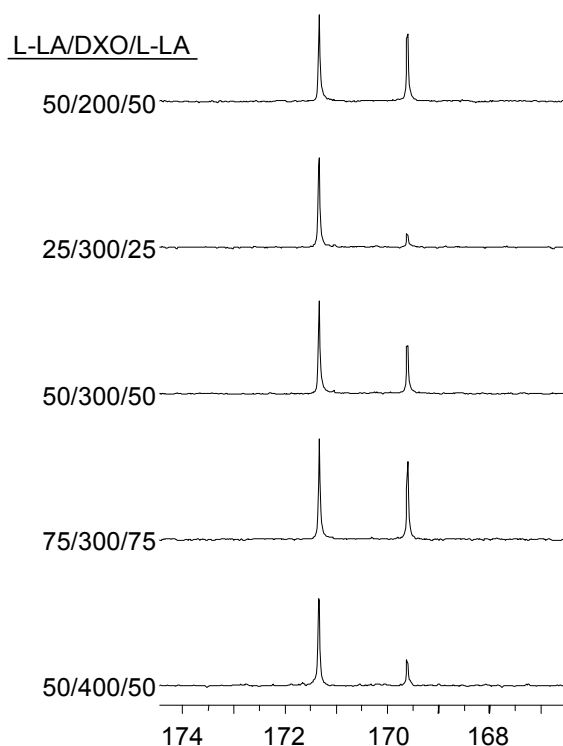


**Figure 5.5.1** The carbonyl region of the  $^{13}\text{C}$ -NMR of the tri-block copolymers. Composition as indicated in the figure,  $\text{DP}_0$  of the different blocks are given as L-LA/DXO/L-LA

The figure clearly shows that well-defined block copolymers were formed during synthesis. Two distinct peaks assigned to the DXO-DXO-DXO (DDD) and L-LA-L-LA-L-LA (LLL) existed. An insignificant amount of transesterification reactions was taking place during block copolymerization, since this type of reaction would give rise to the signals observed in the random copolymers. The carbonyl region of random poly(DXO-*co*-L-LA) has additional peaks at 170.8, 170.7, 170.1 and 169.7 ppm,<sup>[50]</sup> due to DDL, LDL, LLD, and DLL sequences. When the L-LA was added to the polyDXO macro-



initiator, the polymerization took place at the tin-alkoxide end-group to give the desired ABA block copolymers in high yield.

### 5.5.2 Influence of the block copolymer composition on the thermal properties

Thermal properties of the block copolymers prepared were investigated with differential scanning calorimetry (DSC) on thin films of the tri-block copolymers cast from dichloromethane solution. According to DSC, all of the copolymers prepared were crystalline except the poly(L-LA-*b*-DXO-*b*-L-LA) sample containing 93% DXO.

During evaporation of the solvent, crystallization occurred and well-defined spherulites developed, as shown in Figure 5.5.2. The spherulites varied in size from approximately 5  $\mu\text{m}$  to 50  $\mu\text{m}$ , larger spherulites were found in the samples containing higher proportions of L-LA. The composition of the block copolymers is given in the figure as the mol-% DXO/mol-% L-LA. The polymer containing 89% DXO and 11% L-LA showed some crystallinity according to DSC but no spherulites could be observed by SEM. The crystalline domains were probably too small to be visible on the surface.

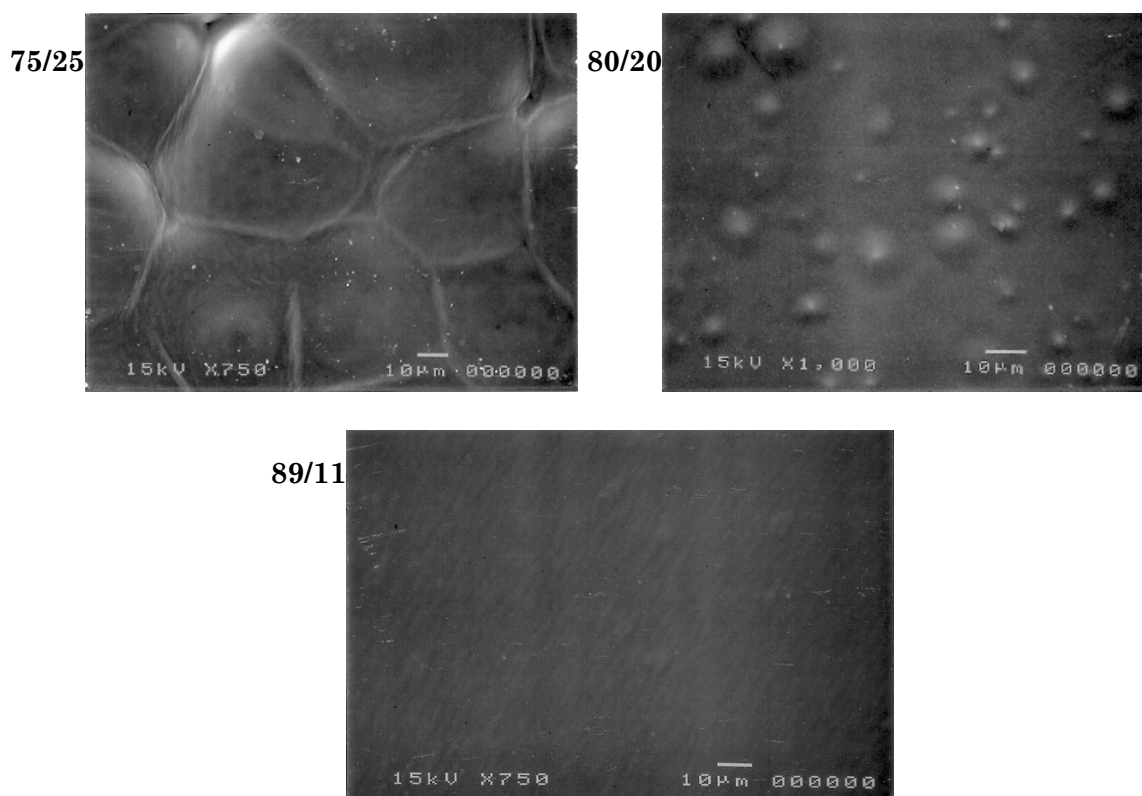


**Figure 5.5.2** SEM micrographs of the poly(L-LA-*b*-DXO-*b*-L-LA) films of different composition, cast from dichloromethane solution. The DXO/L-LA compositions are given in the figure.

DSC analysis was used to characterize the thermal properties of the tri-block copolymers produced. The influence of composition and molecular weight on the resulting thermal characteristics was investigated. Figure 5.5.3 shows the glass transition temperature,  $T_g$ , of the DXO and L-LA tri-block copolymers.

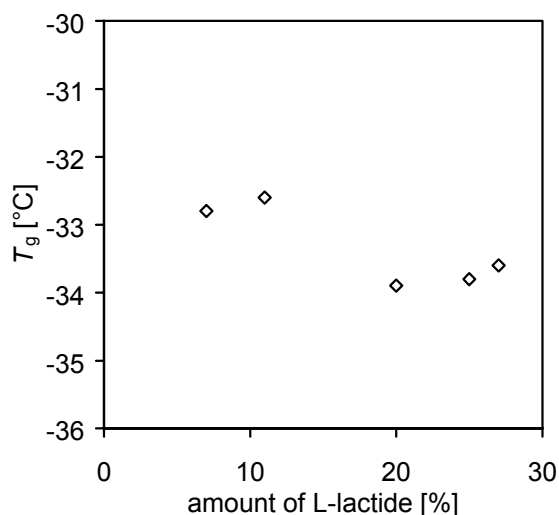


**Figure 5.5.3** The glass transition temperature of the tri-block copolymers as a function of the amount of L-lactide in the material.

The results in figure 5.5.3 demonstrate an almost constant  $T_g$ , independent of the tri-block copolymer composition or the molecular weight, as expected for a two-phase system. The random copolymers showed an increasing  $T_g$  with an increasing amount of L-LA in the copolymer.<sup>[50]</sup>

It has been reported that the melting point is highly affected by the molecular weight of the polylactide.<sup>[115]</sup> The  $T_m$  increases towards a constant value of 184°C as the molecular weight increases. Figure 5.5.4 shows the melting point for the crystalline samples. It is clear that an increase in the L-lactide block length (*i.e.* an increase in molecular weight) led to an increase in melting point. Also, an increase in the DXO block length with constant L-LA block length (*i.e.* an increase in the overall DXO content) lowered the melting temperature.

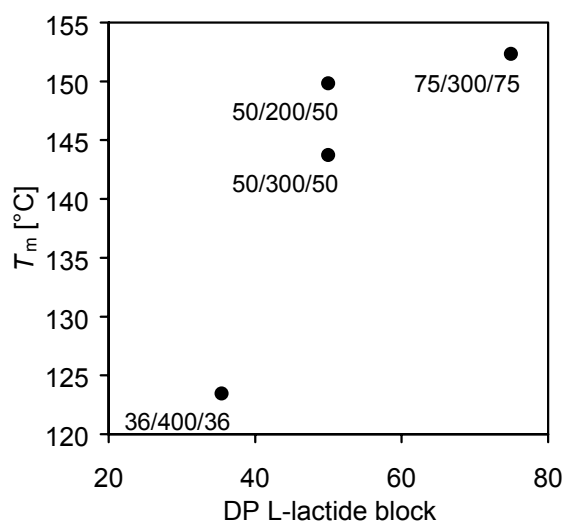


**Figure 5.5.4** The melting temperature of the tri-block copolymers as a function of the average L-LA block length.

The heat of fusion (a measure of the crystallinity of the material) was determined during the second scan. Figure 5.5.5 shows the heat of fusion as a function of the amount of L-LA in the copolymer.

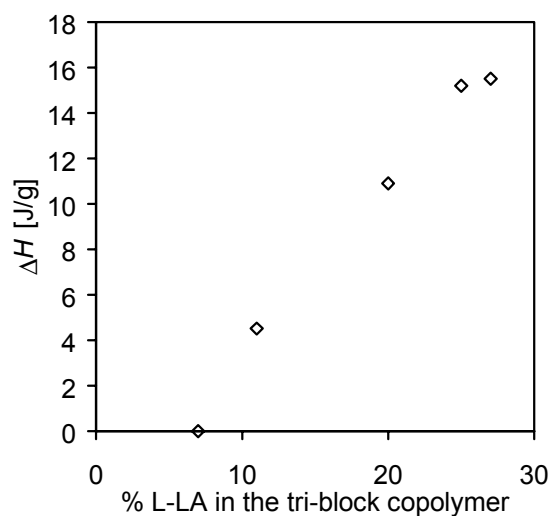


**Figure 5.5.5** The heat of fusion as a function of the amount of L-LA in the tri-block copolymers.

The heat of fusion of the crystalline poly(L-LA) decreases as expected with a decrease in the proportion of L-lactide units in the block copolymer. This is due to poly(DXO) being totally amorphous, and not able to crystallize.

## 5.6 Hydrolytic degradation of poly(L-lactide-*b*-1,5-dioxepan-2-one-*b*-L-lactide)

The tri-block copolymers were hydrolyzed in order to study the effects of copolymer composition and molecular weight on the *in vitro* degradation. The hydrolysis was performed in a saline phosphate buffer solution at 37°C. The hydrolytic degradation of the polymers leads to a decrease in molecular weight, weight loss, morphological changes, and the formation of degradation products.

Properties of the original tri-block poly(L-lactide-*b*-1,5-dioxepan-2-one-*b*-L-lactide)s subjected to hydrolytic degradation are summarized in Table 5.6.1. These copolymers were selected to provide representative information about the influence of composition, molecular weight and crystallinity on the degradation pathway. All polymers except No. 1 exhibited initially some degree of crystallinity.

**Table 5.6.1.** Molecular characteristics and thermal properties of the tri-block copoly(L-lactide-*b*-1,5-dioxepan-2-one-*b*-L-lactide) prior to hydrolysis

Polym. No.	DXO/L-LA <sup>a</sup> [%]	$\bar{M}_n$ <sup>b</sup>	$\bar{M}_w$ <sup>b</sup>	$T_g$ <sup>c</sup> [°C]	$T_m$ <sup>c</sup> [°C]	$\Delta H$ <sup>c</sup> [J/g]
1	93/7	65100	88900	-32,8	-	-
2	89/11	74900	97700	-32,6	123,4	4,52
3	87/13	64900	80800	-32,7	130,3	7,67
4	80/20	68400	88900	-33,9	143,7	10,9
5	77/23	77300	96100	-33,8	152,3	15,2
6	75/25	65400	84900	-33,0	154,0	16,7
7	75/25	53700	70100	-33,6	149,8	15,5

<sup>a)</sup> molar composition of the copolymer as determined by <sup>1</sup>H-NMR

<sup>b)</sup> molecular weight of the tri-block copolymer as determined by SEC, chloroform as mobile phase

<sup>c)</sup> determined by differential scanning calorimetry, heating rate 10°C/min

The molecular weights of the original and degraded samples were determined by SEC, with chloroform as mobile phase. The molecular weight values were not absolute but relative to polystyrene standards. This was sufficient for this study which was concerned with the changes in molecular weight of the hydrolyzed samples relative to the original material to evaluate degradation.

### 5.6.1 The influence of copolymer composition and original molecular weight on the rate of degradation

Figure 5.6.1 gives the number-average molecular weight,  $\bar{M}_n$ , of the films during hydrolytic degradation in phosphate buffer solution, pH = 7.4 at 37°C. In general, the number-average molecular weight started to decrease immediately after immersion in the buffer solution. The molecular weight of the samples decreased rapidly during the first 10 weeks of hydrolysis, and the rate of degradation thereafter decreased due to the increase in the proportion of crystalline poly(L-LA) in the remaining polymer sample. After this first stage, the degradation rate decreases strongly because further degradation can occur only in the crystalline phase.

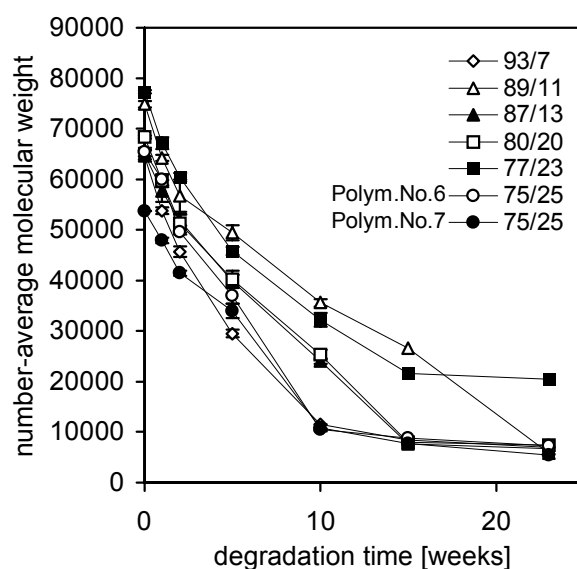


**Figure 5.6.1** The number-average molecular weight of the remaining copolymer films during hydrolytic degradation.

The composition of the polymers had no significant effect on the rate of degradation. The main factor influencing the degradation rate was the initial number-average molecular weight, although the variation in the rate was not very great. The fastest rate was found for the polymers with the lowest initial molecular weight.

The SEC analysis revealed the formation of low molecular weight compounds resulting in a multimodal molecular weight distribution. This is probably due to the poly(L-LA) crystalline phase being more resistant to water penetration and subsequent hydrolytic degradation. It has been reported that the cleavage of ester bonds starts in the amorphous phase and proceeds until most of the non-crystallized polymer has reacted completely.<sup>[142,143]</sup>

### 5.6.2 Changes in the copolymer composition during degradation.

The changes in copolymer composition during hydrolytic degradation were determined by  $^1\text{H-NMR}$ . Figure 5.6.2 shows the proportions of DXO and L-LA in the remaining copolymer sample. In general, the original copolymer films contained an excess of poly(DXO). The L-LA content of the copolymers increased as the degradation of the polymers proceeded. This is also probably because the poly(L-LA) crystalline phase is more resistant to water penetration and subsequent hydrolytic degradation, as discussed above.

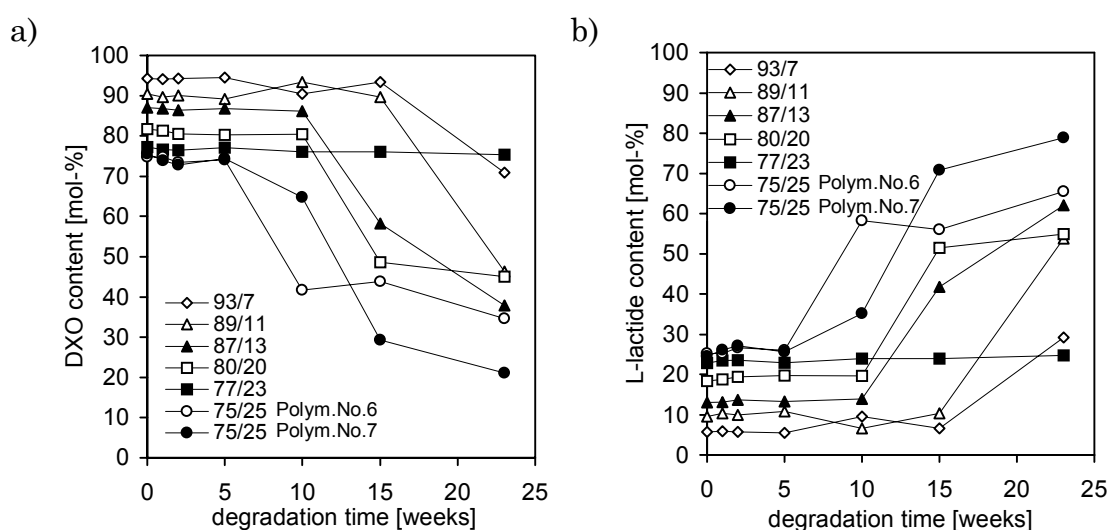


**Figure 5.6.2** The copolymer composition as a function of the degradation time. a) DXO content, and b) L-LA content in the remaining polymer.

The onset of the increase in proportion of L-LA in the polymer coincided with the onset of weight loss.

### 5.6.3 Influence of the decrease in weight-average molecular weight on the weight loss

Changes in the weight-average molecular weight and residual weight were determined by SEC and gravimetry. Figure 5.6.3 shows the  $\bar{M}_w$  and residual weight as a function of the degradation time for all copolymers investigated. A decrease in the residual weight was observed during the first week due to diffusion of low molecular weight compounds out from the polymer matrix. Residual monomer or solvent may be present in the original material, and this can be removed when it is immersed into the buffer solution. The weight loss was clearly dependent on the molecular weight. The rate of weight loss increased substantially when the  $\bar{M}_w$  had decreased sufficiently. It started when the weight-average molecular weight had reached a value lower than approximately 40 000.

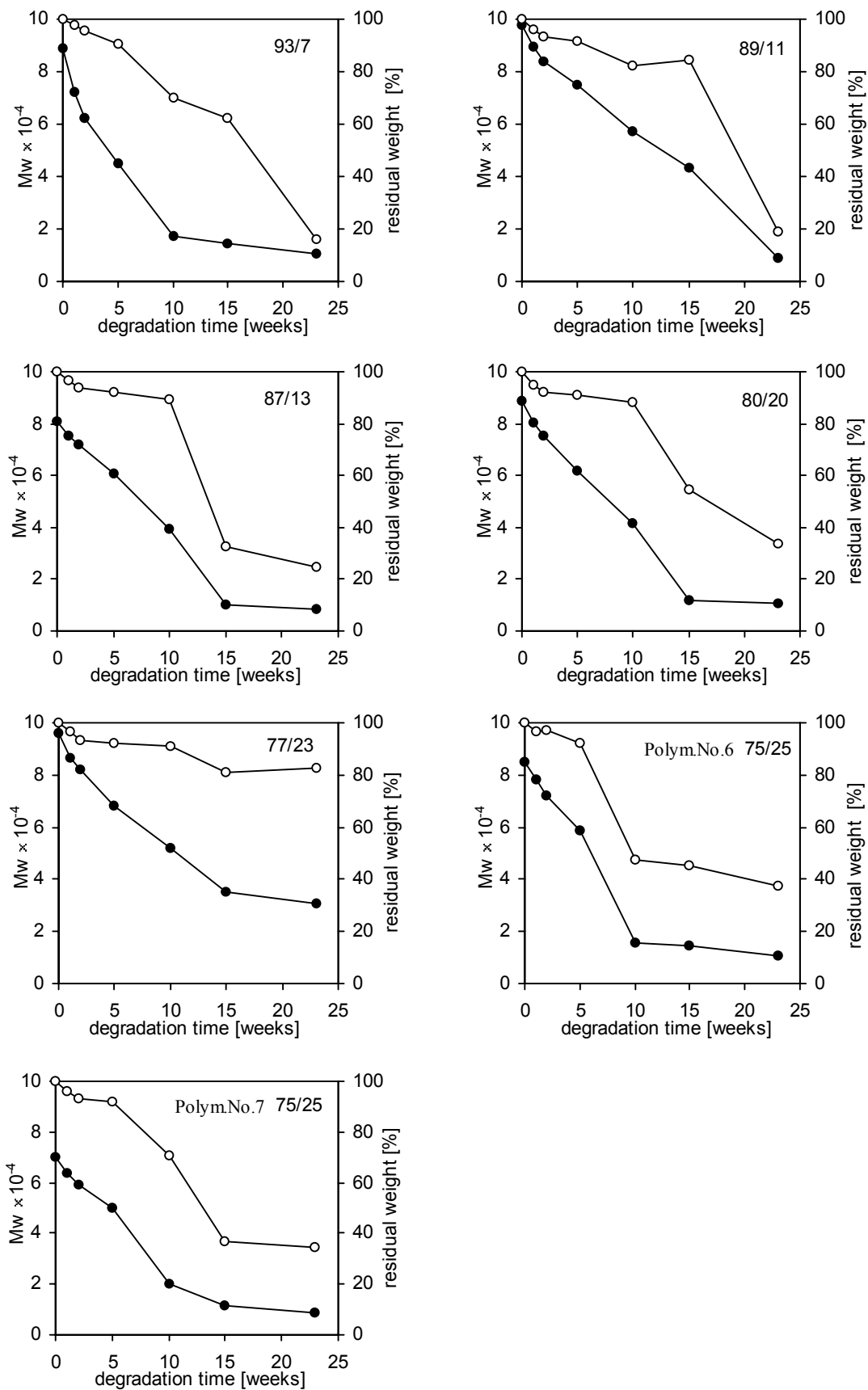


**Figure 5.6.3** The weight-average molecular weight (●) and residual weight (○) as a function of degradation time.

### 5.6.4 Degradation products

The degradation products formed during the hydrolysis of poly(L-LA-*b*-DXO-*b*-L-LA) in phosphate buffer solution have been identified and quantified with gas chromatography - mass spectrometry. The compounds released from the polymer matrix were identified by comparison with library spectra and examination of the fragmentation pattern. Figure 5.6.4 shows the mass spectrum of the degradation products. The products formed during hydrolysis were identified as 3-(2-hydroxyethoxy)-propanoic acid and lactic acid.

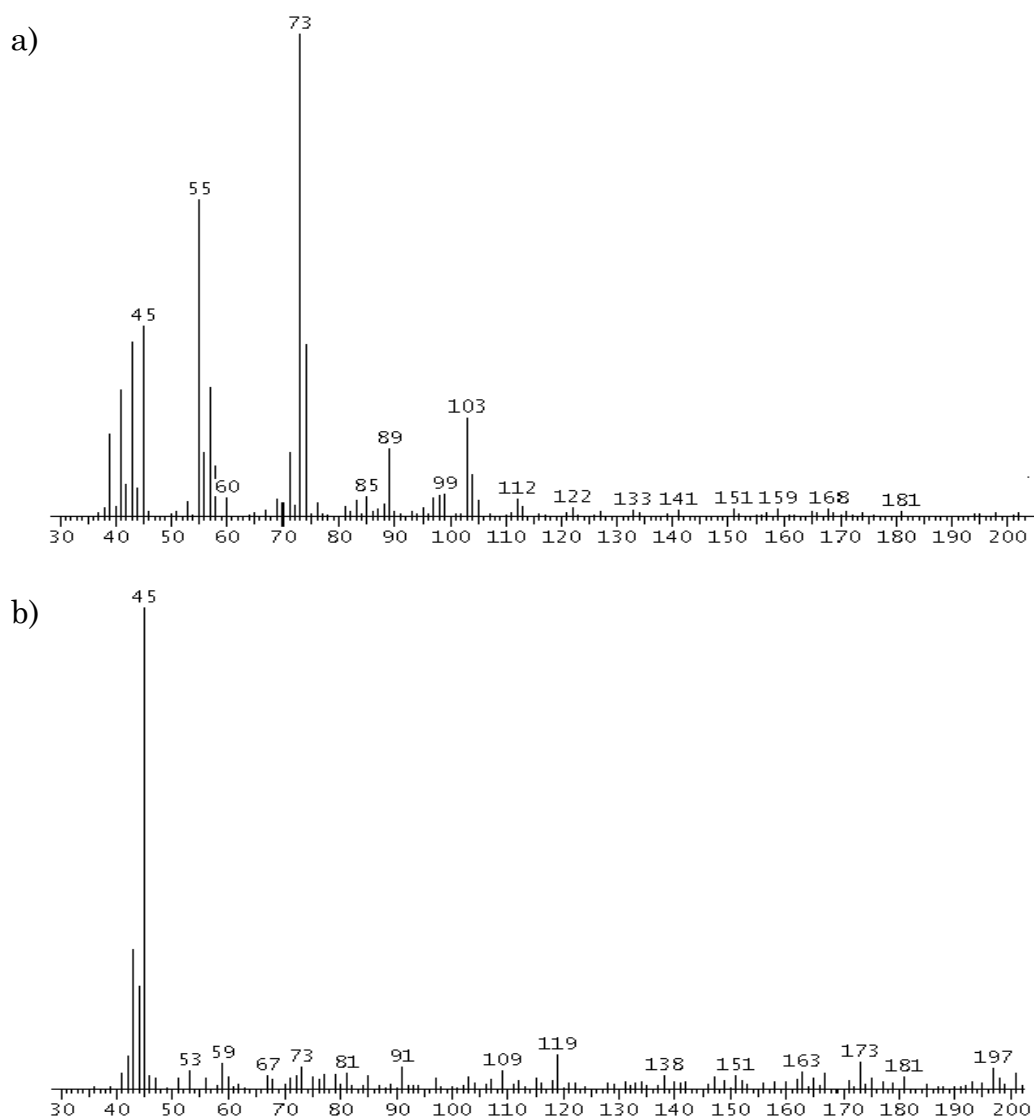


**Figure 5.6.4** The mass spectra of a) 3-(2-hydroxyethoxy)-propanoic acid b) lactic acid formed during hydrolytic degradation.

It is important to know which low molecular weight compounds are formed during hydrolysis, to be able to predict the biocompatibility of the material.

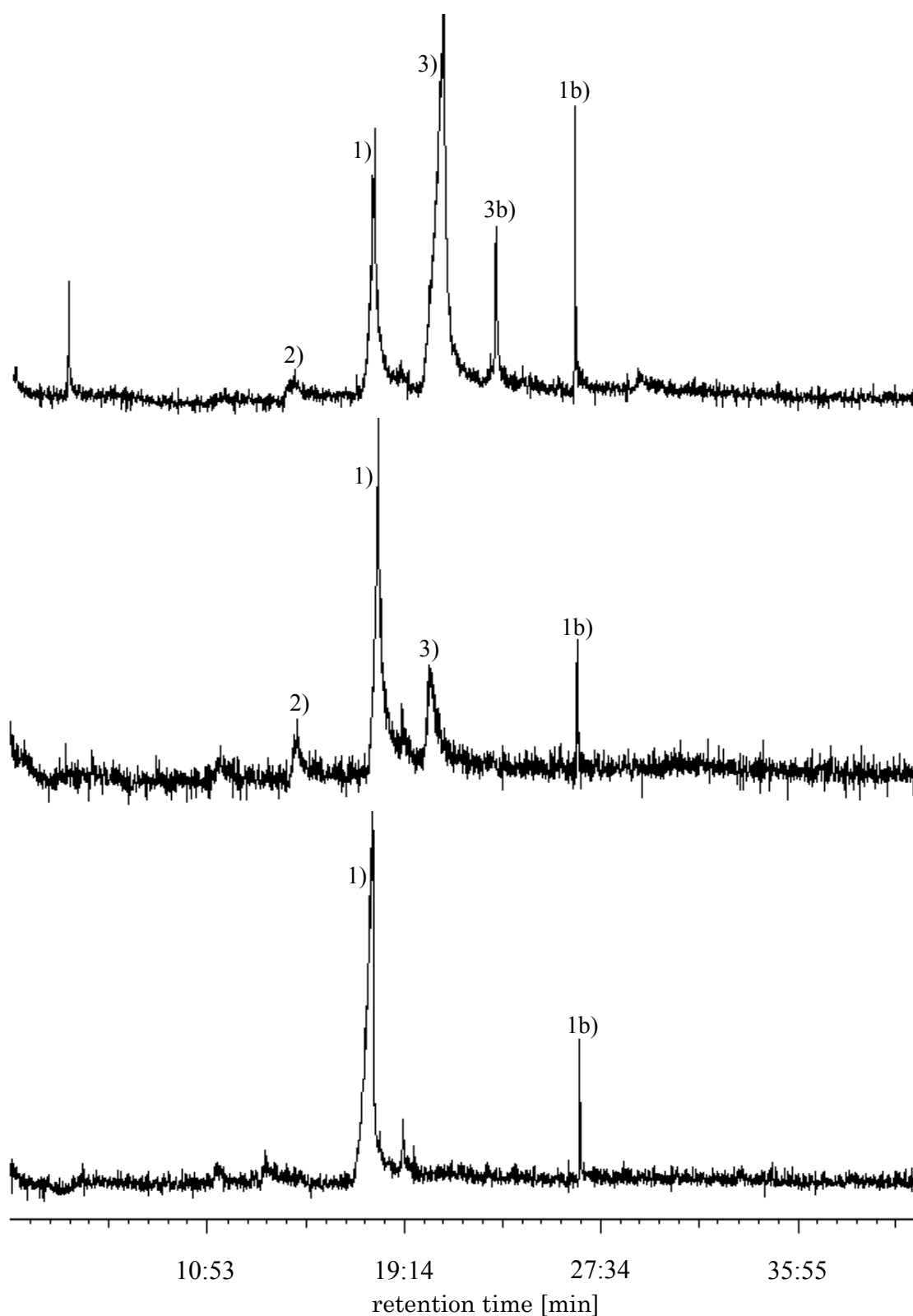


Figure 5.6.5 shows the gas chromatograms of the hydrolysis products formed after 1, 10, and 23 weeks in buffer solution. The formation of lactic acid and 3-(2-hydroxyethoxy)-propanoic acid has previously been reported for the hydrolysis of random copolymers of L-LA and DXO.<sup>[118,144]</sup> The structures of the degradation products indicate that hydrolysis proceeded by ester bond cleavage, also that the ether bond in the DXO repeating unit remained unattacked.

An internal standard was added to the sample solution before analysis in order to determine the amount of degradation products released into the aqueous buffer solution. The 2-hydroxy valeric acid sodium salt was selected as internal standard due to its resemblance to the analyzed products and the favorable retention time. Figure 5.6.6 shows the release of degradation products and the residual weight as a function of degradation time. The amount of products formed and released into the buffer solution was determined by comparison with the amount of internal standard.

The copolymer samples showed a drop in the residual weight during the first weeks of degradation. This was attributed to the diffusion of low molecular weight compounds (*e.g.* residual monomer or solvent) from the polymer matrix. After this initial decrease, the samples retained most of their weight during the following weeks. The release of degradation products started after five weeks of degradation, which coincided with the significant decrease in residual weight. A good correlation was observed between the weight loss in the degraded samples and the rate of production of degradation products, lactic acid and 3-(2-hydroxyethyl)-propanoic acid.

The pH of the degradation medium remained stable for the first 10 weeks. It then started to decrease and the pH dropped down to at most a value of 6.6, in agreement with the release of degradation products into the aqueous medium.



**Figure 5.6.5** Gas chromatogram showing the aqueous degradation products formed after 1, 10, and 23 weeks of hydrolysis of poly(L-lactide-*b*-1,5-dioxepan-2-one-*b*-L-lactide). Peak notation: (1) 2-hydroxy valeric acid (internal standard), (1b) methyl ester of no. 1, (2) lactic acid, (3) 3-(2-hydroxyethoxy)-propanoic acid, and (3b) methyl ester of no. 3

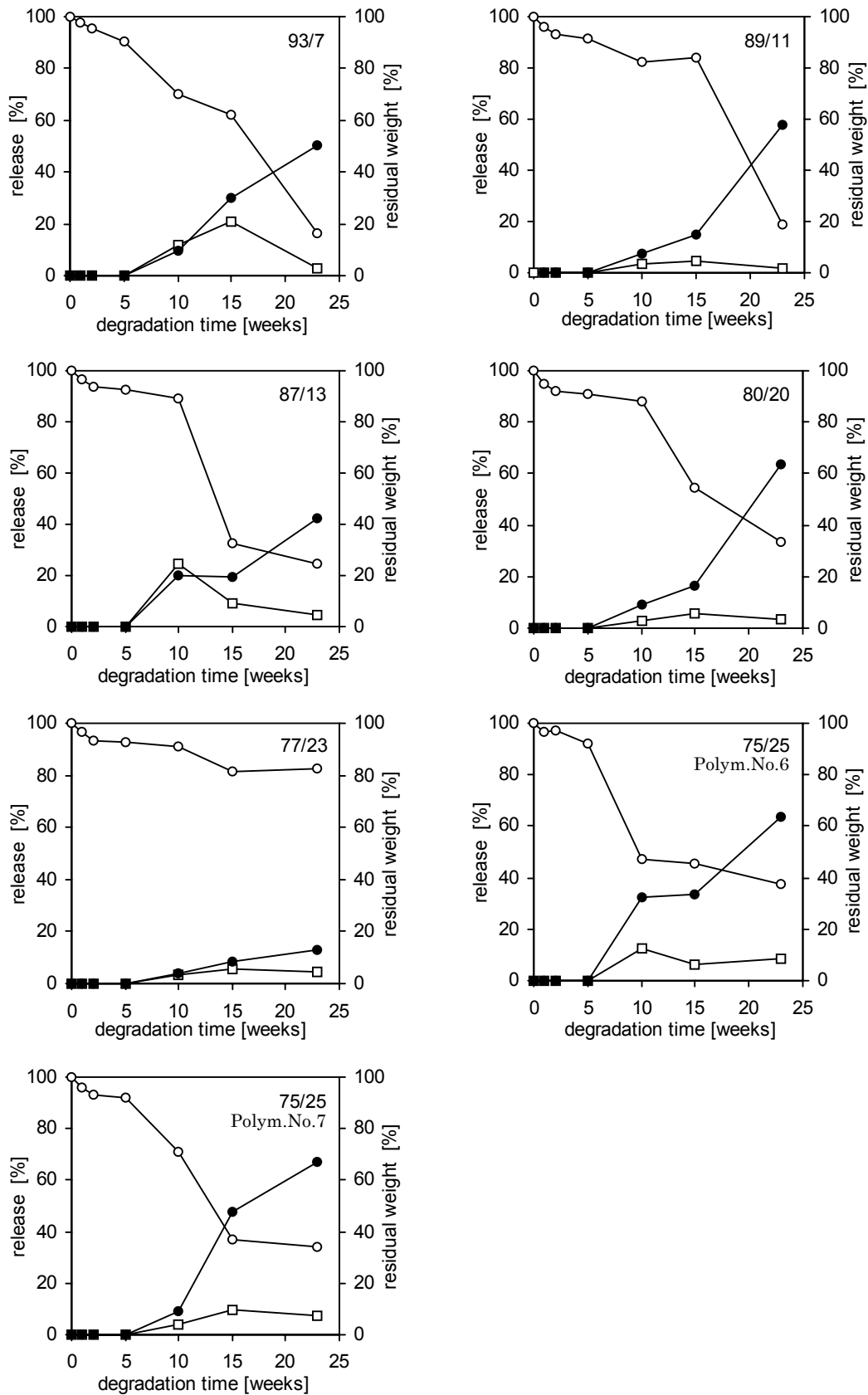


**Figure 5.6.6** The release of degradation products and residual weight (○) as a function of degradation time. (●) 3-(2-hydroxyethoxy)-propanoic acid, (□) lactic acid.

### 5.6.5 Dependence of the thermal properties on the composition and molecular weight

The hydrolytic degradation of poly(L-LA-*b*-DXO-*b*-L-LA) caused changes in the morphology as observed by differential scanning calorimetry (DSC). In general, the thermograms originally exhibited a single glass transition and a single melting endotherm when heated. The relative size of the melting peak of the original polymer samples increased with increasing proportion of L-LA in the copolymer. In general, all polymers exhibited crystallinity except No. 1 (93/7 DXO/L-LA), Table 5.6.1. The block copolymer containing 93 mol-% DXO / 7mol-% L-LA shows only a glass transition due to the excess of the amorphous polyDXO in this material.

Figure 5.6.7 shows the evolution of the DSC thermograms of polymer No. 6, Table 5.6.1. The thermograms recorded after 0, 1, 2, and 5 weeks of degradation show only a distinct melting endotherm. After approximately 10 weeks of degradation the melting region exhibited double melting peaks or shoulders, as shown in Figure 5.6.7.

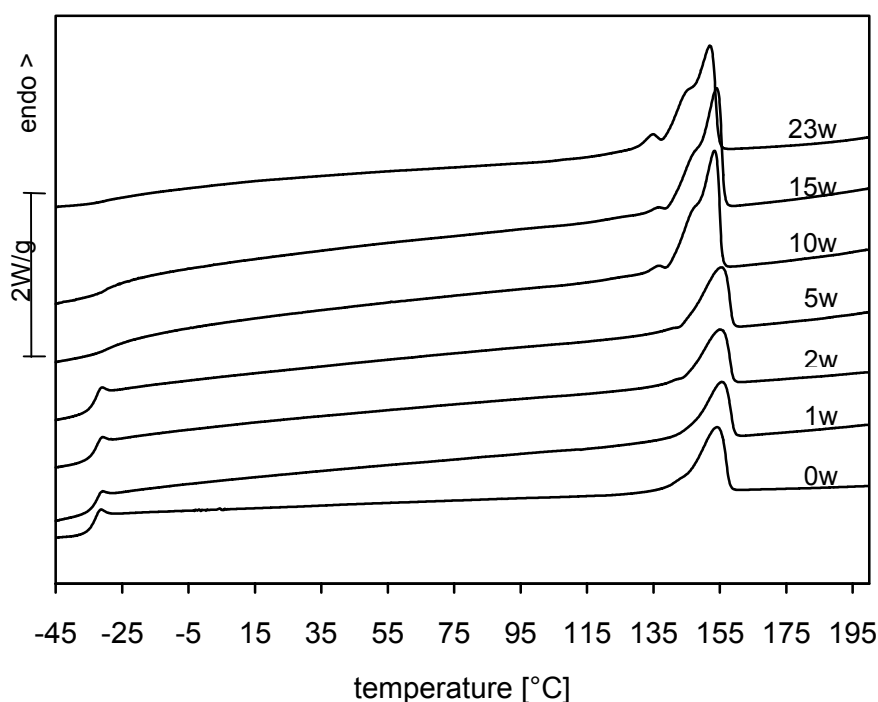


**Figure 5.6.7** Evolution of the DSC thermograms of tri-block copolymer No. 6, Table 5.6.1, during hydrolytic degradation, second heating.

The increase in degradation time resulted in a multimodal melting endotherm. This was probably due to the crystallization of chain segments of different sizes produced by hydrolysis of the polymer back bone. The appearance of double melting peaks has been reported for the hydrolysis of

pure poly(L-LA).<sup>[145]</sup> This was due to different degradation rates in the crystalline and amorphous phases, which resulted in the formation of macromolecular chains of different molecular weights. These macromolecules of a number of sizes tend to form crystallites of different dimensions.

Figure 5.6.9 shows the melting temperature of the second heating as a function of the degradation time. The plot shows that the  $T_m$  increases during the first week of degradation. This phenomenon was partly attributed to the diffusion of low molecular weight products from the polymer sample as detected by gravimetry and GC-MS. It has previously been shown that monomer intentionally added to poly(D,L-lactide) eluted from the sample films upon immersion in buffer solution, without polymer degradation.<sup>[146]</sup> The presence of low molecular weight compounds strongly influences the properties of the polymer.<sup>[147]</sup> The behavior was also partly due to thermal rearrangements in the polymer due to the plasticizing effect of water causing an increase the  $T_m$ .

The  $T_m$  starts to decrease as the molecular weight of the polymer chains decreases. It has been reported that the melting temperature is largely affected by the molecular weight of the sample.<sup>[115]</sup> When the polymer becomes enriched in L-lactide, the  $T_m$  increases again.

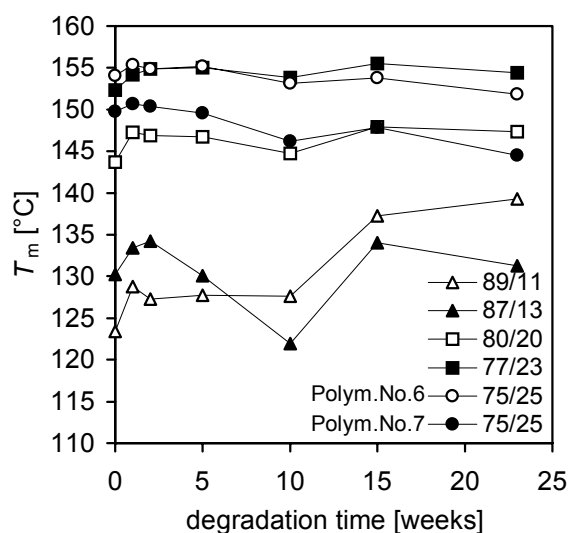


**Figure 5.6.9** The melting point of the polymer as a function of degradation time. Melting temperature determined from the second heating. Molar compositions of the tri-block copolymers are indicated in the figure.

Figure 5.6.8 shows the glass transition temperature as a function of the degradation time. The polymers originally exhibited similar  $T_g$  values, despite the difference in L-LA content. The variation was within one degree.

This is contrary to what has been reported for the random copolymers where an increase in L-LA content from 10 to 25 mol-% resulted in an increase of approximately 10 degrees.<sup>[50]</sup> This indicates that most of the amorphous phase consisted of poly(DXO). The glass transition of the pure polyDXO has previously been reported to be  $-39^{\circ}\text{C}$ .<sup>[148]</sup>

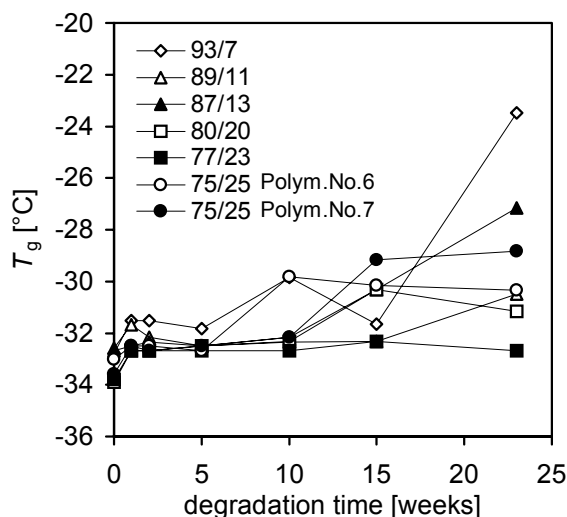


**Figure 5.6.8** The glass transition temperature versus degradation time for the tri-block copolymers. Molar ratios of the copolymers are indicated in the figure.

The glass transition temperature remained constant until the onset of weight loss. The  $T_g$  then increased due to the increase in the proportion of L-LA in the remaining polymer matrix.

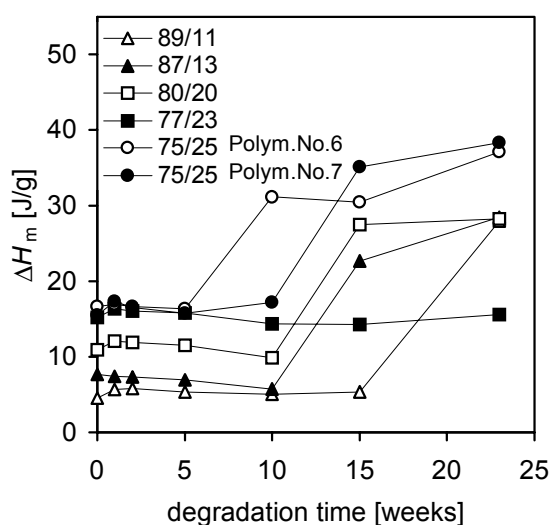


**Figure 5.6.10** Melting enthalpy of the crystalline fraction of the tri-block copolymers as a function of degradation time. Molar ratios of the copolymers are indicated in the figure.

The heat of fusion is shown in Figure 5.6.10 as a function of the degradation time for the melting endotherm recorded during the second scan. The tendency is clear, the heat of fusion generally increased with increasing degradation time. The increasing value of  $\Delta H$  was explained by the increase in L-LA content in the remaining polymer matrix, which was confirmed by NMR measurements. The poly(DXO) phase is totally amorphous and does not contribute to the amount of crystalline material in the polymer matrix.





## 6 CONCLUSIONS

The ring-opening polymerization technique was developed to achieve a controlled synthesis. The initiator 1,1,6,6-tetra-*n*-butyl-1,6-distanna-2,5,7,10-tetraoxacyclodecane proved to be useful in the synthesis of well-defined dihydroxy terminated polymers. Our study showed that the experimental conditions influenced the properties of the polymer formed. The highest molecular weight poly(1,5-dioxepan-2-one) was synthesized at a reaction temperature of 40°C under otherwise equal conditions. The polymerization of poly(L-lactide) was slower than the polymerization of DXO and therefore conducted at 60°C. The mild reaction conditions allowed us to perform the polymerization with only a negligible amount of side-reactions such as inter- and intramolecular transesterification reactions taking place. Bulk polymerization was not useful since no correlation between the monomer-to-initiator ratio and the obtained molecular weight was observed at the conditions used.

Nuclear magnetic resonance spectroscopy proved to be a useful tool to investigate the progress of the reaction. NMR of the reaction mixture revealed the existence of tin-alkoxide end groups before precipitation and hydroxyl terminated end groups after precipitation and termination in methanol. The polymerization was shown to follow an insertion mechanism, where both tin-alkoxide groups were active in propagation. The kinetics was first order with respect to the monomer. The external order with respect to the initiator changed with the initiator concentration, due to aggregation/deaggregation of the initiator.

Hybrid density functional methods were found to be useful in the theoretical investigation of the reaction mechanism of ring-opening polymerization with stannous octoate as catalyst. According to calculations, the catalyst is first transferred into a tin-alkoxide complex through reaction between hydroxyl-containing co-initiators or impurities and stannous octoate. The tin-alkoxide complex formed loosely coordinates a monomer, and

propagation proceeds through insertion of the monomer into the tin-oxygen bond through acyl-oxygen bond rupture.

A new family of well-defined tri-block copolymers containing the amorphous poly(1,5-dioxepan-2-one) as the middle segment and the semi-crystalline poly(L-lactide) as outer blocks has been synthesized. The polymerization procedure was based on a two-step sequential addition of monomers to a controlled polymerization system utilizing the cyclic tin-alkoxide 1,1,6,6-tetra-*n*-butyl-1,6-distanna-2,5,7,10-tetraoxacyclodecane as initiator.

The hydrolytic degradation pathway of poly(L-lactide-*b*-1,5-dioxepan-2-one-*b*-L-lactide) films were determined. The degradation of the tri-block copolymers proceeded in two steps. During the first step the molecular weight decreased rapidly without significant mass loss. In the second step, mass loss occurred and the molecular weight continued to decrease but leveled off. The composition of the block copolymer had a negligible effect on the rate of decrease of the molecular weight. The original molecular weight was the major factor affecting the degradation. The rate of hydrolysis of 1,5-dioxepan-2-one units was much faster than that of lactide units, resulting in an increase in lactide content in the remaining block copolymers. The major degradation products formed were lactic acid and 3-(2-hydroxyethoxy)-propanoic acid.

The study is summarized in the following points:

1. tin-alkoxides are effective initiators in the ring-opening polymerization of lactones and lactides in solution
2. tin-alkoxides react through a coordination-insertion mechanism giving a controlled polymerization
3. hybrid density functional methods are a promising concept to be utilized in the investigation of the reaction mechanism
4. it is possible to effectively produce well-defined tri-block copolymers
5. the block copolymers are degraded in saline buffer solution into lactic acid and 3-(2-hydroxyethoxy)-propanoic acid

## 7 ACKNOWLEDGEMENTS

I wish to express my sincere gratitude to my supervisor Professor Ann-Christine Albertsson, head of the Department of Polymer Technology, for accepting me as her Ph. D. student and for her encouragement and scientific support throughout this work and the writing of this thesis. She is also thanked for providing excellent research resources at the department.

I gratefully acknowledge the Swedish Research Council for Engineering Sciences (TFR) for financial support, which has made this work possible.

I thank the senior scientists in the “Biopolymer”-group for providing scientific knowledge in a range of research areas.

Ulf Bremberg is gratefully acknowledged for help with the NMR instrument. I am grateful to Mats Svensson and Henrik von Schenck for introducing me to “computer polymerization”.

I also thank all my colleagues at the department for creating a pleasant working atmosphere. I especially thank Carina Eldsäter, and Heléne Magnusson for all the great chocolate dinners, exciting journeys and nice discussions about everything, nothing and dogs. Maria Ryner is thanked for being a valuable colleague and travelling companion. Milica Tarabic (and “Stig”), Farideh Khabbaz, Björn Olander and Ulrica Edlund are thanked for interesting conversations about all subjects.

I am very thankful to Margareta Andersson, Charlotte Warding, Maria Bozena Anderz and Emma Hareide for all their administrative help.

I wish to thank the former and present members of ABB for all the fun times. I would especially like to mention Karin Jakobsson, Thierry Glauser, Martin Bellander, Mikael Krook and Petter Eriksson who have given me many unforgettable memories.

I thank my friends, you know how you are, for giving me opportunities to experience more than polymer chemistry.

I would like to thank my family, Christina, Torbjörn, Jonas, Jenny for endless support in all kinds of matters.

Finally, I would like to thank Andreas for his love and support during my writing of this thesis.



## 8 REFERENCES

- <sup>1</sup> Mathisen T., Ph. D. Thesis, "Synthesis, characterization and hydrolytic degradation of aliphatic polyesters", KTH, **1988**
- <sup>2</sup> Lundmark S., Ph. D. Thesis, "Synthesis, characterization and degradation of aliphatic polyanhydrides", KTH, **1989**
- <sup>3</sup> Löfgren A., Ph. D. Thesis, "New degradable, biomedical copolymers of 1,5-dioxepan-2-one and lactones and lactides: Synthesis, characterization and degradation behaviour", KTH, **1994**
- <sup>4</sup> Eklund M., Ph. D. Thesis, "Designed aliphatic polymers of carbonate, ester and anhydride units for degradable biomaterials: Synthesis, characterization and hydrolytic degradation", KTH, **1995**
- <sup>5</sup> Palmgren R., Ph D. Thesis, "Degradable elastomers", KTH, **1997**
- <sup>6</sup> Carothers W. H.; Dorough G. L.; van Natta F. J., The reversible polymerization of six-membered cyclic esters, *J. Am. Chem. Soc.*, **1932**, *54*, 761
- <sup>7</sup> van Natta F. J.; Hill J. W.; Carothers W. H.,  $\epsilon$ -Caprolactone and its polymers, *J. Am. Chem. Soc.*, **1934**, *56*, 455
- <sup>8</sup> Hill J. W., Adipic Anhydride, *J. Am. Chem. Soc.*, **1930**, *52*, 4110
- <sup>9</sup> Carothers W. H.; van Natta F. J., Glycol esters of carbonic acid, *J. Am. Chem. Soc.*, **1930**, *52*, 314
- <sup>10</sup> Duda A.; Penczek S., Determination of the absolute propagation rate constants in polymerization with reversible aggregation of active centers, *Macromolecules*, **1994**, *27*, 4867
- <sup>11</sup> Kricheldorf H.; Kreiser-Saunders I.; Boettcher C., Polylactones 31. Sn(II)Octoate-initiated polymerization of L-lactide – A mechanistic study, *Polymer*, **1995**, *36*, 1253
- <sup>12</sup> Degée Ph.; Dubois Ph.; Jérôme R., Bulk polymerization of lactides initiated by aluminum isopropoxide, 3. Thermal stability and viscoelastic properties, *Macromol. Chem. Phys.*, **1997**, *198*, 1985
- <sup>13</sup> Pitt C.; Gu Z.-W., Modification of the rates of chain cleavage of poly( $\epsilon$ -caprolactone) and related polyesters in the solid state, *J. Controlled Release.*, **1987**, *4*, 283
- <sup>14</sup> Jérôme R.; Henriouille-Granville M.; Boutevin B.; Robin J. J., Telechelic polymers: Synthesis characterization and applications, *Prog. Polym. Sci.*, **1991**, *16*, 837

- 15 Sosnowski S.; Gadzinowski M.; Slomkowski S., Poly(L,L-lactide) microspheres by ring-opening polymerization, *Macromolecules*, **1996**, *29*, 4556
- 16 Gadzinowski M.; Sosnowski S.; Slomkowski S., Kinetics of the dispersion ring-opening polymerization of  $\epsilon$ -caprolactone initiated with diethylaluminum ethoxide, *Macromolecules*, **1996**, *29*, 6404
- 17 Brode G. L.; Koleske J. V., Lactone polymerization and polymer properties, *J. Macromol. Sci. – Chem.*, **1972**, *A6(6)*, 1109
- 18 Johns D. B.; Lenz R. W.; Luecke A., Lactones, in “Ring-opening polymerization” Eds. Ivin K. J. and Saegusa T., Elsevier, London, **1984**, *Vol. 1*, 464
- 19 Löfgren A.; Albertsson A.-C., Dubois Ph.; Jérôme R., Recent advances in ring-opening polymerization of lactones and related compounds, *J. Macromol. Sci. Rev. Macromol. Chem. Phys.*, **1995**, *C35(3)*, 379
- 20 Mecerreyes D.; Jérôme R.; Dubois Ph., Novel macromolecular architectures based in aliphatic polysters: Relevance of the “coordination-insertion” ring-opening polymerization, *Adv. Polym. Sci.*, **1999**, *147*, 1
- 21 Kricheldorf H.; Kreiser-Saunders I., Polylactides – Synthesis, characterization and medical application, *Macromol. Symp.*, **1996**, *103*, 85
- 22 Saegusa T.; Kobayashi S.; Hayashi K., Polymerization via zwitterion. 17. Alternating copolymerization of 2-phenylimino-1,3-dioxolane with  $\beta$ -propiolactone, *Macromolecules*, **1978**, *11*, 360
- 23 Cherdron H.; Ohse H.; Korte F., Die polymerization von lactonen, Teil 1: Homopolymerization 4-, 6- und 7-gliedriger lactone mit kationischen inititoren, *Macromol. Chem.*; **1962**, *56*, 179
- 24 Albertsson A.-C.; Palmgren R., Cationic polymerization of 1,5-dioxepan-2-one with Lewis acids in bulk and solution, *J. Macromol. Chem., Pure Appl. Chem.*, **1996**, *A33(6)*, 747
- 25 Rozenberg B. A., Cationic polymerization of  $\epsilon$ -caprolactone in the presence of diols via activated monomer mechanism, *Macromol. Chem., Macromol. Symp.*, **1992**, *60*, 177
- 26 Jérôme R.; Teyssié Ph., in “Comprehensive polymer science”, Eds. Eastmond G. C., Ledwith A., Russo S. and Sigwalt P., **1989**, *Vol. 3, Part 1*, 501
- 27 Penczek S.; Slomkowski S., Progress in anionic ring-opening polymerization, in “Recent advances in anionic polymerization”, Eds. Hogen-Esch T. and Smid J., Elsevier, New York, **1987**, *Chap. 19*, 275
- 28 Jedlinski Z.; Kurcok P.; Kowalczyk M.; Polymerization of  $\beta$ -lactones initiated by potassium solutions, *Macromolecules*, **1985**, *18*, 2679
- 29 Hofman A.; Slomkowski S.; Penczek S., Structure of the active centers and mechanism of the anionic polymerization of lactones, *Macromol. Chem.*, **1984**, *185*, 91
- 30 Jedlinski Z.; Walach W.; Kurcok P.; Adamus G., Polymerization of lactones, 12. Polymerization of L-dilactide and D,L-dilactide in the presence of potassium methoxide, *Macromol. Chem.*, **1991**, *192*, 2051

- <sup>31</sup> Sipos L.; Zsuga M.; Kelen T., Living ring-opening polymerization of L,L-lactide initiated with potassium t-butoxide and its 18-crown-6 complex, *Polym. Bull.*, **1992**, *27*, 495
- <sup>32</sup> Ito K.; Hashizuka Y.; Yamashita Y., Equilibrium cyclic oligomer formation in the anionic polymerization of  $\epsilon$ -caprolactone, *Macromolecules*, **1977**, *10*, 821
- <sup>33</sup> Lundberg R. D.; Cox E. F. Lactones, in "Ring-Opening Polymerization". Ed. Frish K. and Reegen S., Marcel Dekker, New York, **1969**, Vol. 2, 247
- <sup>34</sup> Spassky N.; Wisniewski M.; Pluta C.; Le Borgne A., Highly stereoselective polymerization of rac-(D,L)-lactide with a chiral Schiff's base/aluminium alkoxide initiator, *Macromol. Chem. Phys.*, **1996**, *197*, 2627
- <sup>35</sup> Ovitt T. M.; Coates G. W., Stereoselective ring-opening polymerization of meso-lactide: synthesis of syndiotactic poly(lactic acid), *J. Am. Chem. Soc.*, **1999**, *121*, 4072
- <sup>36</sup> Kricheldorf H.; Bers M.; Scharnagl N., Poly(lactones). 9. Polymerization mechanism of metal alkoxide initiated polymerizations of lactide and various lactones, *Macromolecules*, **1988**, *21*, 286
- <sup>37</sup> Duda A.; Florjanczyk Z.; Hofman A.; Slomkowski S.; Penczek S., Living pseudoanionic polymerization of  $\epsilon$ -caprolactone – poly( $\epsilon$ -caprolactone) free of cyclics and with controlled end groups, *Macromolecules*, **1990**, *23*, 1640
- <sup>38</sup> Bero M.; Czapla B.; Dobrzynski P.; Janeczek H.; Kasperczyk J., Copolymerization of glycolide and  $\epsilon$ -caprolactone, 2. Random copolymerization in the presence of tin octoate, *Macromol. Chem. Phys.*, **1999**, *200*, 911
- <sup>39</sup> Kowalski A.; Duda A.; Penczek S., Polymerization of L,L-lactide initiated by aluminum isopropoxide trimer or tetramer, *Macromolecules*, **1998**, *31*, 2114
- <sup>40</sup> Grijpma D. W.; Pennings A. J., Polymerization temperature effects on the properties of L-lactide and  $\epsilon$ -caprolactone copolymers, *Polym. Bull.*, **1991**, *25*, 335
- <sup>41</sup> Gilding D. K.; Reed A. M., Biodegradable polymers for use in surgery – polyglycolic/poly(lactic acid) homo- and copolymers: 1, *Polymer*, **1979**, *20*, 1459
- <sup>42</sup> Dubois Ph.; Ropson N.; Jérôme R.; Teyssié Ph., Macromolecular engineering of polylactones and polylactides. 19. Kinetics of ring-opening polymerization of  $\epsilon$ -caprolactone initiated with functional aluminum alkoxides, *Macromolecules*, **1996**, *29*, 1965
- <sup>43</sup> Dubois Ph.; Ropson N.; Jérôme R.; Teyssie Ph., Macromolecular engineering of polylactones and polylactides. 19. Kinetics of ring-opening polymerization of  $\epsilon$ -caprolactone initiated with functional aluminum alkoxides, *Macromolecules*, **1996**, *29*, 1965
- <sup>44</sup> Kricheldorf H.; Berl M.; Scharnagl N., Poly(lactones). 9. Polymerization mechanism of metal alkoxide initiated polymerizations of lactide and various lactones, *Macromolecules*, **1988**, *21*, 286
- <sup>45</sup> Bero M.; Kasperczyk J., Coordination polymerization of lactides. 5. Influence of lactide structure on the transesterification processes in the copolymerization with  $\epsilon$ -caprolactone, *Macromol. Chem. Phys.*, **1996**, *197*, 3251

- <sup>46</sup> In't Veld P. J. A.; Velner E. M.; van de Witte P.; Hamhuis J., Dijkstra P. J.; Feijen J., Melt block copolymerization of  $\epsilon$ -caprolactone and L-lactide, *J. Polym. Sci. A, Polym. Chem.*, **1997**, *35*, 219
- <sup>47</sup> Dahlmann J.; Rafler G.; Fechner K.; Mehliis B.; Synthesis and properties of biodegradable aliphatic polyesters, *Brit. Polym. J.*, **1990**, *23*, 235
- <sup>48</sup> Grijpma D. W.; Zondervan G. J.; Pennings A. J., High-molecular weight copolymers of L-lactide and  $\epsilon$ -caprolactone as biodegradable elastomeric implant materials *Polym. Bull.*, **1991**, *25*, 327
- <sup>49</sup> Kricheldorf H.; Meier-Haack J., Polylactones. 22. ABA triblock copolymers of L-lactide and poly(ethylene glycol) *Macromol. Chem.*, **1993**, *194*, 715
- <sup>50</sup> Löfgren A.; Albertsson A.-C., Synthesis and characterization of poly(1,5-dioxepan-2-one-co-L-lactide) and poly(1,5-dioxepan-2-one-co-D,L-lactide), *J. Macromol. Sci., Pure Appl. Chem.*, **1995**, *A32(1)*, 41
- <sup>51</sup> Albertsson A.-C.; Gruvegård M., Degradable high-molecular weight random copolymers based on  $\epsilon$ -caprolactone and 1,5-dioxepan-2-one, with non-crystallizable unite inserted in the crystalline structure, *Polymer*, **1995**, *36*, 1009
- <sup>52</sup> Kowalski A.; Duda A.; Penczek S., Kinetics and mechanism of cyclic esters polymerization initiated with tin(II) octoate, 1. Polymerization of  $\epsilon$ -caprolactone, *Macromol. Rapid Commun.*, **1998**, *19*, 567
- <sup>53</sup> Schwach G.; Coudane J.; Engel R.; Vert M., More about the polymerization of lactides in the presence of stannous octoate, *J. Polym. Chem.*, **1997**, *35*, 3431
- <sup>54</sup> Degée Ph.; Dubois Ph.; Jacobsen S.; Fritz H.-G.; Jérôme R., Beneficial effect of triphenylphosphine on the bulk polymerization of L,L-lactide promoted by 2-ethylhexanoic acid tin (II) salt, *J. Polym. Sci., Polym. Chem.*, **1999**, *37*, 2413
- <sup>55</sup> Ouhadi T.; Stevens C.; Teyssié P., Mechanism of  $\epsilon$ -caprolactone polymerization by aluminum alkoxides, *Macromol. Chem., Suppl.*, **1975**, *1*, 191
- <sup>56</sup> Dubois Ph.; Jacobs C.; Jérôme R.; Teyssié Ph., Macromolecular engineering of polylactones and polylactides. 4. Mechanism and kinetics of lactide homopolymerization by aluminum isopropoxide, *Macromolecules*, **1991**, *24*, 2266
- <sup>57</sup> Bero M.; Kasperczyk J.; Jedlinski Z., Coordination polymerization of lactides. 1. Structure determination of obtained polymers, *Macromol. Chem.*, **1990**, *191*, 2287
- <sup>58</sup> Löfgren A.; Albertsson A.-C.; Dubois Ph.; Jérôme R.; Teyssié Ph., Synthesis and characterization of biodegradable homopolymers and block copolymers based on 1,5-dioxepan-2-one, *Macromolecules*, **1994**, *27*, 5556
- <sup>59</sup> Löfgren A.; Renstad R.; Albertsson A.-C., Synthesis and characterization of a new degradable thermoplastic elastomer based on 1,5-dioxepan-2-one and  $\epsilon$ -caprolactone, *J. Appl. Polym. Sci.*, **1995**, *55*, 1589
- <sup>60</sup> Quirk R.; Lee B., Experimental conditions for living polymerization, *Polym. Int.*, **1992**, *27*, 359
- <sup>61</sup> Gold L., Statistics of polymer molecular size distribution for an invariant number of propagating chains, *J. Chem. Phys.*, **1958**, *28*, 91



- <sup>62</sup> Dubois Ph.; Jacobs C.; Jérôme R.; Teyssié Ph., Macromolecular engineering of polylactones and polylactides. 4. Mechanism and kinetics of lactide homopolymerization by aluminum isopropoxide, *Macromolecules*, **1991**, *24*, 2266
- <sup>63</sup> Duda A.; Florjanczyk Z.; Hofman A.; Slomkowski S.; Penczek S., Living pseuduanionic polymerization of  $\epsilon$ -caprolactone. Poly( $\epsilon$ -caprolactone) free of cyclics and with controlled end groups, *Macromolecules*, **1990**, *23*, 1640
- <sup>64</sup> Montaudo G.; Montaudo M. S.; Puglisi C.; Samperi F.; Spassky N.; Le Borgne A.; Wisniewski M., Evidence for ester-exchange reactions and cyclic oligomer formation in the ring-opening polymerization of lactide with aluminum complex initiators, *Macromolecules*, **1996**, *29*, 6461
- <sup>65</sup> Duda A.; Penczek S., Kinetics of  $\epsilon$ -caprolactone polymerization on dialkylaluminum alkoxides, *Macromol. Chem., Macromol. Symp.*, **1991**, *47*, 127
- <sup>66</sup> Duda A., Polymerization of  $\epsilon$ -caprolactone initiated by aluminum isopropoxide carried out in the presence of alcohols and diols. Kinetics and mechanism, *Macromolecules*, **1996**, *29*, 1399
- <sup>67</sup> Jacobs C.; Dubois Ph.; Jérôme R.; Teyssié Ph., Macromolecular engineering of polylactones and polylactides. 5. Synthesis and characterization of diblock copolymers based on poly- $\epsilon$ -caprolactone and poly(L,L or D,L)lactide by aluminum alkoxides, *Macromolecules*, **1991**, *24*, 3027
- <sup>68</sup> Miola C.; Hamaide T.; Spitz R., End-functionalized poly( $\epsilon$ -caprolactone) oligomers through heterogeneous catalysis in protic conditions: a mechanistic approach, *Polymer*, **1997**, *38*, 5667
- <sup>69</sup> Mehrothra R. C.; Gupta V. D., Preparation and properties of some organotin compounds I. Dibutyltin glycolates, *J. Organometal. Chem.*, **1965**, *4*, 145
- <sup>70</sup> J. Considine, Organotin chemistry. VIII\*. The reaction of dibutyltin oxide with vic-glycols, *J. Organomet. Chem.*, **1966**, *5*, 263
- <sup>71</sup> Kricheldorf H.; Sumbél M.; Kreiser-Saunders I., Polylactones. 20. Polymerization of  $\epsilon$ -caprolactone with tributyltin derivatives: A mechanistic study, *Macromolecules*, **1991**, *24*, 1944
- <sup>72</sup> Kricheldorf H.; Boettcher C.; Tönnies K.-U., Polylactones: 23. Polymerization of racemic and meso D,L-lactide with various organotin catalysts – stereochemical aspects, *Polymer*, **1992**, *33*, 2817
- <sup>73</sup> Kemnitzer J.; McCarty S. P.; Gross R. A., Syndiospecific ring-opening polymerization of  $\beta$ -butyrolactone to form predominantly syndiotactic poly( $\beta$ -hydroxybutyrate) using tin(IV) catalysts, *Macromolecules*, **1993**, *26*, 6143
- <sup>74</sup> Kemnitzer J.; McCarty S. P.; Gross R. A., Preparation of predominantly syndiotactic poly( $\beta$ -hydroxybutyrate) by the tributyltin methoxide catalyzed ring-opening polymerization of racemic  $\beta$ -butyrolactone, *Macromolecules*, **1993**, *26*, 1221
- <sup>75</sup> Kricheldorf H.; Lee S.-R., Polylactones. 35. Macrocyclic and stereoselective polymerization of  $\beta$ -D,L-butyrolactone with cyclic dibutyltin initiators, *Macromolecules*, **1995**, *28*, 6718
- <sup>76</sup> McLain S. J.; Drysdale N. E., Yttrium and rare earth compounds catalyzed lactone polymerization, US Patent 5 028 667, **1991**

- <sup>77</sup> McLain S.; Ford T.; Drysdale N., Living ring-opening polymerization of (L,L)-lactide by yttrium and lanthanum alkoxides, *Polym. Prep., Am. Chem. Soc.*, **1992**, *33*, 463
- <sup>78</sup> Stevels W.; Dijkstra P.; Feijen J., New initiators for the ring-opening polymerization of cyclic esters, *Trends Polym. Sci.*, **1997**, *5*, 300
- <sup>79</sup> Stevels W.; Ankoné M.; Dijkstra P.; Feijen J., Kinetics and mechanism of L-lactide polymerization using two different yttrium alkoxides as initiators, *Macromolecules*, **1996**, *29*, 6132
- <sup>80</sup> McLain S.; Drysdale N., Living ring-opening polymerization of  $\epsilon$ -caprolactone by yttrium and lanthanide alkoxide, *Polym. Prep., Am. Chem. Soc.*, **1992**, *33*, 174
- <sup>81</sup> Yasuda H.; Furo M.; Yamamoto H., New approach to block copolymerizations of ethylene with alkyl methacrylates and lactones by unique catalysis with organolanthanide complexes, *Macromolecules*, **1992**, *25*, 5115
- <sup>82</sup> Nomure R.; Endo T., Synthesis of poly( $\epsilon$ -caprolactone-*b*-tetrahydrofuran-*b*- $\epsilon$ -caprolactone) through the samarium iodide-induced transformation, *Macromolecules*, **1995**, *28*, 5372
- <sup>83</sup> Stevels W.; Ankoné M.; Dijkstra P.; Feijen J., Well defined block copolymers of  $\epsilon$ -caprolactone and L-lactide using  $Y_5(\mu-O)(O^iPr)_{13}$  as an initiator, *Macromol. Chem. Phys.*, **1995**, *196*, 1153
- <sup>84</sup> Shen Y.; Shen Z.; Zhang Y.; Yao K., Novel rare earth catalysts for the living polymerization and block copolymerization of  $\epsilon$ -caprolactone, *Macromolecules*, **1996**, *29*, 8289
- <sup>85</sup> Yasuda H.; Ihara E., Rare-earth-metal initiated polymerizations of polar and nonpolar monomers to give high-molecular weight polymers with extremely narrow molecular weight distribution, *Macromol. Chem. Phys.*, **1995**, *196*, 2417
- <sup>86</sup> Le Borgne A.; Pluta Ch.; Spassky N., Highly reactive yttrium alkoxide as new initiator for the polymerization of  $\beta$ -butyrolactone, *Macromol. Rapid Commun.*, **1994**, *15*, 955
- <sup>87</sup> Xu J.; McCarty S. P.; Gross R. A., Racemic  $\alpha$ -methyl- $\beta$ -propiolactone polymerization by organometallic catalyst systems, *Macromolecules*, **1996**, *29*, 4565
- <sup>88</sup> Hall H. K.; Schneider A. K., Polymerization of cyclic esters, urethanes, ureas and imides, *J. Am. Chem. Soc.*, **1958**, *80*, 6409
- <sup>89</sup> Saiyasombat W.; Molloy R.; Nicholson T. M.; Johnson A. F.; Ward I. M.; Poshachinda S., Ring-strain and polymerizability of cyclic esters, *Polymer*, **1989**, *39*, 5581
- <sup>90</sup> Kurcok P.; Matuszowicz A.; Jedlinski A.; Kricheldorf H.; Dubois Ph.; Jérôme R., Substituent effect in anionic polymerization of  $\beta$ -lactones initiated by alkali metal alkoxides, *Macromol. Rapid Commun.*, **1995**, *16*, 513
- <sup>91</sup> Hiltunen K.; Härkönen M.; Seppälä J.; Väänänen T., Synthesis and characterization of lactic acid based telechelic prepolymers, *Macromolecules*, **1996**, *29*, 8677
- <sup>92</sup> Kylmä J.; Seppälä J., Synthesis and characterization of biodegradable thermoplastic poly(ester urethane) elastomer, *Macromolecules*, **1997**, *30*, 2876

- <sup>93</sup> Hiltunen K.; Seppälä J.; Härkönen M., Lactic acid based poly(ester-urethane)s: The effect of different polymerization conditions on the polymer structure and properties, *J. Appl. Polym. Sci.*, **1997**, *64*, 865
- <sup>94</sup> Stevels W. M.; Bernard A.; van de Witte P.; P. J. Dijkstra P. J.; Feijen J., Block copolymers of poly(L-lactide) and poly( $\epsilon$ -caprolactone) or poly(ethylene glycol) prepared by reactive extrusion, *J. Appl. Polym. Sci.*, **1996**, *62*, 1295
- <sup>95</sup> Noshay A.; McGrath J. E., in "Block copolymers, overview and critical survey", Academic Press, New York, **1977**, *Chap. 3*, 24
- <sup>96</sup> Kim S. H.; Kim Y. H., Biodegradable star-shaped poly-L-lactide, *Biodegradable Plastics and Polymers*, **1994**, 464
- <sup>97</sup> Arvanitoyannis I.; Nakayama A.; Kawasaki N.; Yamamoto N., Novel star-shaped polylactide with glycerol using stannous octoate or tetraphenyl tin as catalyst: 1. Synthesis, characterization and study of their biodegradability, *Polymer*, **1995**, *36*, 2947
- <sup>98</sup> Grijpma D.; Joziassse C.; Pennings A. J., Star-shaped polylactide-containing block copolymers, *Macromol. Chem., Rapid Commun.*, **1993**, *14*, 155
- <sup>99</sup> Choi Y. K.; Bae Y. H.; Kim S. W., Star-shaped poly(ether-ester) block copolymers: Synthesis, characterization, and their physical properties, *Macromolecules*, **1998**, *31*, 8766
- <sup>100</sup> Vainionpää S.; Rokkanen P.; Törmälä R., Surgical applications of polymers in human tissue, *Prog. Polym. Sci.*, **1989**, *14*, 679
- <sup>101</sup> Amass W.; Amass A.; Tighe B., A review of biodegradable polymers: Uses, current development in the synthesis and characterization of biodegradable polyesters, blends of biodegradable polymers and recent advances in biodegradation studies, *Polym. Int.*, **1998**, *47*, 89
- <sup>102</sup> Kulkarni R. K.; Pani K. C.; Neuman C.; Leonard F., Polylactic acid for surgical implants, *Arch. Surg.*, **1966**, *93*, 839
- <sup>103</sup> Vert M.; Li S. M.; Spenlehauer G.; Guerin P., Bioresorbability and biocompatibility of aliphatic polyesters, *J. Mater. Sci., Mater. Med.*, **1992**, *3*, 432
- <sup>104</sup> Frazza E. J.; Schmitt E. E., A new absorbable suture, *J. Biomed. Mater. Res. Symp.*, **1971**, *1*, 43
- <sup>105</sup> Pitt C. G.; Chasalow F. I.; Hibionada Y. M.; Klimas D. M.; Schindler A., Aliphatic polyesters I. The degradation of poly( $\epsilon$ -caprolactone) in vivo, *J. Appl. Polym. Sci.*, **1981**, *26*, 3779
- <sup>106</sup> Pitt C. G.; Gratzl M. M.; Kimmel G. L.; Surles J.; Schindler A., Aliphatic polyesters II. The degradation of poly(DL-lactide), poly( $\epsilon$ -caprolactone), and their copolymers in vivo, *Biomaterials*, **1981**, *2*, 215
- <sup>107</sup> Holland S.; Tighe B.; Gould P., Polymers for biodegradable medical devices. 1. The potential of polyesters as controlled macromolecular release systems, *J. Controlled Release*, **1986**, *4*, 155
- <sup>108</sup> Göpferich A., Mechanisms of polymer degradation and erosion, *Biomaterials*, **1996**, *17*, 103

- <sup>109</sup> Mayer J.; Kaplan D., Biodegradable materials: Balancing degradability and performance, *Trends Polym. Sci.*, **1994**, *2*, 227
- <sup>110</sup> Albertsson A.-C.; Lundmark S., Synthesis, characterization and degradation of aliphatic polyanhydrides, *Brit. Polym. J.*, **1990**, *23*, 205
- <sup>111</sup> Heller J.; Sparer R.; Zentner G., Poly(ortho esters), *Biodegrad. Polym.*, **1990**, *45*, 121
- <sup>112</sup> Albertsson A.-C.; Eklund M., Influence of molecular structure on the degradation mechanism of degradable polymers: *in vitro* degradation of poly(trimethylene carbonate), poly(trimethylene carbonate-co-caprolactone) and poly(adipic anhydride), *J. Appl. Polym. Sci.*, **1995**, *57*, 87
- <sup>113</sup> Grijpma D.; Pennings A., (Co)polymers of L-lactide, 1. Synthesis, thermal properties and hydrolytic degradation, *Macromol. Chem. Phys.*, **1994**, *195*, 1633
- <sup>114</sup> Leenslag J. W.; Pennings A. J., Synthesis of high molecular weight poly(L-lactide) initiated with tin 2-ethylhexanoate, *Macromol. Chem.*, **1987**, *188*, 1809
- <sup>115</sup> Jamshidi K.; Hyon S.-H.; Ikada Y., Thermal characterization of polylactides, *Polymer*, **1988**, *29*, 2229
- <sup>116</sup> Kalb B.; Pennings A. J., General crystallization behaviour of poly(L-lactic acid), *Polymer*, **1980**, *21*, 607
- <sup>117</sup> Edlund U.; Albertsson A.-C., Novel drug delivery microspheres from poly(1,5-dioxepan-2-one-co-L-lactide); *J. Polym. Sci., Polym. Chem.*, **1999**, *37*, 1877
- <sup>118</sup> Löfgren A.; Albertsson A.-C., Copolymers of 1,5-dioxepan-2-one and L- or D,L-dilactide: Hydrolytic degradation behavior, *J. Appl. Polym. Sci.*, **1994**, *52*, 1327
- <sup>119</sup> Löfgren A.; Albertsson A.-C.; Zhang Y. Z.; Bjursten L.-M., Copolymers of 1,5-dioxepan-2-one and L- or D,L-dilactide: In vivo degradation behaviour, *J. Biomater. Sci. Polym. Ed.*, **1994**, *6*, 411
- <sup>120</sup> Shalaby S.; Kafrawy A., Synthesis and some properties of isomorphic copolymers of  $\epsilon$ -caprolactone and 1,5-dioxepan-2-one, *J. Polym. Sci., Polym. Chem.*, **1989**, *27*, 4423
- <sup>121</sup> Shalaby S., Isomorphic copolymers of  $\epsilon$ -caprolactone and 1,5-dioxepan-2-one, US Patent 4 190 720, 1980 (Ethicon Inc.)
- <sup>122</sup> Bornstein, J.; La Liberte, B. R.; Andrews, T. M.; Montermoso, J. C., Formation of a cyclic ester from the reaction of di-*n*-butyltin dichloride with ethylene glycol, *J. Org. Chem.*, **1959**, *24*, 886
- <sup>123</sup> Mathisen T.; Albertsson A.-C., Polymerization of 1,5-dioxepan-2-one. 1. Synthesis and characterization of the monomer 1,5-dioxepan-2-one and its cyclic dimer 1,5,8,12-tetraoxacyclotetradecane-2,9-dione, *Macromolecules*, **1989**, *22*, 3838
- <sup>124</sup> Considine J., Organotin chemistry VIII. The reaction of dibutyltin oxide with vic-glycols, *J. Organomet. Chem.*, **1966**, *5*, 263
- <sup>125</sup> Bornstein J.; La Liberte B. R.; Andrews T. M.; Montermosos J. C., Formation of a cyclic ester from the reaction of di-*n*-butyltin dichloride with ethylene glycol, *J. Org. Chem.*, **1959**, *24*, 886

- <sup>126</sup> Kricheldorf H.; Lee S.-R.; Bush S., Polylactones. 36. Macrocyclic polymerization of lactides with cyclic Bu(2)Sn initiators derived from 1,2-ethanediol, 2-mercaptoethanol, and 1,2-dimercaptoethane, *Macromolecules*, **1996**, *29*, 1375
- <sup>127</sup> Bradley D. C.; Mehrothra R. C.; Gaur D. P., in "Metal alkoxides" Academic press, London, **1978**
- <sup>128</sup> Nelissen M.; Keul H.; Höcker H., Ring-closing depolymerization of poly( $\epsilon$ -caprolactone), *Macromol. Chem. Phys.*, **1995**, *196*, 1645
- <sup>129</sup> Höcker H.; Thermodynamic recycling – on ring-opening polymerization and ring-closing depolymerization, *J. Macromol. Sci., Pure Appl. Chem.*, **1993**, *A30(9&10)*, 595
- <sup>130</sup> Duda A.; Penczek S., Kinetics of polymerization involving reversible deactivation due to aggregation of active centers. Analytical vs. numerical solution for the  $\epsilon$ -caprolactone/dialkylaluminum alkoxide system, *Macromol. Rapid Commun.*, **1994**, *15*, 559
- <sup>131</sup> Biela T.; Duda A., Solvent effect in the polymerization of  $\epsilon$ -caprolactone initiated with diethylaluminum ethoxide, *J. Polym. Sci. Polym. Chem.*, **1996**, *34*, 1807
- <sup>132</sup> Penczek S.; Duda A., Anionic and pseudoanionic polymerization of  $\epsilon$ -caprolactone, *Macromol. Chem., Macromol. Symp.*, **1991**, *42/43*, 135
- <sup>133</sup> Ouhadi T.; Hamitou A.; Jérôme R.; Teyssié Ph.; Soluble bimetallic  $\mu$ -oxo-alkoxides. 8. Structure and kinetic behaviour of the catalytic species in unsubstituted lactone ring-opening polymerization, *Macromolecules*, **1976**, *9*, 927
- <sup>134</sup> Chisholm M.; Iyer S.; McCollum D.; Pagel M.; Werner-Zwanziger U., Microstructure of poly(lactide). Phase-sensitive HETCOR spectra of poly(*meso*-lactide), poly(*rac*-lactide), and atactic poly(lactide), *Macromolecules*, **1999**, *32*, 963
- <sup>135</sup> Kasperczyk J., Microstructural analysis of poly[(L,L-lactide-co-(glycolide))] by <sup>1</sup>H and <sup>13</sup>C n.m.r. spectroscopy, *Polymer*, **1996**, *37*, 201
- <sup>136</sup> Thakur K.; Kean R.; Hall E.; Doscotch M.; Siepmann I.; Munson E., High-resolution <sup>13</sup>C and <sup>1</sup>H NMR study of poly(lactide), *Macromolecules*, **1997**, *30*, 2422
- <sup>137</sup> Kricheldorf H.; Jonte J.; Berl M., Polylactones 3. Copolymerization of glycolide with L,L-lactide and other lactones, *Macromol. Chem. Suppl.* **1985**, *12*, 25
- <sup>138</sup> Barakat I.; Dubois Ph.; Jérôme R.; Teyssié Ph., Macromolecular engineering of polylactones and polylactides. 10. Selective end-functionalization of poly(D,L)-lactide, *J. Polym. Sci. Polym. Chem.*, **1993**, *31*, 505
- <sup>139</sup> Albertsson A.-C.; Palmgren R., Polymerization and degradation of 1,5-dioxepan-2-one, *J. Macromol. Sci., Pure Appl. Chem.*, **1993**, *A30(12)*, 919
- <sup>140</sup> Gilding D.K., Biodegradable polymers, in "Biocompatibility of clinical implant materials", Ed. William D., CRC Press, Florida, **1981**, *Vol. 2*, 209
- <sup>141</sup> Albertsson A.-C.; Ljungqvist O., Degradable polymers. II. Synthesis, characterization, and degradation of an aliphatic thermoplastic block copolyester, *J. Macromol. Sci., -Chem.*, **1986**, *A23(3)*, 411
- <sup>142</sup> Fisher E. W.; Sterzel H.; Wegner G., Investigation of the structure of solution grown crystals of lactide copolymers by means of chemical reactions, *Kolloid – Z. u. Z. Polym.*, **1973**, *251*, 980

- <sup>143</sup> Li S., Hydrolytic degradation characteristics of aliphatic polyesters derived from lactic and glycolic acids, *J. Biomater. Med. Res. (Appl. Biomater.)*, **1999**, *48*, 342
- <sup>144</sup> Karlsson S.; Hakkarainen M.; Albertsson A.-C., Identification by headspace gas chromatography – mass spectrometry of in vitro degradation products of homo- and copolymers of L- and D,L-lactide and 1,5-dioxepan-2-one, *J. Chromatography*, **1994**, *688*, 251
- <sup>145</sup> Li S.; Garreau H.; Vert M., Structure-property relationship in the case of the degradation of massive poly( $\alpha$ -hydroxy acids) in aqueous media, Part 3. Influence of the morphology of poly(L-lactic acid), *J. Mater. Sci., Mater. Med.*, **1990**, *1*, 198
- <sup>146</sup> Hyon S.-H.; Jamshidi K.; Ikada Y., Effects of residual monomer on the degradation of DL-lactide polymer, *Polym. Int.*, **1998**, *46*, 196
- <sup>147</sup> Leenslag J.; Pennings A. J.; Bos R.; Rozema F.; Boering G., Resorbable materials of poly(L-lactide). VII. In vivo and in vitro degradation, *Biomaterials*, **1987**, *8*, 311
- <sup>148</sup> Mathisen T.; Masus K.; Albertsson A.-C., Polymerization of 1,5-dioxepan-2-one. 2. Polymerization of 1,5-dioxepan-2-one and its cyclic dimer, including a new procedure for the synthesis of 1,5-dioxepan-2-one, *Macromolecules*, **1989**, *22*, 3842